Gabriela Idania Vargas Zúñiga

2013

The Dissertation Committee for Gabriela Idania Vargas Zúñiga Certifies that this is the approved version of the following dissertation:

Synthesis, Anion Binding, and Photophysical Properties in Polypyrrolic Systems

Committee:

Jonathan L. Sessler, Supervisor

Eric V. Anslyn

Guangbin Dong

Jennifer Brodbelt

Sean M. Kerwin

Synthesis, Anion Binding, and Potphysical Properties of Polypyrrolic Systems

by

Gabriela Idania Vargas Zúñiga, B.S.; M.S.; M.A

Dissertation

Presented to the Faculty of the Graduate School of

The University of Texas at Austin

in Partial Fulfillment

of the Requirements

for the Degree of

Doctor of Philosophy

The University of Texas at Austin

December 2013

¨Nature is the source of true knowledge. She has her own logic, her own laws. She has no effect without cause, no invention without necessity¨.

Leonardo Da Vinci

Acknowledgements

I would like to thank my advisor Prof. Jonathan L. Sessler, for his constant belief in my abilities and support, and for encourages me to learn more and always do my best no matter the adversities or limitations.

Thank you very much to every single Sessler group member, for the good time I have had in the lab.

I really appreciate the hard work and great help of Dr. Vincent Lynch, who has recorded all the X-ray crystallographic analyses presented in this dissertation.

Dr. Sung Kuk Kim, you have been a great labmate, and have taught me everything I know. I appreciate a lot all the good words that you have always had for me. All the help that you have given to me related to chemistry has been of a great value for me.

I would also like to thank to Dr. Jonathan Arambula and Derric Brothwick for their help with the HLPC samples.

Christian, Christopher, Elizabeth, and Vladimir thank you very much for your friendship.

Special thanks go for RT, Yerim, Murat, Dong Sub, and Min Hee. All of you have been very nice and respectful. It has been a lot of fun to share the office with you.

Christina, Eric, and Aaron, you are great friends and labmates. I always find myself laughing all the time when I am with your company: you a sourced joy.

I would also like to express my gratitude to my family for their constant support and love

Synthesis, Anion Binding, and Photophysical Properties of Polypyrrolic Systems

Gabriela Idania Vargas Zúñiga, Ph. D.

The University of Texas at Austin, 2013

Supervisor: Jonathan L. Sessler

Anion binding has emerged as an important field of study due to the role that anionic species play in nature. As a consequence, considerable effort has been focused on the generation of anion receptors. These receptors have been designed to recognize anions through interactions, such as hydrogen bonding, donor-acceptor, and hydrophofic effects, in order to achieve higher sensitivity and selectivity. Another approach involves ion pair recognition, wherein the anions and cations are bound to the same system. Specifically, receptors bearing both hydrogen bonding donor and cation coordination sites have been of great interest as systems that lead to anion recognition and enhanced anion selectivities. Chapter 1 of this dissertation describes efforts to develop systems on the basis of modified Schiff-base calixpyrroles. This modification was achieved by incorporating a "strap" across the macrocycle to produce the so-called strapped Schiff-base calixpyrroles. The strap bearing amides are known to act as hydrogen bonding donors that can isolate the binding site from the medium. On the other hand, Schiff-base calixpyrroles have been widely studied as multidentate ligands for metal cation coordination. Therefore, the synthetic combination of these two moieties might provide a system wherein an ion pair complex is formed. Strapped Schiff-base calixpyrrole palladium complex were found to bind selectively cyanide anions.

The effects of direct substitution on one *meso* position on the optical and photophysical properties of porphycenes was recently found to be dependent of the electronic properties of the substituten (e.g., electron donor or electron withdrawing group). However, the effects on the electronic and optical properties properties as a result of substitution through a conjugated spacer are as yet unknown. This led to the synthesis of four *meso* substituted etioporphycenes, which are described in Chapter 2. Here, the substitution through an ethenyl group was stablished by analytical and structural means. This chapter provides of a description of the spectroscopic, structural and voltamperometric features of these compounds. Experimental procedures and characterization data are reported in Chapter 3.

Table of Contents

List of Tables

List of Figures

List of Schemes

Chapter 1: Synthesis of Novel Strapped Schiff-Base Calixpyrrole Macrocycles

1.1 INTODUCTION

Over the past decades, considerable effort has been devoted in the preparation of receptors capable of selectively binding and recognizing anionic substrates. Particular interest has been focused on areas such as nuclear waste remediation, environmental chemistry, and biology.[1] In recent years, Lee, Sessler, and coworkers have reported the use of "strapped" calix[4]pyrroles systems, wherein the binding domain derived from the pyrrole NH protons is effectively defined and isolated from the medium.[1,2] Studies of these new systems revealed that strapping one face of the calix[4]pyrrole served to enhance anion affinities. Moreover, improved selectivities were observed compared with analogous compounds with lower levels of preorganization. However, the relatively small cavity of strapped calix[4]pyrrole macrocycles limits their capacity to bind larger anionic substrates. This provides a motivation to synthesize larger strapped macrocycles similar to calix[4]pyrrole.

Core expanded porphyrins constitute a diverse class of ligands that have been used as platforms for the preparation of new metal complexes. They have been used to study reactivity patterns that can be compared with the natural porphyrins. An example is the calixpyrrole Schiff-base macrocycle 1.1 (*cf.* Figure 1.1), wherein the flexible dipyrromethane unit present in calix[4]pyrrole is linked by four Schiff-base units. This macrocycle has been used widely as a ligand for metal cation coordination.

The goal of this study was to synthesize a strapped system that incorporates a larger cavity for anion binding, and enough structurally flexibility to undergo a change in conformation upon addition of substrates. With such considerations in mind, the system

chosen was calix[4]pyrrole Schiff-base. This Chapter includes a brief introduction to calix[4]pyrrole and strapped calix[4]pyrrole chemistry and their use as anion receptors and ion pair receptors. Also, the author provides a short summary of calixpyrrole Schiff-base macrocycle chemistry. Finally, this chapter describes the preparation and spectroscopic characterization of new strapped Schiff-base calixpyrrole macrocycles 1.33 and 1.43 (*cf*. Figure 1.1). Upon addition of certain metallic salts to 1.43, the corresponding homo binuclear complexes were obtained. Finally, studies of the anion binding properties of 1.43 and its metal complexes were performed.

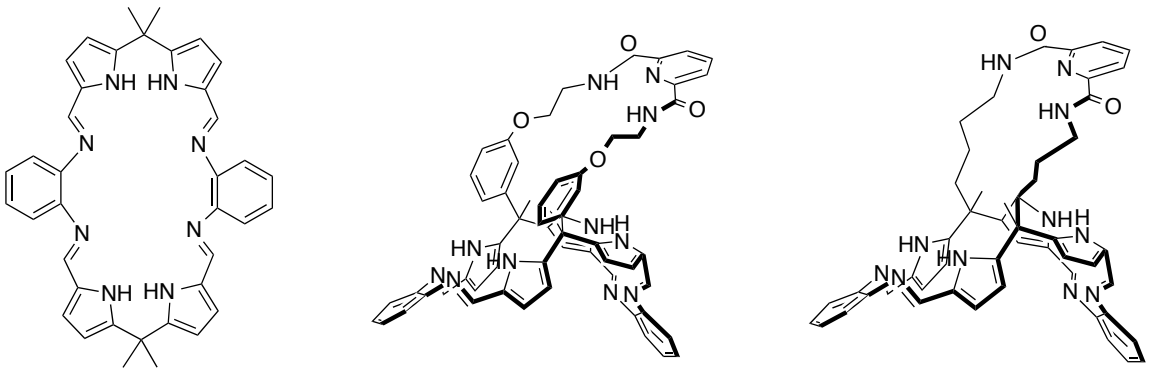

1.1 **1.2** **1.3**

Figure 1.1: Schiff-base calixpyrrole **1.1**, and strapped Schiff-base calixpyrroles **1.2** and **1.3**.

1.2 STRAPPED CALIX[4]PYRRLOE MACROCYCLES

Calix[4]pyrrole **1.4** is a macrocycle composed for four pyrrole units linked by four di-substituted *meso*-carbons. This porphyrinogen was originally reported by Baeyer[2] in 1886 and later studied as a ligand for metal coordination (*cf*. Figure 1.2).[3] In 1996 Sessler and coworkers reported the use of this macrocycle as an anion binding agent in organic media. They found it bound Lewis basic anions and underwent a change in conformation (from the so-called 1,3-alternate to the "cone" conformation) in analogy to what is seen for calix[4]arenes.[4] Since the discovery of its anion binding properties, efforts have been devoted to the modification of calix[4]pyrrole to improve its ability to recognize anions. Most of these modifications have been focused on functionalization of either the β-pyrrolic and *meso*-positions. However, such modifications are subject to important limitations and in many instances do not improve significantly the anion affinities.

An alternative approach used to enhance the affinity and selectivity of receptors is to isolate the binding domain from the medium. In the particular case of calix[4]pyrrole this was achieved by introducing a strap across one face. This 'locks' the conformation of the macrocycle in the cone conformation. By manipulating the strap length, the size of the cavity can be manipulated. This led in 2002 to the preparation of a series of compounds called "strapped calixpyrroles", which displayed increased anion affinities (*cf*. Figure 1.2). For instance, the strapped calix[4]pyrrole **1.5** displayed a chloride affinity of one order of magnitude larger than **1.4** (K_a = 1.4 × 10^6 M^{-1} *vs*. 1.4 × 10^5 M^{-1}, respectively in acetonitrile).[5, 6] Single crystal X-ray analyses revealed that a chloride anion was located within the cavity and was bound to the cavity through N-H•••Cl hydrogen bonds. The macrocycle itself existed in a cone-like conformation.

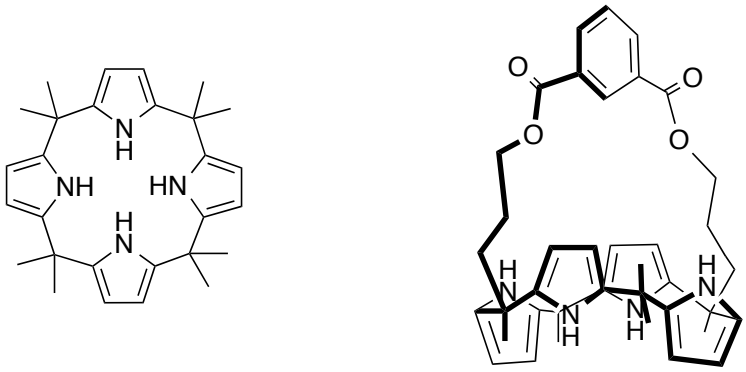

1.4 **1.5**

Figure 1.2: Calix[4]pyrrole **1.4** and *cis* ester calix[4]pyrrole **1.5**.

Further investigations involving changes in the length of the strap revealed that by modifying the length of the strap, even greater affinity enhancements for one specific anion could be achieved. For instance, as detailed in Table 1.1, for receptors **1.6** and **1.7**, the highest affinity for bromide anion was observed when the receptor contained the largest strap, in this case **1.7** (n = 3). Conversely, the largest affinity for chloride was seen with receptor **1.6** (n = 1), (*cf*. Figure 1.3). On this basis, it was concluded that not only is the size of the cavity important, but also the ability of the strap to stabilize the anionic guests (Cl^-, Br^-) *via* hydrogen bond interactions is crucial for achieving selective anion binding.[7]

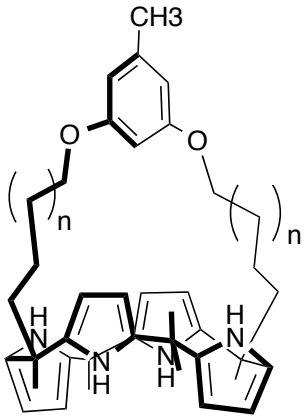

1.6 (n = 1)
1.7 (n = 3)

Figure 1.3: *Cis* ether strapped calix[4]pyrroles **1.6** and **1.7**.[7]

Table 1.1: Association constants K_a (M^{-1}) for the binding of halide anions to the receptors **1.4**-**1.7** as determined by ITC (isothermal titration calorimetry) measurements carried out in acetonitrile at 303 K using the corresponding tetrabutylammonium (TBA) salts.[6, 7]

	1.4	**1.5**	**1.6**	**1.7**
Cl^-	1.4×10^5	1.4×10^6	3.6×10^6	1.4×10^6
Br^-	3.4×10^3	7.5×10^3	3.0×10^4	1.2×10^5

The incorporation of additional hydrogen binding donors within the strap in an effort to increase the anion affinity even further led to the synthesis of receptors **1.8**-**1.10** shown in Figure 1.4. In this case the presence of amide groups in the strap was thought to enhance the anion binding. However, binding studies revealed that the affinity of the anions was independent of the length of the strap. Such unexpected behavior was explained as the anion binding occurred outside the central pocket defined by the strap. ^{1}H NMR spectroscopic titrations of receptor **1.8** in the presence of TBACl led to the suggestion that at high concentration of the receptor, the addition of small amount of anion produced a 2 : 1 (receptor : anion) complex. In contrast, the formation of a 1 : 1 complex is observed when the concentration of the chloride anion increases.[7,8]

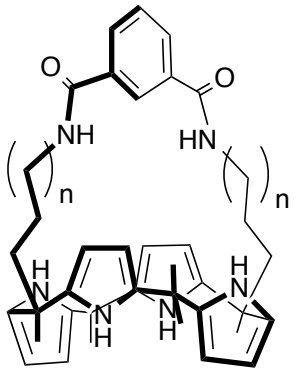

1.8 (n = 0)
1.9 (n = 2)
1.10 (n = 3)

Figure 1.4: *Cis* amide strapped calix[4]pyrroles **1.8**-**1.10**.[8]

The introduction of strapped calixpyrroles containing fluorophores, such as coumarin **1.11**[9] or acridine **1.12**,[10] in the strap permitted selective recognition and sensing of halide anions (*cf*. Figure 1.5). In the case of **1.11**, the fluorescence emission properties of the macrocycle were dependent of the addition on appropiate cations and anions. For instance, the fluorescence intensity was enhanced by the addition of sodium cations. This was attributed to the binding of these species to the carbonyl moiety in the coumarin, which produced a photoinduced electron transfer (PET) process. In contrast, the addition of anions resulted in a reduction of the fluorescence intensity due to the binding of the anionic species within the calix[4]pyrrole cavity. Most of these studies focused on the binding of halide anions.[9]

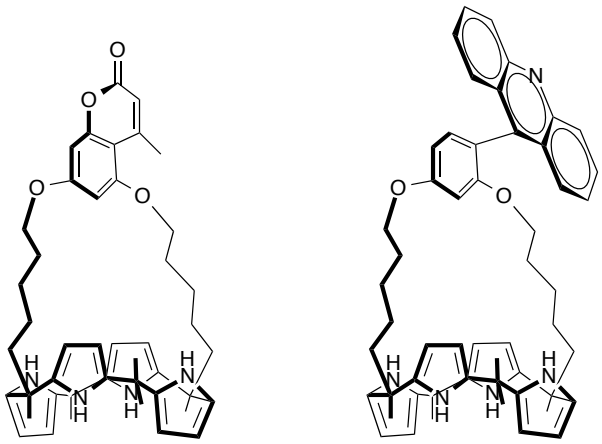

1.11 **1.12**

Figure 1.5: Coumarin-strapped calix[4]pyrrole **1.11** and acridine-strapped calix[4]pyrrole **1.12**.

In 2007, Lee and coworkers reported the preparation of the strapped chiral binol-derived calix[4]pyrroles **1.13** and **1.14** (*cf*. Figure 1.6). These receptors contained in an (*R*) or (*S*)-binol (1,1'-bi(2-naphthol)) diether strap attached to the calix[4]pyrrole core.[11] As presented in Figure 1.6, receptor **1.14** was found to bind both chiral (*R*) and (*S*)-2-phenylbutyrate ((*R*) and (*S*)-PB) in acetonitrile with high affinities. However, the pair (*S*)-guest-(*S*)-host had association constants ten times larger than the corresponding pair (*R*)-guest-(*S*)-host. This behavior was attributed to favorable interactions between the phenyl group of the guest and one of the naphthyl groups in the host. In constrast, the smaller association constant were observed for (*R*)-PB was rationalized in terms of unfavorable steric interactions between the chiral receptor and the phenyl group of the guest.[11]

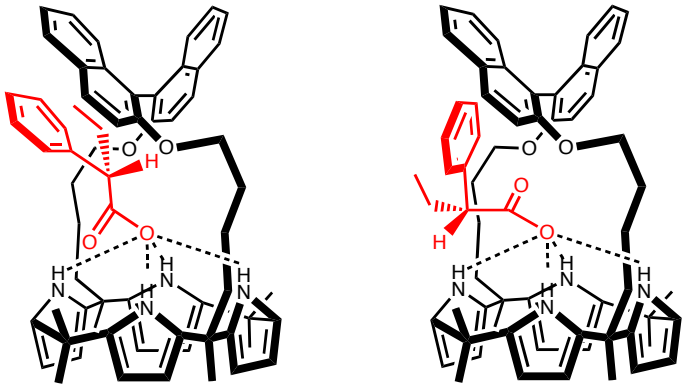

1.14/(*R*)-PB **1.14**/(*S*)-PB

Figure 1.6: Proposed binding modes between **1.14** and (*R*)-2-phenylbutyrate (left), and (*S*)-2-phenylbutyrate (right).[11]

In 2009, Gale and coworkers reported receptor **1.15**, Figure 1.7. This 1,2,3-triazole strapped calix[4]pyrrole was prepared using so-called click chemistry. The anion binding properties of this receptor where exploited to achieve the transport of chloride

anions through membranes made of POPC (1-palmitoyl-2-oleoylphosphatidyl choline), or POPC containing 30 mol% cholesterol. In this study, the strapped calix[4]pyrrole **1.15** functioned as a chloride anion transporter. Two mechanisms were proposed to account for the release of chloride anion. These mechanisms involved ion-pair co-transport and chloride-nitrite antiport, respectively.[12] In order to improve the chloride anion transport efficiency, another set of strapped calix[4]pyrroles, **1.16**-**1.18**, bridged by two triazoles through alkyl chains, were reported by the same research group. Increasing the length of alkyl chain between the two triazoles (i.e. **1.18**, n = 3, Figure 1.7), produced a transporter in which a chloride/nitrate antiport process proved predominant.[13] Recently, Samanta *et al*. reported a new catechol derived diether strap **1.19**. This receptor contains a binding domain more constrained than the macrocycles described above. The association constant calculated by ITC revealed that **1.19** displays relative higer affinity towards chloride and fluoride than bromide, or dihydrogen phosphate.[14]

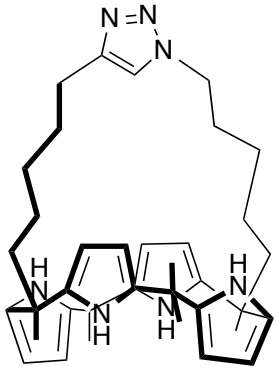

1.15

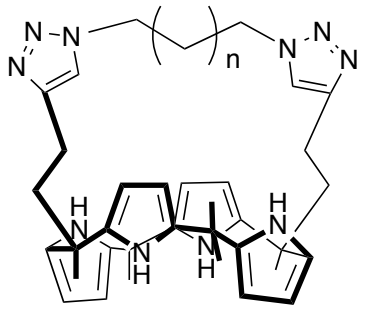

1.16 (n = 1)
1.17 (n = 2)
1.18 (n = 3)

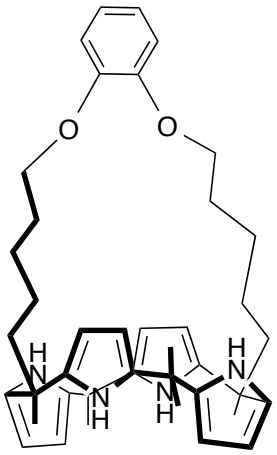

1.19

Figure 1.7: Triazole-strapped calix[4]pyrrole **1.15** and bis-triazole strapped calix[4]pyrrole **1.16**-**1.18**, and catechol-strapped calix[4]pyrrole **1.19**

1.3 CALIX[4]PYRROLE-BASED ION PAIR RECEPTORS

Since the first strapped calix[4]pyrrole report was published in 2002, a number of strapped calix[4]pyrroles have been synthesized. As detailed in the previous section, the introduction of different groups within and modifying the length of the straps offers the possibility of tuning the anion recognition properties of these systems.[5,7] Another approach involves ion pair recognition. In this case, the receptor is able to bind simultaneously cations and anions. This approach is particularly attractive because these receptors might allow enhanced ion selectivities, greater levels of control over ion recognition, extraction, and transportation through membranes than the corresponding strap-free calix[4]pyrroles. These potential benefits lead to the preparation of Ni(II)porphyrin-capped calix[4]pyrroles **1.20**-**1.22** by Lee and coworkers (*cf*. Figure 1.8).[15] These receptor contained a metal center (porphyrin-nickel complex) and a hydrogen binding donor (calix[4]pyrrole). ^{1}H NMR spectroscopic binding studies carried out in deuterated dichloromethane revealed that this system displays a selective affinity for fluoride anions over other anions such as Cl^-, Br^-, and I^-.[15] This selectivity was attributed to a combination of the coordination of the anion to the metal center and stabilization *via* hydrogen bonding interaction.

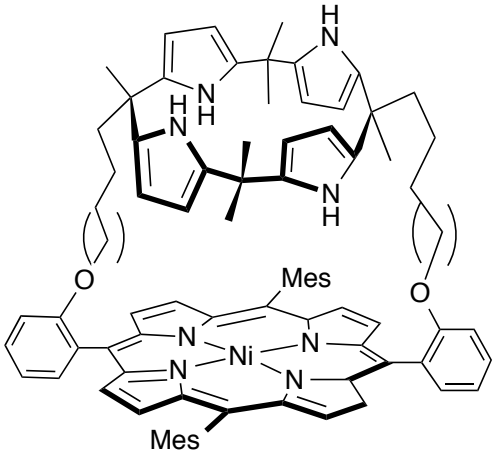

1.20 (n = 1)
1.21 (n = 2)
1.22 (n = 3)

Figure 1.8: Metalloporphyrin-capped calix[4]pyrroles **1.20**-**1.22**.

In 2008, Kim *et. al* reported receptor **1.23**. As shown in Figure 1.9, receptor **1.23** contains two strong ion binding sites (a calix[4]arene crown-6 for the Cs^+ ions and a calix[4]pyrrole for anions).[16] Isothermal titration calorimetric (ITC) and ^1H NMR spectroscopic data revealed that receptor **1.23** forms stable 1:1 complexes with CsF (K_a = 3.8×10^5 M^{-1} in acetonitrile).[16] Single crystal X-ray diffraction analysis revealed that the ion pair complex is preserved in solid state, wherein a methanol molecule from the solvent was located between Cs^+ and F^- in a solvent-bridged fashion. Later, another strapped calix[4]pyrrole ion pair receptor (**1.24**) that contained a weak cation recognition site (calix[4]arene) instead the strong Cs^+ binding site present in **1.23**, was reported. It was found to bind CsX salts (CsX, X = F^-, Cl^-, Br^-, and NO_3^-).[17] Interestingly, ^1H NMR spectroscopic analyses in mixture of deuterated methanol-chloroform (1:9, v/v) revealed that the binding of Cs salts was dependent on the counterion. In this case, receptor **1.24** was able to stabilize three different ion pair binding modes with the Cs^+ cation (solvent-bridged, contact, and host-separated) (*cf*. Figure 1.9).[17] These findings led to the proposal

that receptor **1.24** as an extractant of radioactive cesium cations. In 2012, another ion pair receptor, **1.25**, similar to **1.23** was synthesized, (*cf.* Figure 1.9).[18] This strapped calix[4]pyrrole was found to function as an extractant for cesium cations in a novel-release cycle. Specifically, upon contact of an aqueous $KClO_4$ solution with the cesium salt complex of **1.25** a cation metathesis takes place. The incoming cation (K^+) occupies a different binding site, but nevertheless serves to eject the initial recovery of Cs^+ cations. Additional exposure of the potassium salt complex of **1.25** to a nitrobenzene-chloroform mixture and water resulted in the release of potassium salt from the cavity to obtain the ion-free receptor.[18] This allowed regeneration of the original receptor system.

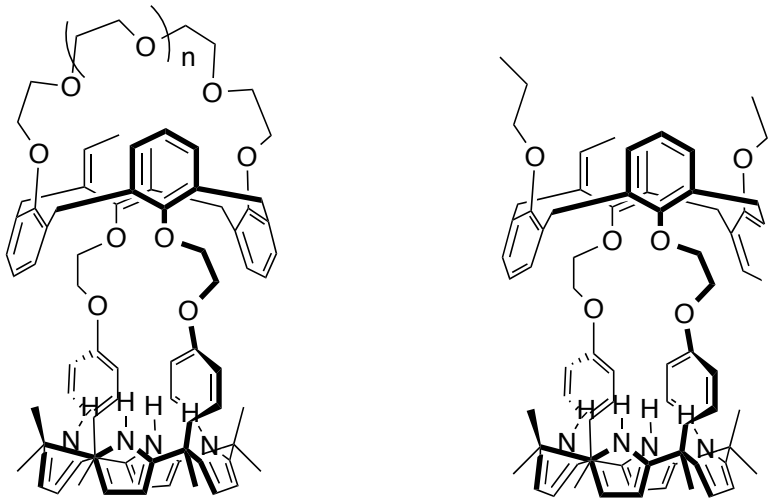

1.23 n = 0
1.25 n = 1

1.24

Figure 1.9: Crown-calix[4]arene-capped calix[4]pyrrole **1.23**, and **1.25** ion pair receptors (left), and calix[4]arene-capped calix[4]pyrrole **1.24** ion pair receptor (right).

Recently, Sessler and coworkers reported the synthesis of receptor **1.26** capable of forming a strong anion complex with fluoride and chloride anions, and also ion pair complexes with alkali metal ions, such as, Li^+, K^+, and Cs^+.[19] ^1H NMR spectroscopic studies in deuterated acetonitrile revealed that receptor **1.26** binds fluoride and chloride with high affinities. In contrast, studies of the ion pair complexes with $NaClO_4$ or $LiClO_4$ salts revealed different binding tendencies. For instance, as shown in Scheme 1.1, when cesium perchlorate was added to **1.27** an ion pair complex was formed, in which the Cs^+ cations were located in the "cup" of the calix[4]pyrrole moiety. Addition of $NaClO_4$ or $LiClO_4$ to **1.27** resulted in a complete decomplexation of fluoride anions from the phenyl moieties in the strap. Upon addition of K^+ cations to receptor **1.27** produced an ion pair complex, in which K^+ cations were situated in the oligoether moiety.[19] These differences served to underscore the subtle nature of the binding events and how they could be tuned to favor the recognition of one particular ionic guest.

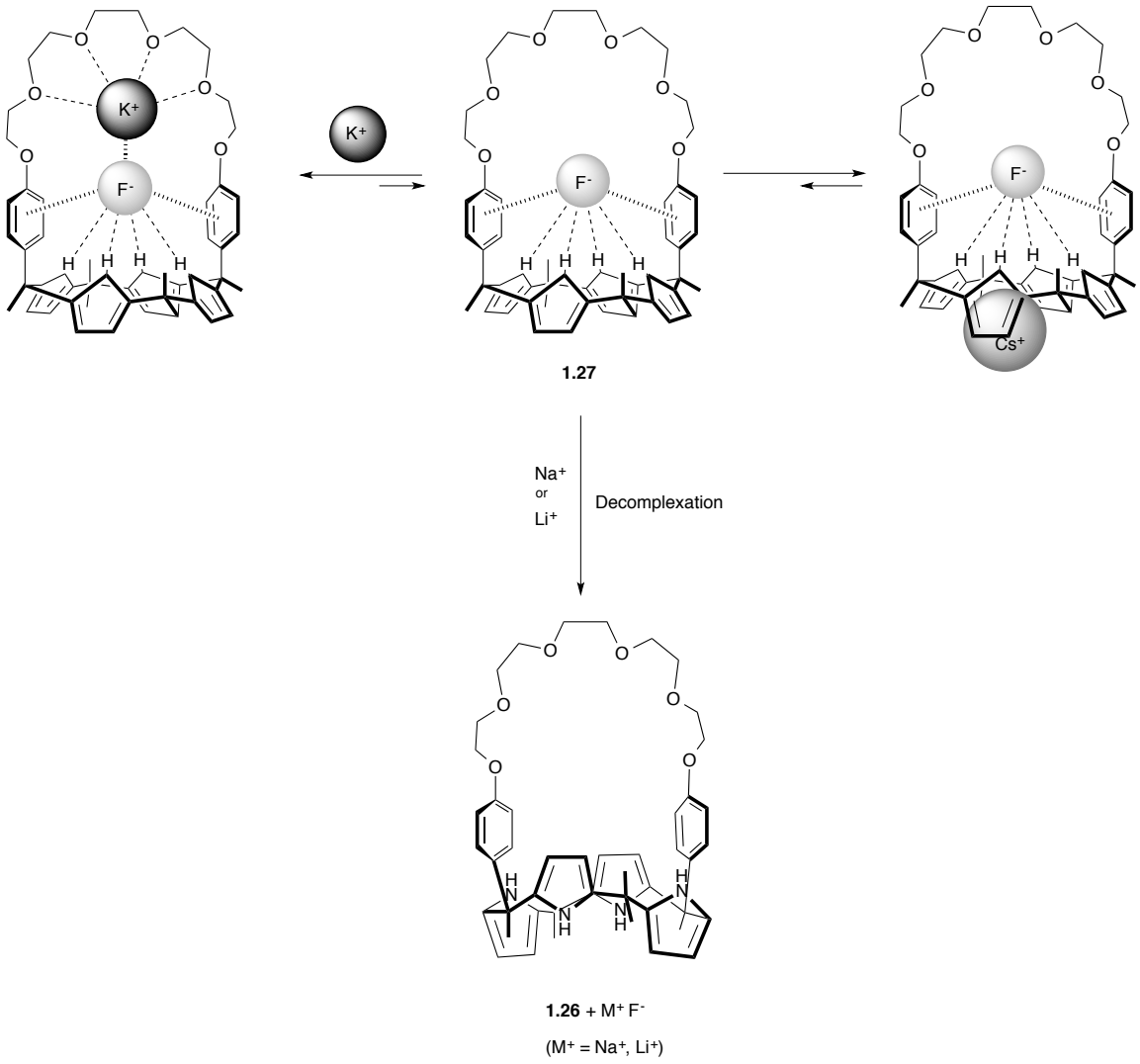

Scheme 1.1: Cation-induced changes that occur to receptor **1.27** upon addition of $NaClO_4$ or $LiClO_4$ salts.

1.4 SCHIFF-BASE CALIXPYRROLES

Although calix[4]pyrrole has been widely studied as an anion receptor due its affinity for small anions, such as fluoride and chloride, its capacity to bind large anions is

still limited by the size of its cavity. In an effort to create receptors capable of binding of larger anions, several expanded macrocycles containing dipyrromethane units have been synthesized. In 1996, Sessler and coworkers reported Schiff-base calixpyrrole 1.1 (*cf.* Figure 1 in Section 1.1).[20] This macrocycle contains two flexible dipyrromethane units that are present in calix[4]pyrrole, which are linked by four imine units (Schiff-base). Due to these characteristics this new macrocycle was named Schiff-base calixpyrrole. Unlike calix[4]pyrrole that displays strong affinity for halide anions (e.g., fluoride and chloride),[20] the free base of receptor 1.1 revealed moderate binding affinities for anions such as chloride and bromide (i.e., for chloride anions in acetonitrile, $K_a = 1.6 \times 10^4$ M^{-1} *vs*, $K_a = 1.4 \times 10^5$ M^{-1} for calix[4]pyrrole). ITC studies revealed that in acetonitrile, the mono and diprotonated forms of 1.1 posses chloride anion affinities that are up to fifty times higher than that of calix[4]pyrrole ($K_a = 9.8 \times 10^5$, $K_1 = 1.6 \times 10^4$ and K_2 7.61×10^6 M^{-1}, for the mono, and diprotonated forms of 1.1, respectively).[20] This increase in the affinity for chloride anions was attributed to the presence of the extra positive charges provided by protonation of the imine groups in the macrocycle. Unlike calix[4]pyrrole that diplays conformational behavior upon addition of anions, crystallographic analysis of Schiff-base calixpyrrole revealed that 1.1 undergoes a complete change in geometry when a chloride anion is bound in its cavity.

The wide nitrogen-rich cavity of the Schiff-base calixpyrrole led to the use analogues of 1.1 (e.g., 1.28) as a ligand for metal complexation. This work was carried out independently by Sessler and Love research groups, with the vast majority of the contributions coming from the latter team.[21] As shown in Scheme 1.2, upon addition of two equivalents of transition metal salts a binuclear metal complex, such as, 1.29 is formed. Cation complexation induces conformational change from a nonplanar chair conformation in the free base form of ligand 1.28 to a "Pacman-like" conformation in which the two aryl groups ends come together in a face-to-face fashion similar to Pacman porphyrins.[22] Compared to the difficult multistep synthesis of Pacman porphyrins, Schiff-base calixpyrroles offer an easier-to-access alternative in that synthesis is facile and easy

purification is required.[22] In the case of the binuclear complexes containing Fe(II), Ru(II), or Co(II), the metal centers were bound to an atom of oxygen, or to a molecule of oxygen. In fact, the dicobalt complex 1.29c has been proposed as a catalyst for dioxygen reduction.[21] The versatility of 1.28 and its derivatives as multidentate ligands for metal cations has been explored by Arnold, Love, and coworkers who reported the coordination of lanthanide and actinide cations, such as Ce(III) 1.30,[23] Sm(III) 1.31, or Y(III) 1.32 (as an uranyl-lanthanide complex),[24] and more recently, the coordination of two uranyl cations 1.33 (*cf*. Figure 1.10).[25]

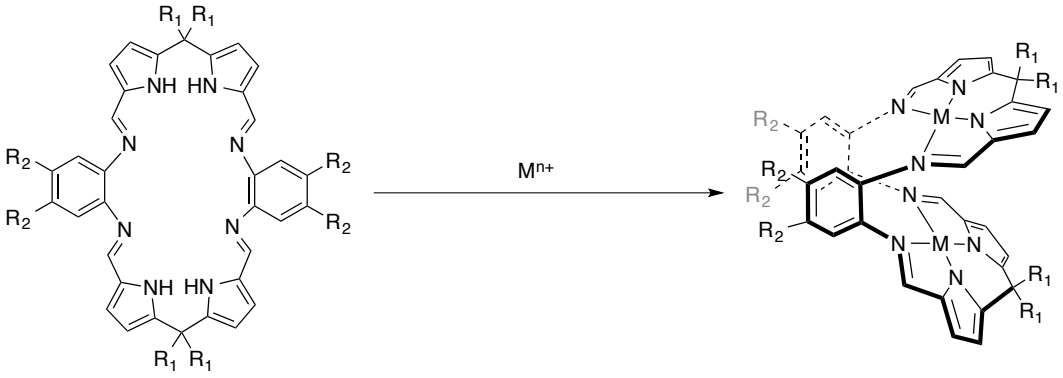

1.28

1.29a M = Fe, R_1 = CH_3, R_2 = OCH_3
1.29b M = Cu, R_1 = CH_3, R_2 = CH_3, or OCH_3
1.29c M = Co, R_1 = CH_3, or fluorenyl , R_2 = CH_3
1.29d M = Pd, R_1 = CH_3,or Ph, R_2 = H
1.29e M = Zn, R_1 = CH_3, R_2 = H
1.29f M = Ni, R_1 = CH_3, R_2 = H
1.29g M = Cd, R_1 = CH_3, R_2 = OCH_3
1.29h M = Cp^*Ru, or PhRu, R_1 = CH_3, R_2 = H

Scheme 1.2: Examples of binuclear transition metal complexes of **1.28** and their synthesis of its derivatives. Some ligands bridging the metal centers have been excluded for clarity.

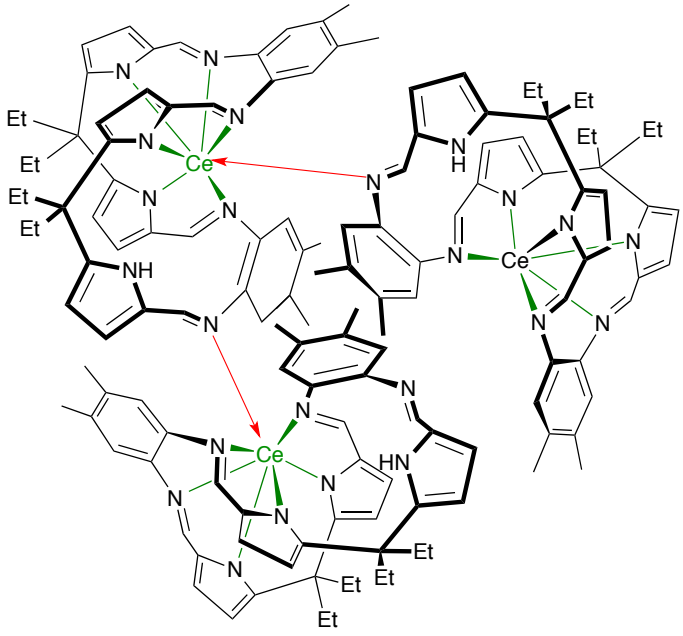

1.30

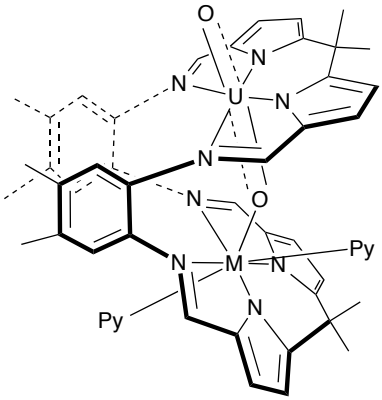

1.31 M = Sm
1.32 M = Y

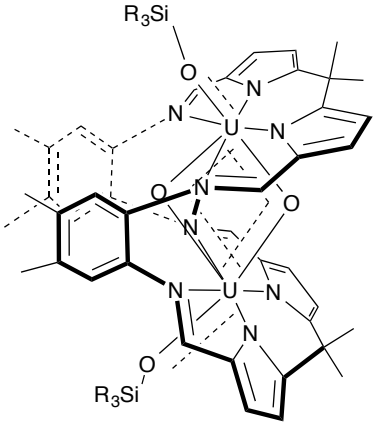

1.33 R = $SiMe_3$, or $SiMe_2Ph$

Figure 1.10: Schiff-base calixpyrrole metal complexes, Ce(III) complexes **1.30** (top), uranyl-lanthanide complexes **1.31** and **1.32** (left), and binuclear uranyl complex **1.33** (right).

Inspired by the chemistry observed with **1.28**, an effort was made to replace the aryl moiety attached to the imine groups in this original system by1,8-disubstituted anthracene. This led to the synthesis of the anthracenyl-based Schiff-base calixpyrrole macrocycle **1.34**. In this complex, the zinc cations preorganize the two nitrogen donor compartments into a cofacial binuclear conformation as shown in Figure 1.11.[26] X-ray diffraction analysis of **1.34** revealed that the Lewis acidic zinc cations accommodate a chloride or a hydroxide anion between the two metal centers. ITC studies in THF led to the conclusion that **1.34** displayed selective affinity for chloride anions in a 1:1 stoichiometry over other halides. The association constant of the zinc complex **1.34** for chloride anions was $K_a = 3.2 \times 10^7$ M^{-1} in THF.[26] This provides support for the notion that preorganization of the binding sites, combined with the use of Lewis acidic cations, facilitates the binding of small anions (i.e., Cl^-).

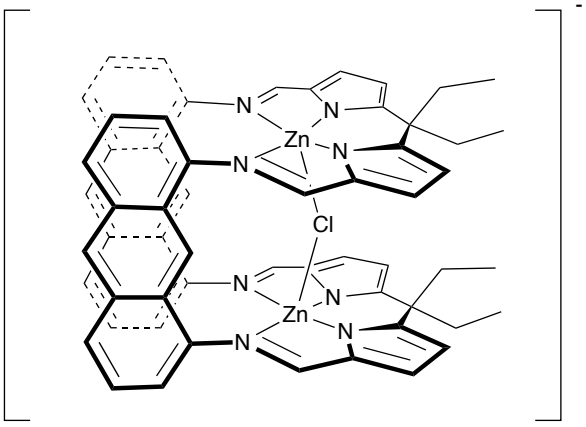

1.34

Figure 1.11: Schematic representation showing how anion may be bound by the binuclear "Pacman" complex **1.34**.

Finally, the metal cation coordination properties of Schiff-base calixpyrrole have used by Bejger *et al*. to stabilize a mixed-valence radical dimer of tetrathiafulvalene (TTF).[27] This was achieved by introducing two tetrathiafulvanlene (TTF) annulated subunits in the macrocycle to form compound **1.35** as shown in Scheme 1.3.[27] This TTF-Schiff-base calixpyrrole was obtained by the condensation of TTF phenylenediamine with diformyldipyrromethane in the presence of *p*-toluenesulfonic acid. Reacting **1.35** with palladium acetate in the presence of triethylamine afforded the binuclear palladium complex in moderate yields. The formation of the palladium binuclear complex **1.36**, served to constrain the two TTF subunits to a Pacman-like conformation. Single crystal X-ray analysis revealed that the TTF groups in **1.36** are proximate, and ^{1}H NMR studies provided evidence that this conformation was preserved in solution.[27] Cyclic voltammetry (CV), UV-Vis, and EPR spectroscopic analyses were consistent with the suggestion that in the metal complex **1.36** a mixed valence radical state in the TTF subunits is stabilized upon oxidation.

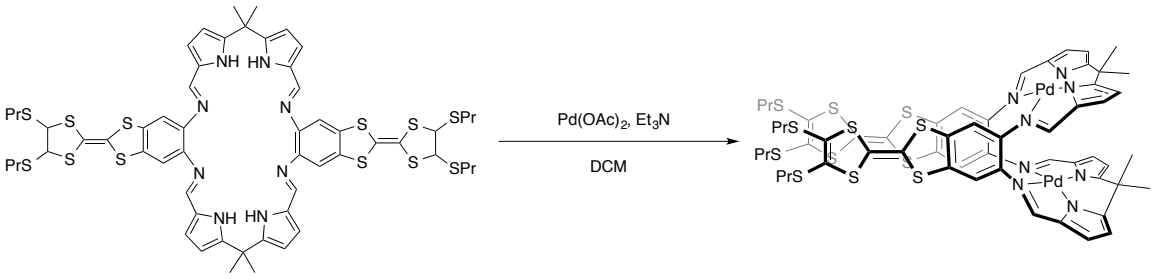

1.35 **1.36**

Scheme 1.3: Synthesis of bis-Pd(II) complex **1.36**.

1.5 Design and Synthetic Strategy

The following section describes the preparation of the polypyrrolic macrocyclic strapped Schiff-base calixpyrroles 1.2, 1.3, and the binuclear metal complexes 1.44-1.47. The introduction of a strap to the Schiff-base calixpyrrole was envisioned to enhance the anion binding properties of the macrocycle. However, as will be discussed in the following sections, the stability of strapped calixpyrrole Schiff-base 1.37 is dependent of the acidity of the medium. It was found to be too unstable for effective use as an anion receptor. The hydrolysis of compound 1.37 was analyzed under three different pH values and the formation of the hydrolysis products were followed using UV-vis spectroscopy.

Compound **1.43** was designed to have a more flexible strap than prior Schiff-base pyrrole macrocycles. This feature was expected to enhcance the stability of the macrocycle under acidic conditions. Once synthesized, the anion binding properties were tested. Similar to what was found to be for other Schiff-base calixpyrrole macrocycles, **1.43** generally exists in a bowl-like conformation, wherein the aryl groups in the macrocycle are oriented to opposite sides with no association between the π-faces (*cf.* Scheme 1.4). Upon the addition of two equivalents of a transition metal salt, a folded form with rigid clip-like or "Pacman" conformation is obtained. In this conformation, it is expected that an ion pair complex would be formed, wherein anionic species would bind to the metal centers. Anion binding studies of the palladium(II) and copper(II) complexes were performed and are described in the following sections.

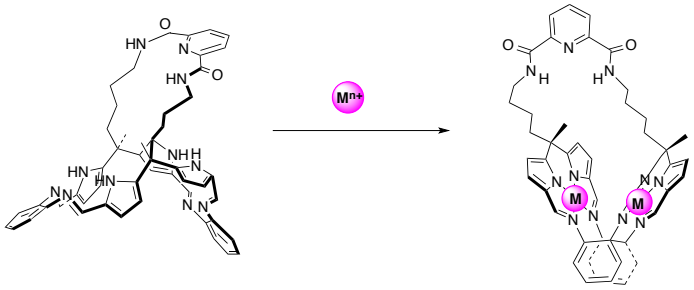

1.3

Scheme 1.4: Representation of the conformational change of **1.3** seen upon coordination of metal cations.

1.6 Results and Discussions

1.6.1 Strapped Schiff-base Calixpyrroles

The synthesis of receptor **1.2** is summarized in Scheme 1.5. Briefly, 3-hydroxyacetophenone **1.37** was reacted with 1,2-dibromoethane in the presence of an excess of K_2CO_3; this afforded **1.38** in a moderate yield (84%). Subsequent reaction of **1.39** with potassium phthalimide followed by condensation with pyrrole under acidic conditions gave dipyrromethane **1.40** in 36% yield. Hydrazinolysis of **1.40** generated amino derivative **1.41**, which was reacted with 2,6-pyridinecarbonyl chloride to produce the strap **1.41a** in 19% yield. This key precursor was formylated using the Vilsmeier-Haack method to obtain compound **1.42.** Macrocyclization of **1.42** with *o*-phenylinediamine afforded macrocycle **1.2** in 10% yield after purification. This macrocycle was purified using a Teledyne CombiFlash Companion with a neutral alumina column using CH_2Cl_2-hexanes, 9:1, v/v to 97% purity, as judjed by high performance liquid chromatography (HLPC).

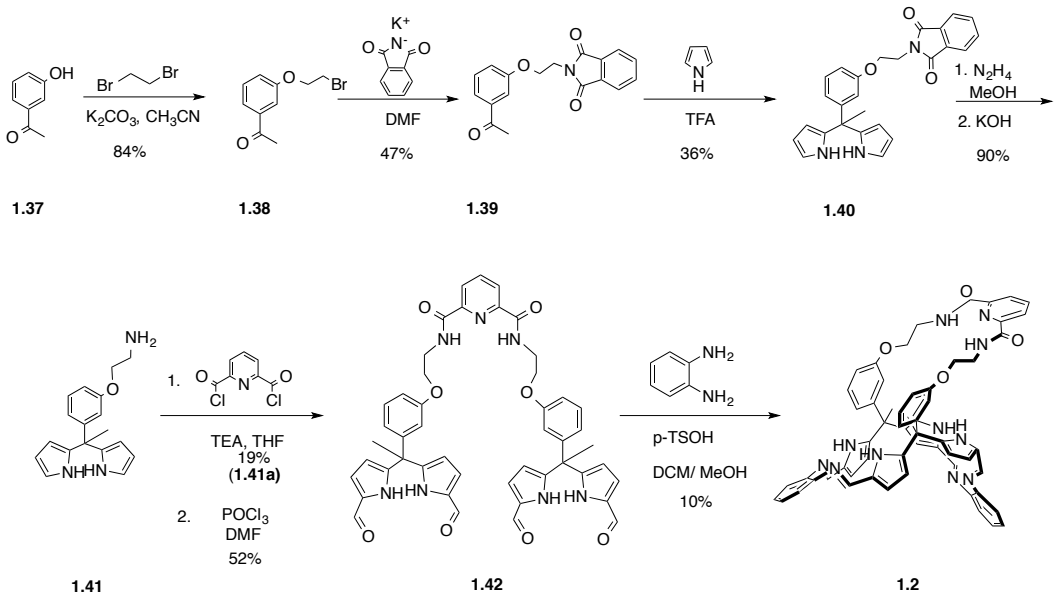

Scheme 1.5: Synthesis of compound **1.2**.

Schiff-base calixpyrrole macrocycle **1.2** was characterized by standard characterization methods, named, ^{1}H and ^{13}C NMR spectroscopy, high-resolution ESI and CI mass spectrometry, and HPLC. Initially, contact of **1.2** dissolved in dichloromethane to thorium chloride aqueous solution (pH = 3.6) produced a change of color in the organic phase from light yellow to bright yellow. This change of color led to the suggestion that **1.2** could be utilized for extraction of Th(IV) cations. Extractions of $ThCl_4$ into an organic phase by macrocycle **1.2** in a mixture of water-dichloromethane (1:1, v/v) revealed that **1.2** presumably had good selectivity for $ThCl_4$ under our model extraction conditions (*cf*. Figure 1.12). On the basis of this observation, titrations of **1.2** with tetrabutylammonium chloride (TBACl) and $ThCl_4$ in 40% v/v water-acetonitrile were separately performed and monitored by UV-Vis spectroscopy. The initial titration of **1.2** using TBACl revealed no change in absorbance, even after the addition of 40 equivalents of the TBACl salt. In contrast, when **1.2** was subjected to increasing additions of $ThCl_4$ under the same conditions a dramatic change in absorbance is observed. Analysis of the UV-Vis spectra revealed a blue shift of the maximum absorbance (λ_{max})

from 338 nm to 300 nm upon addition of $ThCl_4$ to the solution. However, the mass spectrometry analysis (ESI-MS) did not exhibit a peak corresponding to the thorium complex, which led to a reassessment of the initial conclusion and the suggestion that the change in color is due entirely to the protonation of the macrocycle when it is in contact with water. This protonation then leads to a subsequent hydrolysis of the macrocycle in the presence of the initial Lewis acid (Th(IV)).

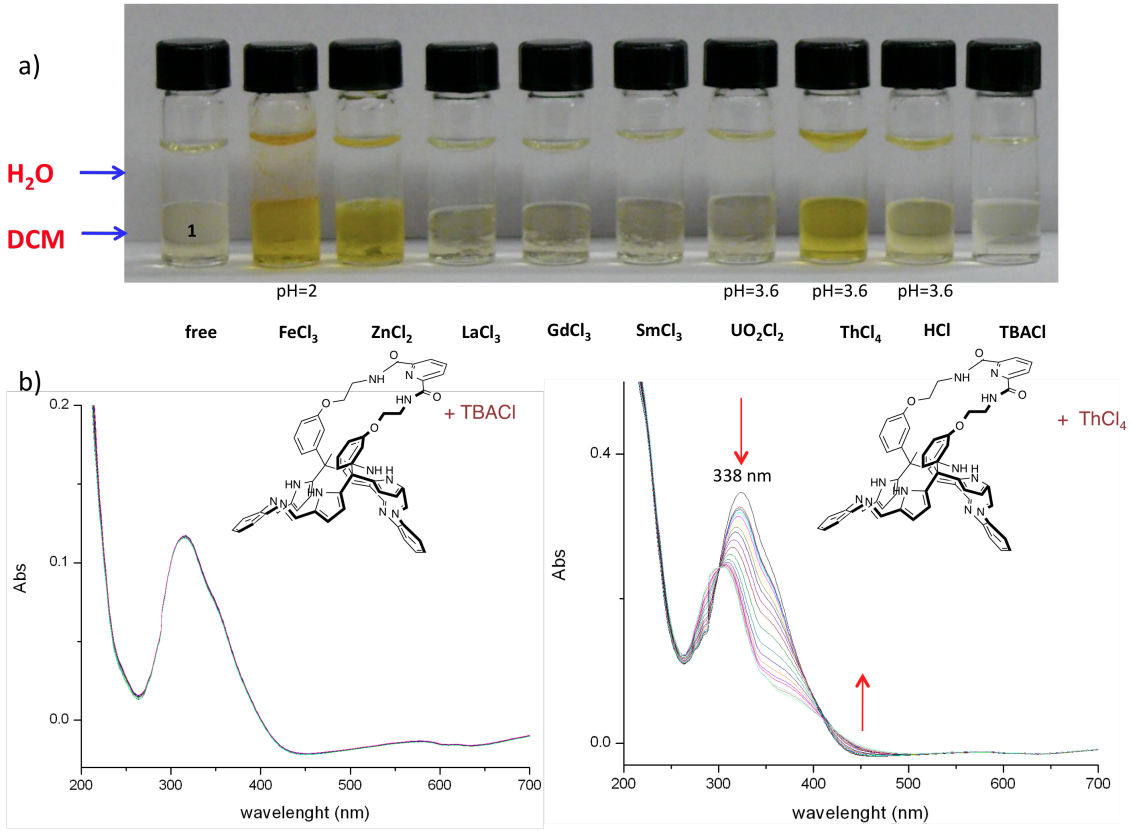

Figure 1.12: a) Color changes seen when the strapped Schiff-base calixpyrrole **1.2** in CH_2Cl_2 is exposed to aqueous solutions of various metallic salts. The pH is not buffered and is approximately 3.7 in the case of the Th(IV) salt. The concentration of **1.2** is 0.2 mM in CH_2Cl_2, and the metallic salt is 2 mM in water. I = 1.0 M NaCl. The pH was measured with a H^+ sensor at 298 K. b) Spectral titrations performed between strapped Schiff-base calix[4]pyrrole macrocycle **1.2** (2.5×10^{-5} M) and TBACl, or $ThCl_4$ in a mixture of CH_3CN-water 6:4, v/v at 298 K (TBA = tetrabutylammonium).

To confirm that **1.2** hydrolyzes in acidic conditions, the stability of **1.2** was tested at three different pH values (3, 6, and 9, using buffers of glycine-HCl, citric acid-sodium citrate, and TRIS-HCl, respectively). The pH values of the aqueous solutions were measured with a H^+ sensor. The hydrolysis products were followed by UV-Vis spectroscopy. The test solutions were prepared by dissolving **1.37** in a mixture of acetonitrile-water, which was buffered to the desired pH. The absorption spectra were then collected every thirty minutes for five hours. The change in absorbance at two wavelengths (329 nm and 283 nm) was monitored. These two wavelengths were chosen they reflect the λ_{max} values of **1.2**, and the tetraaldehyde precursor **1.42**, respectively, (*cf.* Figure 1.13). Analysis of the UV-Vis spectra revealed that at lower pH values (pH = 3 and 6), hydrolysis of **1.2** to **1.42** is complete after four hours. At pH 9 the hydrolysis did not take place in the time frame of the study. This observation was supported by HPLC analysis performed under acidic conditions (using CH_3CN-water (8.4:1.6) (1% v/v TFA)). The HPLC chromatogram revealed the presence of two products; one corresponds to compound **1.2** and a second peak corresponded to the protonated species [**1.2H**]$^+$. Conversely, under conditions of basic hydrolysis (1% v/v TRIS buffer, pH 9) using the same solvent mixture, only one product was detected in the HPLC chromatogram. It corresponded to compound **1.2**, (*cf.* Figure 1.14).

a)

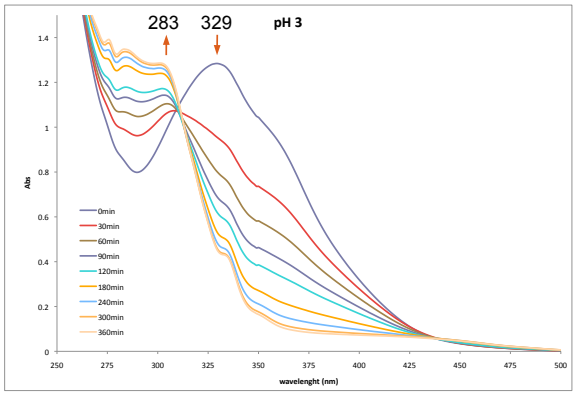
283
329
pH 3
Abs
wavelenght (nm)
0min
30min
60min
90min
120min
180min
240min
300min
360min

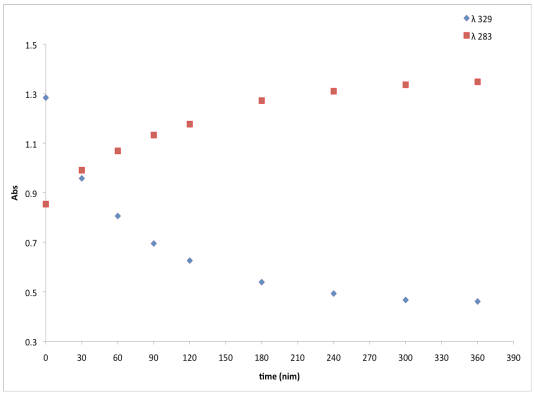
λ 329
λ 283
Abs
time (nim)

b)

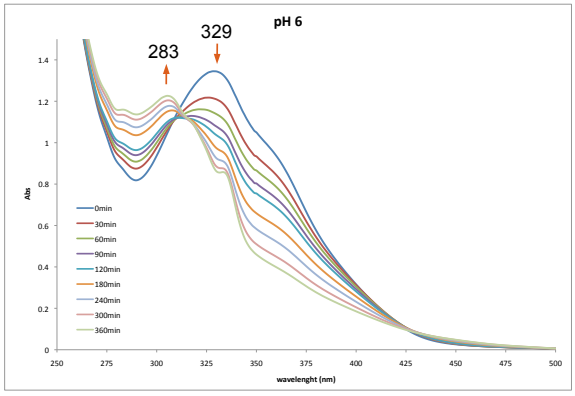
283
329
pH 6
Abs
wavelenght (nm)
0min
30min
60min
90min
120min
180min
240min
300min
360min

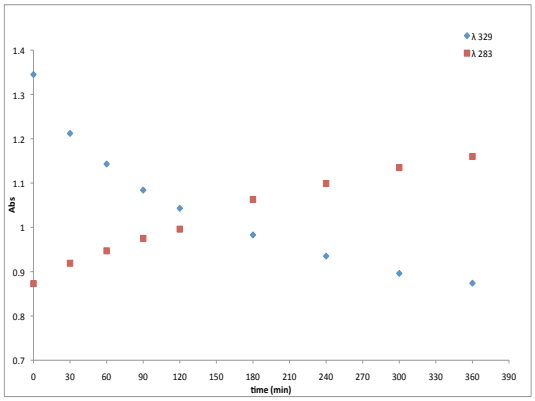
λ 329
λ 283
Abs
time (min)

c)

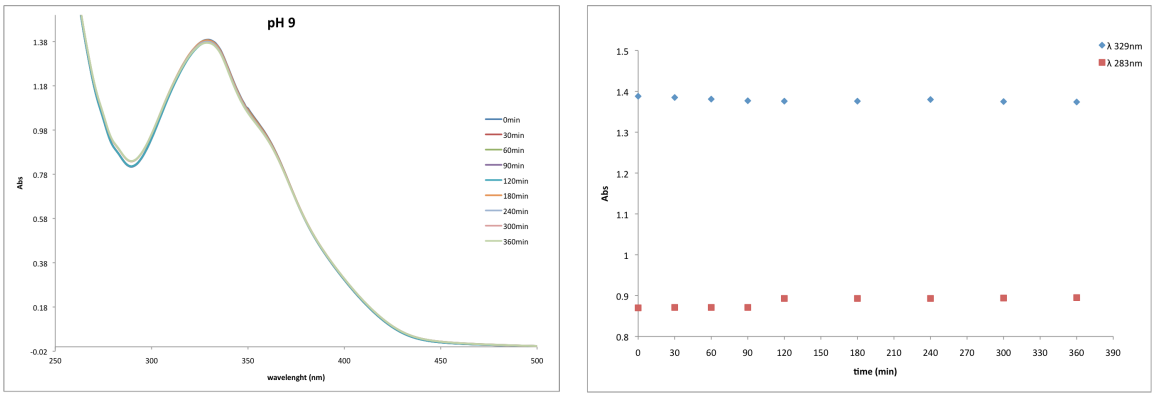

d)

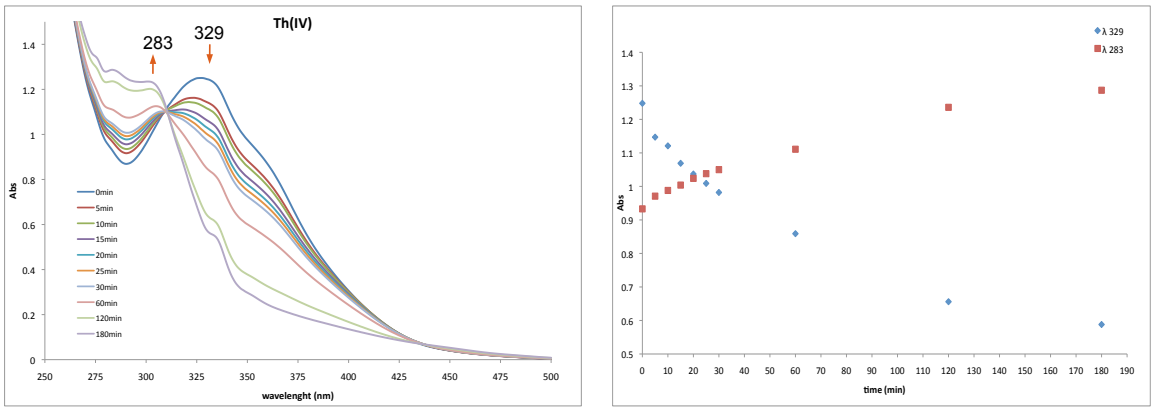

Figure 1.13: Absorption spectra of **1.2** recorded in a CH_3CN-water mixture (8.4:1.6, v/v) at three different pH. Also shown are the spectral changes seen upon exposure to thorium nitrate, a) pH = 3, b) pH = 6, c) pH = 9, and d) Th(IV), respectively. [**1.2**] = 2.5×10^{-5} M, [Th(IV)] = 2.5×10^{-4} M. The buffers employed for these studies were glycine-HCl for pH = 3, citric acid-sodium citrate for pH = 6, and TRIS-HCl for pH = 9. All the experiments were conducted at 298 K.

a)

Chromatogram

clean C:\Documents and Settings\User\Desktop\Group Files\Jonathan\gab\macrocycle.lcd

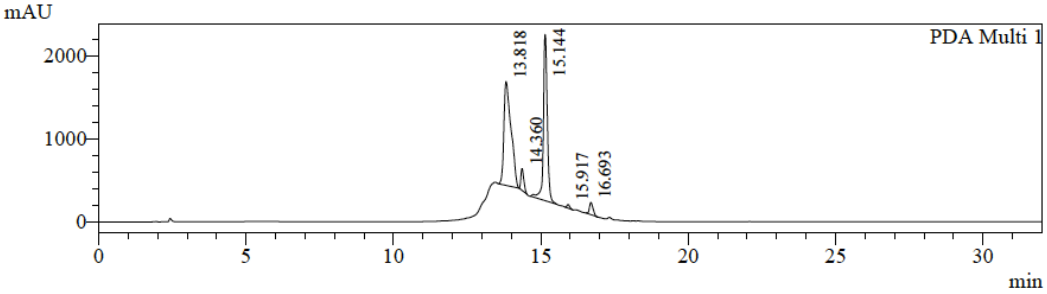

1 PDA Multi 1 / 295nm 4nm

PeakTable

PDA Ch1 295nm 4nm

Peak#	Ret. Time	Area	Area %
1	13.818	21004507	48.978
2	14.360	1798602	4.194
3	15.144	18587986	43.343
4	15.917	280263	0.654
5	16.693	1214294	2.831
Total		42885652	100.000

Spectrum

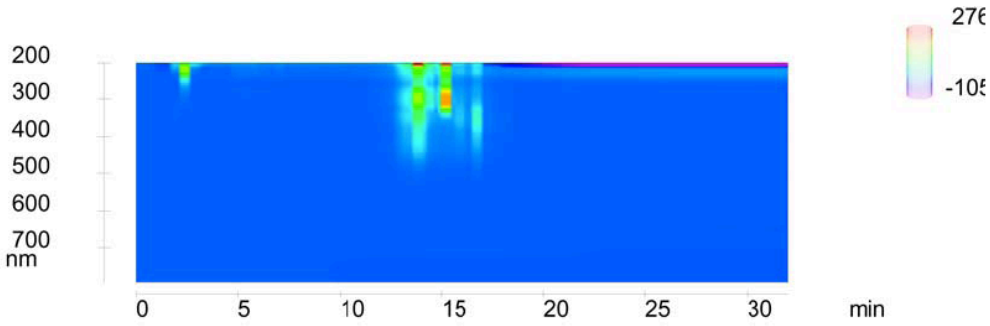

b)

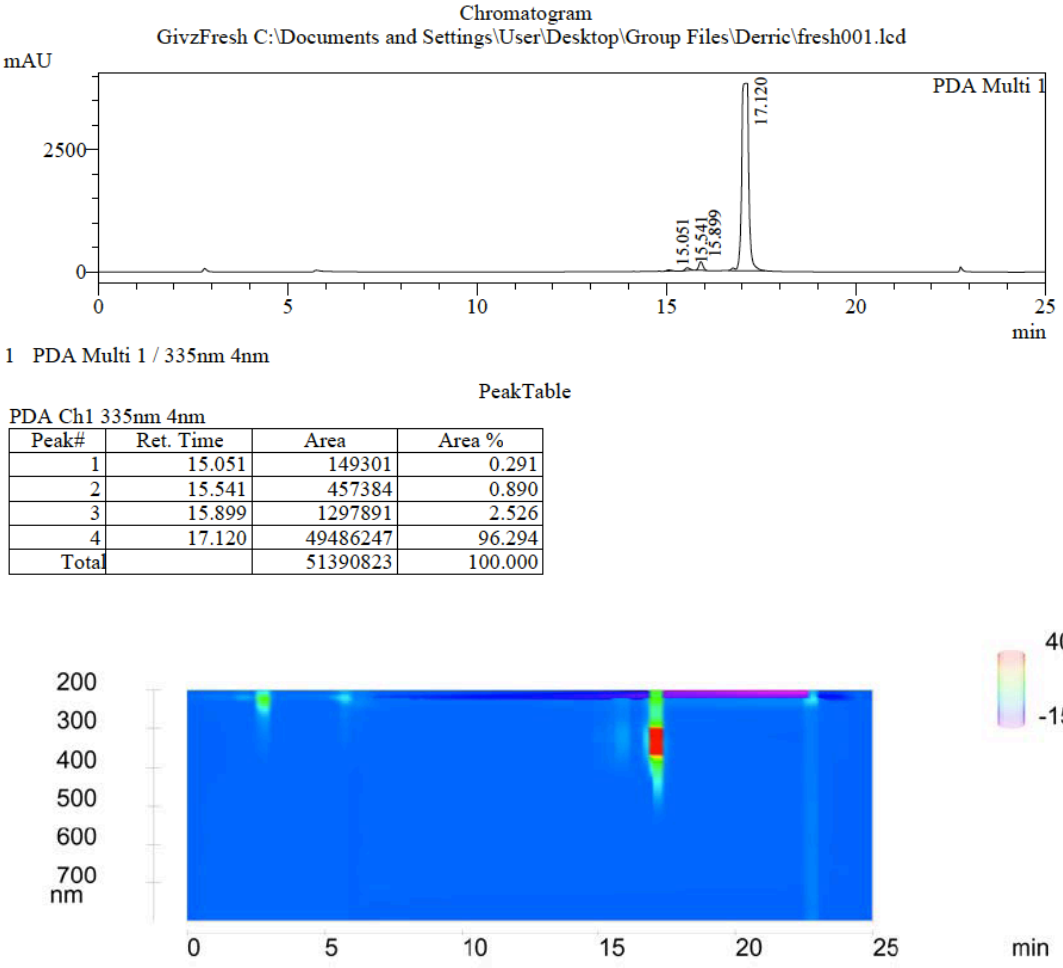

PeakTable

PDA Ch1 335nm 4nm

Peak#	Ret. Time	Area	Area %
1	15.051	149301	0.291
2	15.541	457384	0.890
3	15.899	1297891	2.526
4	17.120	49486247	96.294
Total		51390823	100.000

Figure 1.14: HPLC chromatogram of **1.2** a) using CH_3CN-water (8.4:1.6, v/v) as the mobile phase as determined under acidic conditions (1% v/v TFA) and b) at pH = 9 using (1% v/v TRIS buffer pH 9) in CH_3CN-water (8.4:1.6, v/v).

The hydrolysis products were also analyzed by liquid chromatography-mass spectrometry (LC-MS). Here, two experiments were performed: The first set of reaction was performed in acidic medium using TFA 1% v/v, and the second was carried out using TRIS buffer 1% v/v (pH = 9). The mass assignments observed (m/z = 905, 927,

978, and 1006), correspond to **1.2**, [**1.2** + Na], **1.43**, and [**1.43** + Na] ion peaks (*cf*. Figure 1.15). A single crystal suitable for X-ray diffraction analysis was obtained. It was grown by slow evaporation of a solutions of **1.2** made up in CH_2Cl_2-methanol (1:10, v/v) over a course of two months. In this case, the structure obtained was that of the bis-dipyrromethane tetraaldehyde, **1.42**, (*cf*. Figure 1.16). The remaining solution was evaporated and redissolved in $CDCl_3$ and analyzed by ^1H NMR spectroscopy. The spectrum obtained did not show any signals that could be assigned either to the macrocycle or to the precursors. However, on the basis of the crystal structure obtained, it was assumed that hydrolysis takes place under the crystallization conditions. It is well-known that the formation of the Schiff-base can be facilitated using acidic conditions; however, overly acidic conditions can lead to the protonation of the imine. A nucleophile such as water, is then able to attack the protonated imine inducing the hydrolysis.[28] We speculate that the instability of macrocyle **1.2** under acidic conditions also reflects the strain produced by the rigid strap. However, no independent experimental support for this conclusion is available at present.

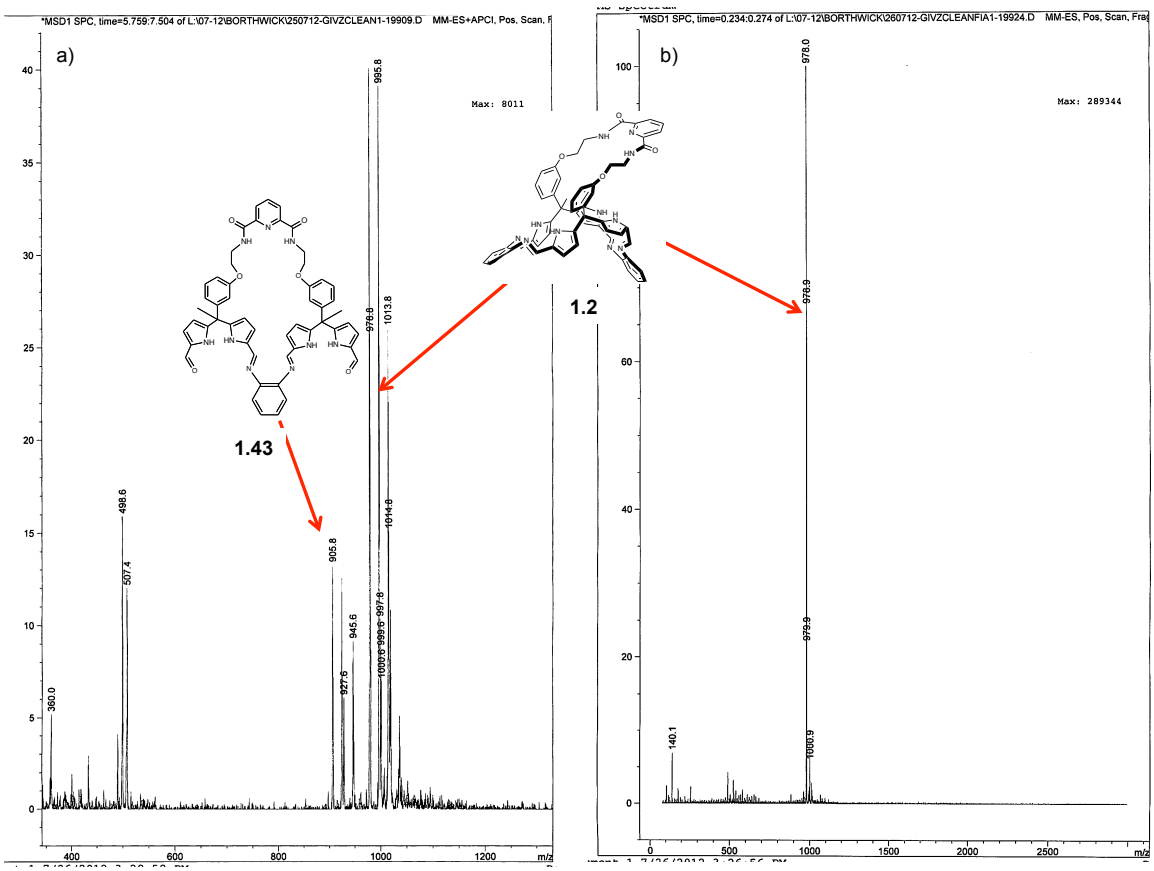

Figure 1.15: Liquid-chromatography mass spectrometric analysis of **1.2** and the hydrolysis products obtained under two different conditions. a) 1% TFA v/v, b) 1% v/v TRIS buffer. The solutions were prepared in CH_3CN-water (8.4:1.6, v/v).

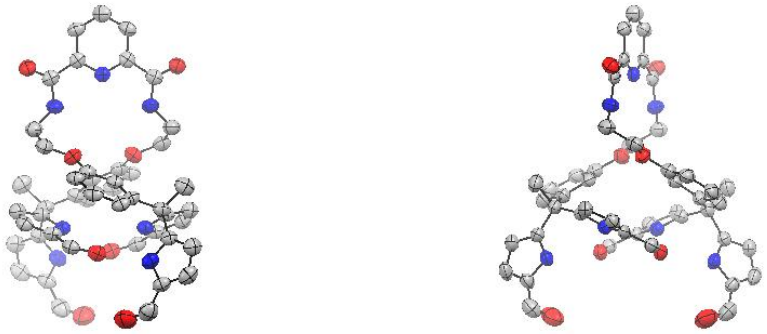

Figure 1.16: Two different views of the single crystal structure of **1.42**. Displayment ellipsoids are scaled to the 50% probability level. The molecule lies on a crystallographic two-fold rotation axis at ¾, ½, z. Atoms with labels appended by "a" are related by 3/2 – x, 1 –y, z. Hydrogen atoms have been removed for clarity.

The above provided a motivation to explore wether modification of the binding site (i.e., by changing the length and the flexibility of the strap) would affect stability. Two strategies were explored in an effort to enhance the stability of the strapped Schiff-base calixpyrrole. The first strategy consisted of preparing an analogue of **1.42** but with an aryl group in the *para* position (compound **1.44**). The second strategy involved the synthesis of a connecting strap containing alkyl chains instead of the aryl groups, persuit of this latter strategy resulted in compounds **1.45**, and **1.46** (*cf*. Figure 1.17). Macrocyclization of the latter straps revealed that only strap **1.46** could give the desired compound **1.3**. In fact, the presence of an extra carbon in the strap resulted in a more stable macrocycle that was obtained in a higher yield than compound **1.2**.

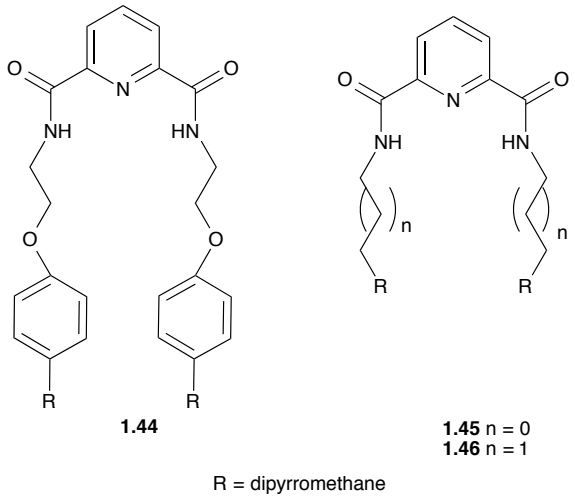

Figure 1.17: Straps **1.44**, **1.45**, and **1.46**.

The strapped macrocycle **1.3** was synthesized according to the synthetic route shown in Scheme 1.6. The synthesis starts with 2-(5-oxohexyl)isoindoline-1,3-dione **1.47**. Reaction of this precursor with pyrrole in the presence of trifluoroacetic acid (TFA) afforded compound **1.48** in 84% yield. Hydrazinolysis of **1.48** gave amino derivative **1.49** in a quantitative yield. Compound **1.49** was reacted with 2,6-pyridinecarbonyl chloride (28% yield) and formylated using the Vilsmeier-Haack method to form **1.46**. Finally, macrocyclization of tetraformyl-**1.46** with *o*-phenylinediamine and subsequent addition of triethylamine afforded macrocycle **1.3** in 43% yield as a pale yellow solid, the compound was used without further purification.

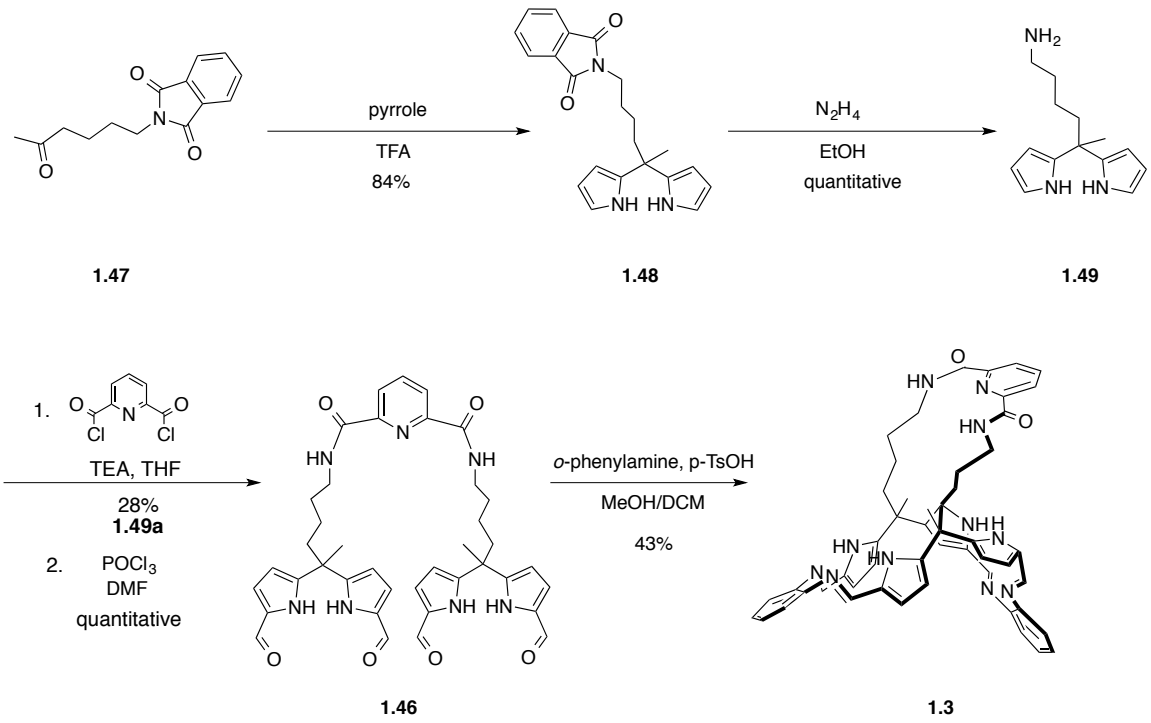

Scheme 1.6: Synthesis of compound **1.3**.

Compound **1.3** was characterized by standard spectroscopic techniques as well as by single crystal X-ray diffraction analysis. A single crystal of the compound **1.3** was obtained by slow evaporation of the reaction mixture consisting of CH_2Cl_2-MeOH (10:1, v/v). The X-ray crystallographic analysis revealed that **1.3** adopts a non-linear, bowl-like conformation around two hydrogen-bonded MeOH molecules in the cavity. A third MeOH molecule is seen in the structure. It interacts with themacrocycle *via* hydrogen bonds with the amide subunits of the strap (*cf*. Figure 1.18). The presence of coordinated methanol molecules within the macrocyclic cavity and interacting with the strap supports the contention that **1.3** can act as a hydrogen-bond donor through interactions between pyrrole NH protons and substrate. In the case of methanol the NH-O distances are N4–O1A 2.915, N7–O1A 2.958, N8–O1B 2.917, N11–O1B 3.176 Å, for the pyrrole NH protons and N1–O1D 3.078, N3–O1D 3.017 Å, for the amide NH protons. Schiff-base

calixpyrroles crystal structures have been obtained previously and revealed the diprotonated forms bind either chloride or *p*-toluensulfonate anions in the cavity. Compound **1.3** crystallized as the free-base form with the methanol molecules interacting with the strap and the macrocycle cavity. To the best of our knowledge, this is the first example of a free-base Schiff-base calixpyrrole crystal. These hydrogen-bonding interactions with methanol provide support for the idea that similar Schiff-base calixpyrroles could be effective anion-binding agents.[20] Also, in the solid state **1.3** was obtained as a single isomer wherein one methyl group in the *meso* position is pointing inside the cavity while the other methyl group is pointing out of the cavity (*cis*). This results in the twist of the strap.

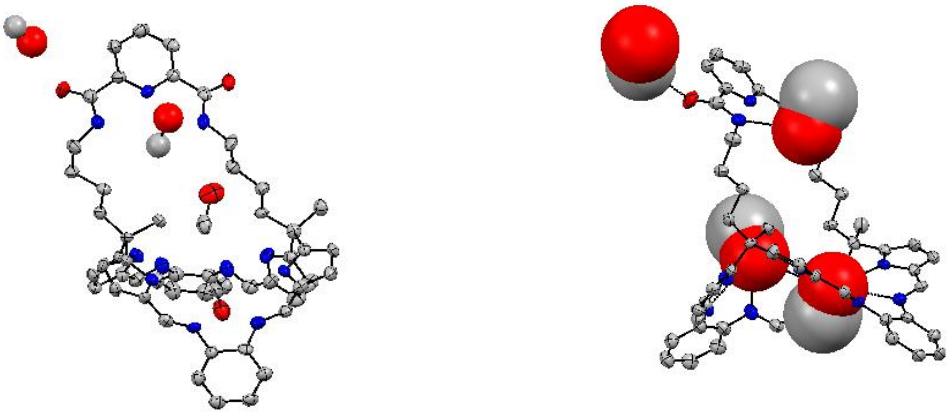

Figure 1.18: Front and side views of the single crystal of the *cis*-strapped Schiff-base calixpyrrole **1.3**•$(MeOH)_4$. Displacement ellipsoids are scaled to the 30% probability level. Hydrogen atoms have been removed from both structural presentations for the sake of clarity.

Unlike amide strapped calix[4]pyrroles that can be obtained as the *cis* and *trans* isomers,[1] compound **1.3** was obtained as a single isomer, the *cis* isomer. This conformation also prevails in solution. ^{1}H NMR spectroscopy of the product obtained by precipitation of **1.3** with trielthylamine from the crude reaction mixture, reveals a spectrum corresponding to only one isomer of **1.3** as shown in Figure 1.19. NMR studies on the remaining liquid after the precipitation did not show any characteristic signals that might reflect the presence of the *trans* isomer.

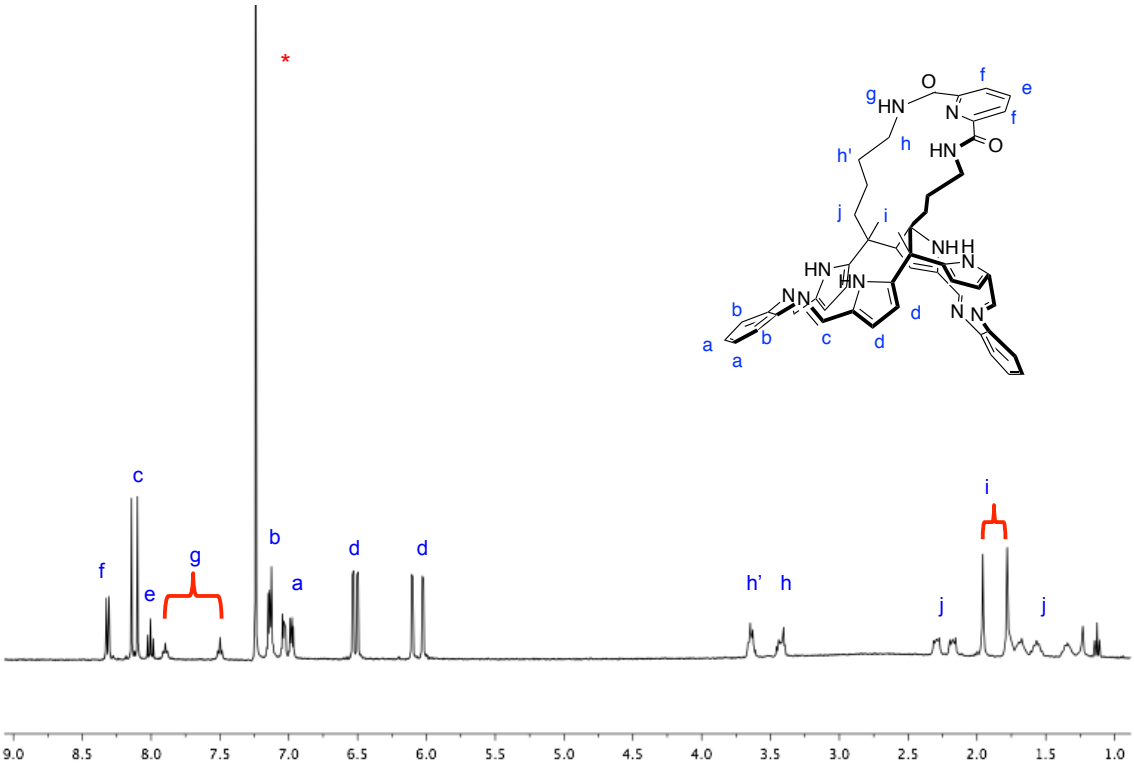

Figure 1.19: ^{1}H NMR spectrum of compound **1.3** recorded in $CDCl_3$. * Denotes peaks ascribed to NMR solvent.

1.6.2 Anion Binding Studies of Compound 1.3

Initial evidence that **1.3** could have an interaction with thorium nitrate ($Th(NO_3)_4$) in solution came from the ^1H NMR spectroscopic analyses shown in Figure 1.18. The titration was carried out in a mixture of $CDCl_3/CD_3CN$ (9.5:0.5, v/v). The NMR spectra revealed that upon addition of increasing quantities of $Th(NO_3)_4$, the protons belonging to the alkyl chain closer to the amide groups in the strap undergo a change in chemical shift from δ = 3.43 to 2.86 ppm (marked as h), while the peaks at 8.00 and 7.50 ppm corresponding to the N-H from the amide groups become broadened (marked as g), Figure 1.20. The peaks corresponding to the macrocycle also become broadened and the peaks corresponding to the β-pyrrolic protons (marked as d) are shifted from δ = 6.52 and 6.06 ppm to 6.98 and 6.23 ppm, respectively. Also, a new broad peak at 8.43 ppm appears after the addition of two equivalents of thorium nitrate. This new peak is attributed to protonation of an imine subunit by H_3O^+ ions present in the solvent, which when the thorium salt comes in contact with water molecules. It is well-known that thorium(IV) is a strong Lewis acid, which in the presence of water releases protons. Although the hydrolytic behavior of Th(IV) in the presence of organic solvents and water has been widely studied, it is complex an still far from fully understood.[28] The hydrolysis of Th(IV) cations is represented in Eq. 1, wherein a proton is transferred from one of the solvent molecules to a molecule of water, giving rise to the hydronium ion (H_3O^+).[28] This led to the assumption that the observed changes in the NMR spectra are due to the protonation of macrocycle **1.3**.

$$mTh^{4+} + rH_2O \leftrightarrow Th_m(OH)_r^{(4m-r)+} + rH_3O^+ \quad \text{Eq. 1}$$

Thus, the addition of a strong acid would produce effects similar to those seen upon the addition of a thorium salt. To test this hypothesis, an ^{1}H NMR titration of **1.3** with trifluoroacetic acid (TFA) was performed. The addition of TFA into a solution of $CDCl_3/CD_3CN$ containing **1.3** gave rise to changes consistent with a complete protonation of the imine subunits after the addition of four equivalents of TFA. This was inferred from the appereance of two broad singlets at δ = 8.81 and 8.78 ppm. The peaks corresponding to the Schiff-base calixpyrrole moiety (marked with the letters c, g, b, a, and d, in Figure 1.21) showed similar chemical shift patterns as the titration with $Th(NO_3)_4$ (Figure 1.20). This led to the conclusion that in the presence of thorium(IV) cations protonation of the imine groups present in **1.3** takes place. However, the peaks corresponding to the C-H protons of the alkyl chain in the strap did not show any shift upon the addition of TFA. This was taken as evidence tha the trifluoroacetate anion does not interact with the strap. Unfortunately, the precipitation of **1.3** was found to take place during course of the titration. This made it difficult to follow the peaks corresponding to the N-H amide protons.

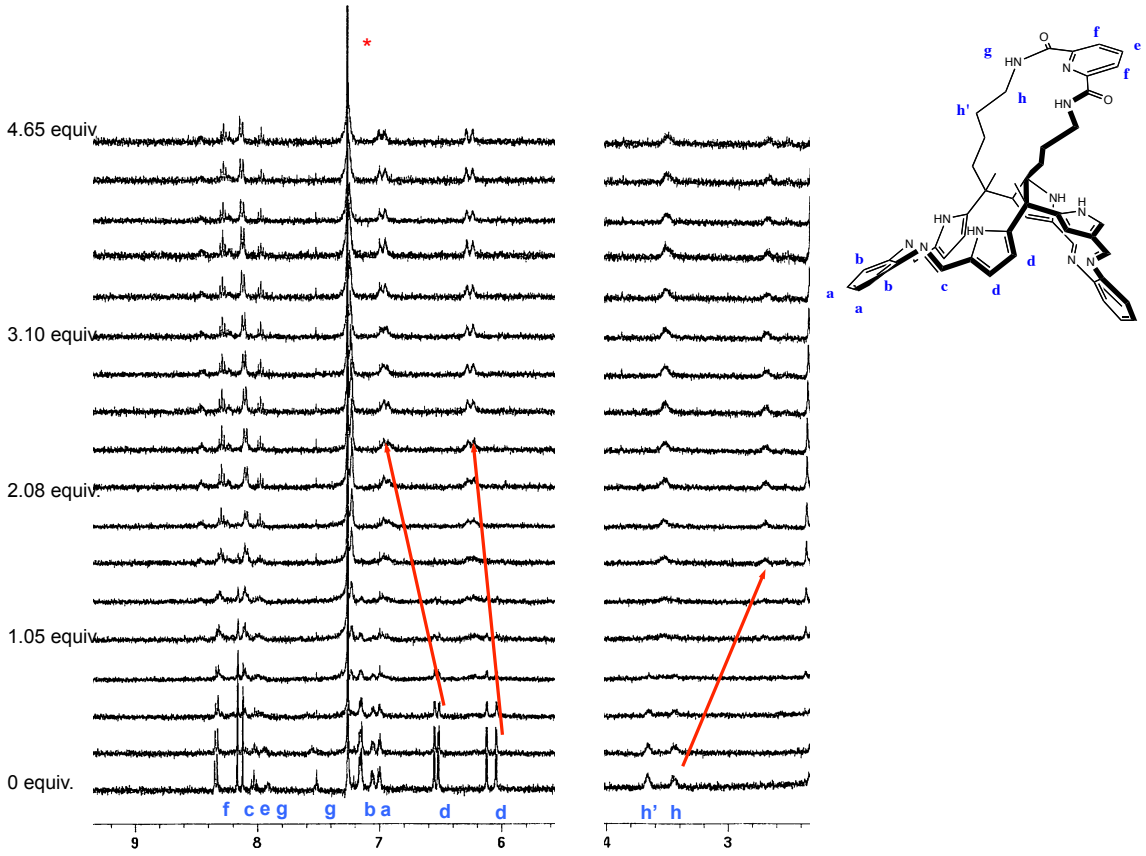

Figure 1.20: Partial ^{1}H NMR spectra for the titration of **1.3** with $Th(NO_3)_4$ in $CDCl_3/CD_3CN$ (9.5/0.5, v/v). The solution was prepared by mixing **1.3** (1.15×10^{-3} M) dissolved in $CDCl_3$ with $Th(NO_3)_4$ (0.176 M) in CD_3CN. * Denotes peaks ascribed to the NMR solvent.

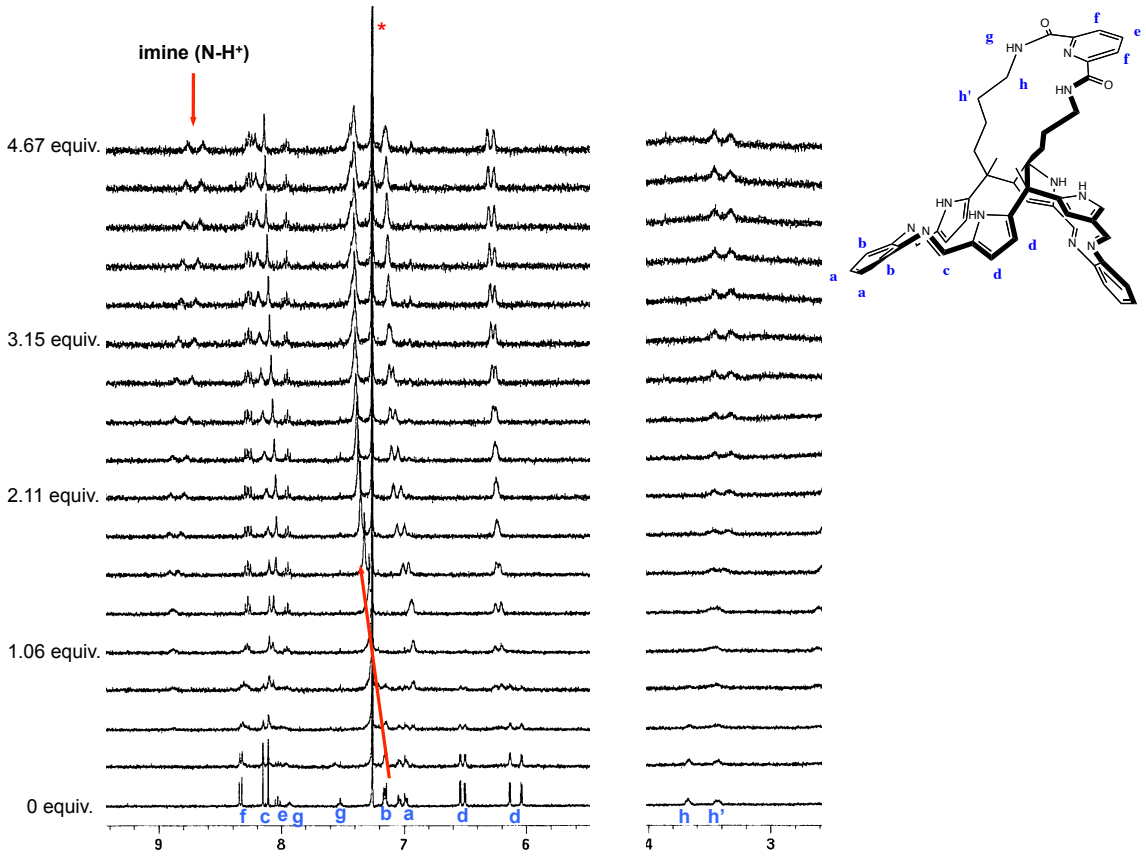

Figure 1.21: Partial ^{1}H NMR spectra for the titration of **1.3** with TFA in $CDCl_3/CD_3CN$ (9.5/0.5, v/v). The solution was prepared by mixing (1.15×10^{-3} M) dissolved in $CDCl_3$ with TFA (0.165 M) in CD_3CN. * Denotes peaks ascribed to the NMR solvent.

Further anion binding studies using ^{1}H NMR sprectoscopy revealed that the nitrate anion (as tetrabutylammonium (TBA) salt), produce a small shift in the signal corresponding to one amide group in the strap in **1.3**. As shown in Figure 1.22, the anion-free form of **1.3** displays two sets of broad triplets for the amide protons (marked with the letter g) at δ = 7.90 and 7.50 ppm. Upon the addition of 3.5 equivalents of $TBANO_3$, one of the amide peaks becomes broadened, while the other shifts from δ = 7.50 to 8.00 ppm.

However, none of the other peaks underwent a change in the presence of nitrate anions. These observations are consistent with the conclusion that the nitrate anion interacts only weakly with the strap but not with the cavity of the macrocycle. In fact, the interaction of the nitrite anion with the strap is thought to be similar to what is seen in the crystal structure wherein methanol is held in place *via* a hydrogen bond with only one of the amide groups of the strap. UV-vis titrations of **1.3** in the presence of $TBANO_3$ revealed that there is no appreciable change in the absorbance that could indicate a strong interaction of the nitrate anions with the strap. This was also confirmed by isothermal titration calorimetry (ITC). wherein no isotherm indicative binding was observed.

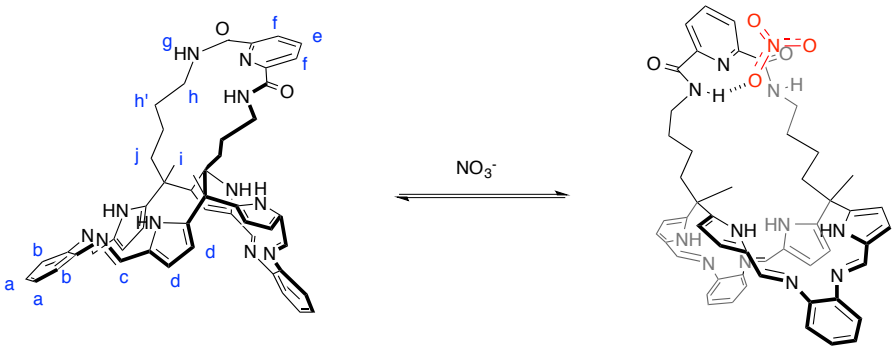
NO3-

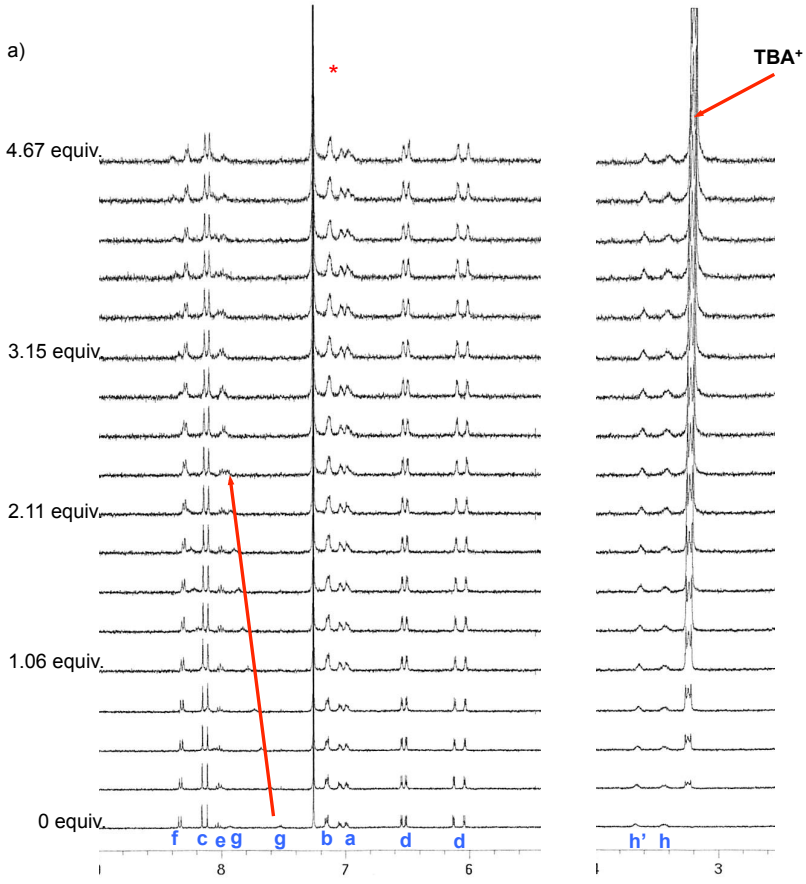
a)
TBA+
4.67 equiv.
3.15 equiv.
2.11 equiv.
1.06 equiv.
0 equiv.
f c e g g b a d d
h' h
8
7
6
3

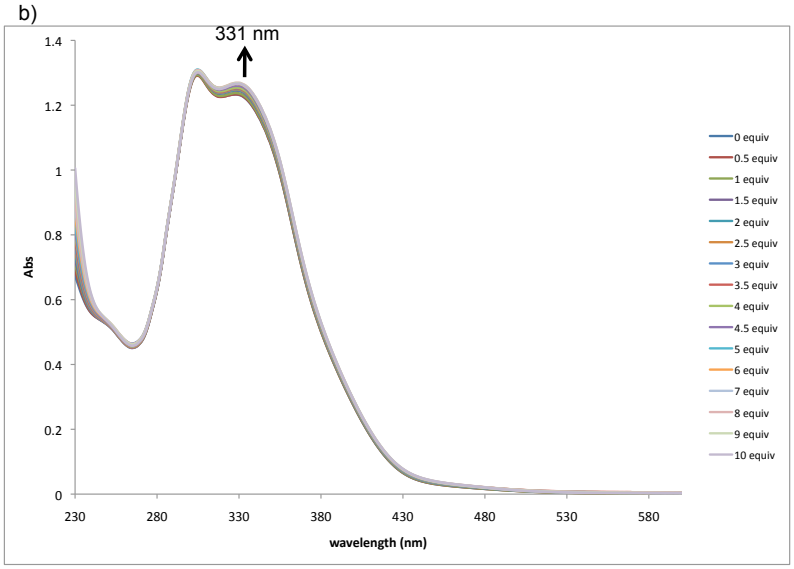

Figure 1.22: a) Partial ^{1}H NMR spectra for the titration of macrocycle **1.3** with $TBANO_3$ in $CDCl_3/CD_3CN$ (9.5/0.5, v/v). The solution was prepared by mixing **1.3** (1.15×10^{-3} M) dissolved in $CDCl_3$ with $TBANO_3$ (0.165 M) in CD_3CN. * Denotes peaks ascribed to the NMR solvent. b) Absorption spectra corresponding to the titration of **1.3** (2.5×10^{-3} M) with $TBANO_3$ (0.15 M) in $CHCl_3$.

Contrary to what was observed in the case of **1.2**, macrocycle **1.3** displays a relative higher stability upon protonation of the imine groups. Hence, the formation of positive charged species from **1.3** could enhance the affinity for anions. In previous anion binding studies performed by our group on the unstrapped Schiff-base calixpyrrole, high affinities for chloride anions were observed when the macrocycle was protonated. This was attributed to the presence of electrostatic interactions that favored anion binding.[20] Thus, UV-Vis and ITC studies of the mono-, di-, and the tetraprotonated forms of **1.3** were carried out in the presence of different anions, such as Cl^-, $H_2PO_4^-$, and NO_3^-, in CH_3CN. To obtain the protonated forms of **1.3**, the free base form was protonated by adding one, two, or four equivalents of TFA. As can be seen from inspection of Figure 1.21, ITC analysis revealed that the addition of chloride anions to the monoprotonated

form of **1.3** is endothermic. Unfortunately, attempts to fit the heat changes curve were unsuccessful using a 1:1 receptor-to-anion binding model. ITC studies of the diprotonated form of **1.3** did not present any isotherm that could be considered reflective of binding chloride anions. Nor was there any evidence of nitrate anion binding as inferred from the ITC analysis. On the other hand, the ITC curves associated with the addition of $H_2PO_4^-$ anions (as their TBA salts) to the tetraprotonated form of **1.3** revealed a binding profile corresponding to a 1:1 receptor-to-anion ratio with an association constant K_a = 2.87 × 10^4 M^{-1} (*cf*. Figure 1.23).

a)

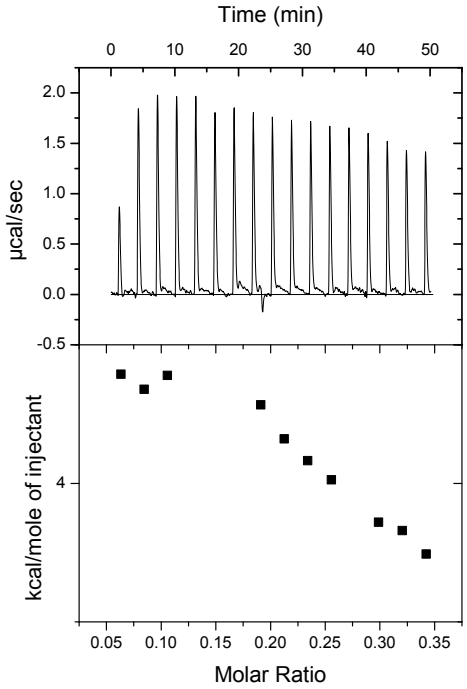

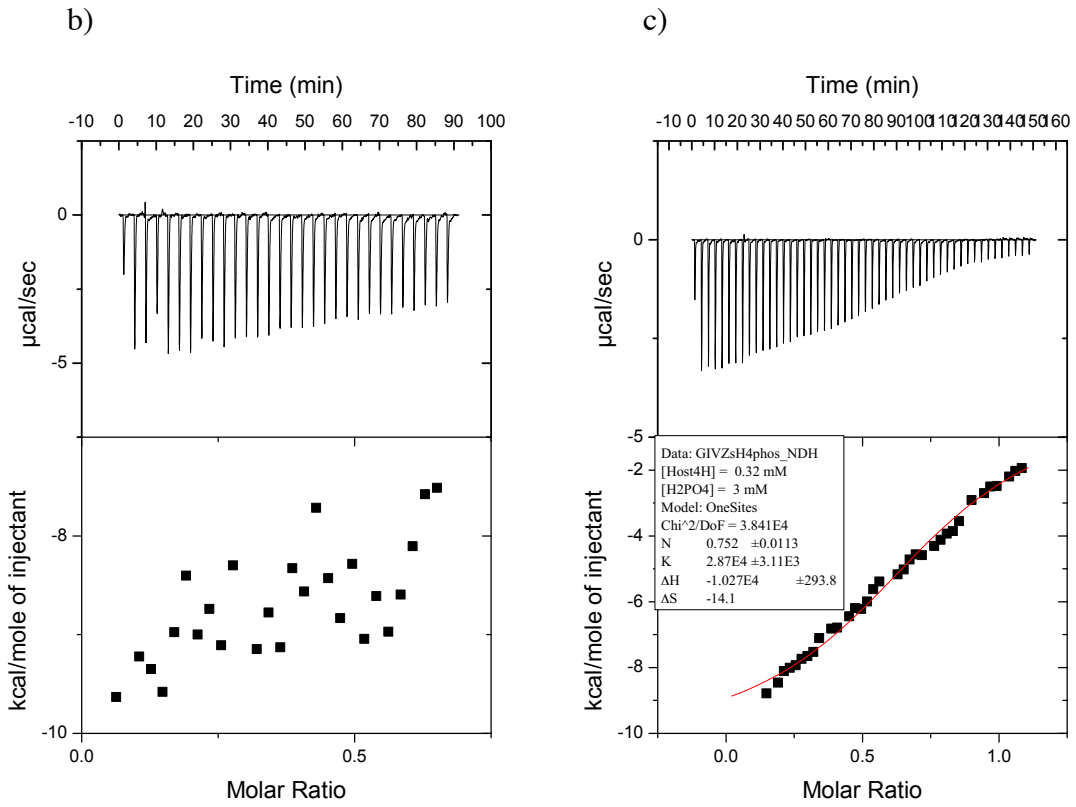

Figure 1.23: ITC traces observed upon the addition of a) TBACl to the monoprotonated form of **1.3** (0.32 mM), b) $TBAH_2PO_4$ to the monoprotonated form of **1.3** (0.32 mM), and c) $TBAH_2PO_4$ to the tetraprotonated form of **1.3** (0.3 mM). All the titrations were performed using acetonitrile as the solvent and were carried out at 298 K.

1.6.3 Strapped Sciff-base Calixpyrrole Metal Complexes

The synthesis of the metal complexes **1.50**-**1.53** is outlined in Scheme 1.7. With exception of **1.53**, the preparative procedure starts with the reaction between **1.3** and 2.2 equivalents of the metallic salt in the presence of NEt_3 or KH; this results in the formation of the corresponding binuclear metal complex in 23-57% yield. Compound **1.53** was synthesized by reacting $[RuCp^*(CH_3CN)_3][PF_6]$ (Cp* = pentamethylcyclopentadienyl) and **1.3** under inert atmosphere in dry CH_2Cl_2 without base. After completion of the reaction, the metal complex was exposed to air and **1.53** was obtained in a 4.3% yield after purification by column chromatography. The metal complexes were characterized by standard spectroscopic techniques unless otherwise indicated as well as by single crystal X-ray diffraction analysis in the case of compound **1.53**. The ^1H NMR spectra of **1.50** and **1.51** revealed a lack of pyrrolic NH peaks, as well as resonances the hydrogens close to the imine that shifted to lower field (i.e., the imine chemical shift for **1.50**, and **1.51** in $CDCl_3$ moves from δ = 8.14 and 8.10 ppm to 7.32 and 7.30 ppm, and 7.15 and 7.12 ppm, respectively). These spectral changes are taken as evidence of cation coordination to the macrocycle (*cf*. Figure 1.24).

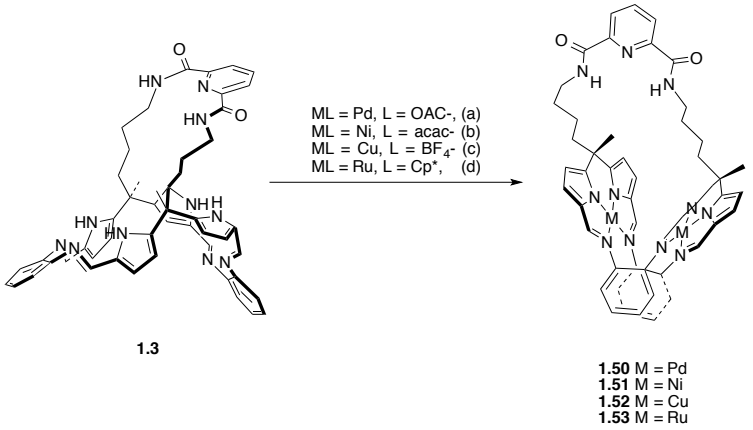

Scheme 1.7: Synthesis of compounds **150**-**1.53**. Conditions: (a) $Pd(OAc)_2$, NEt_3, CH_2Cl_2; (b) $Ni(acac)_2$, NEt_3, $C_2H_4Cl_2$, 60 ºC; (c) $Cu(BF_4)_2 \bullet xH_2O$, NEt_3, CH_2Cl_2-MeOH; (d) $[RuCp^*(CNCH_3)_3][PF_6]$, Ar, CH_2Cl_2.

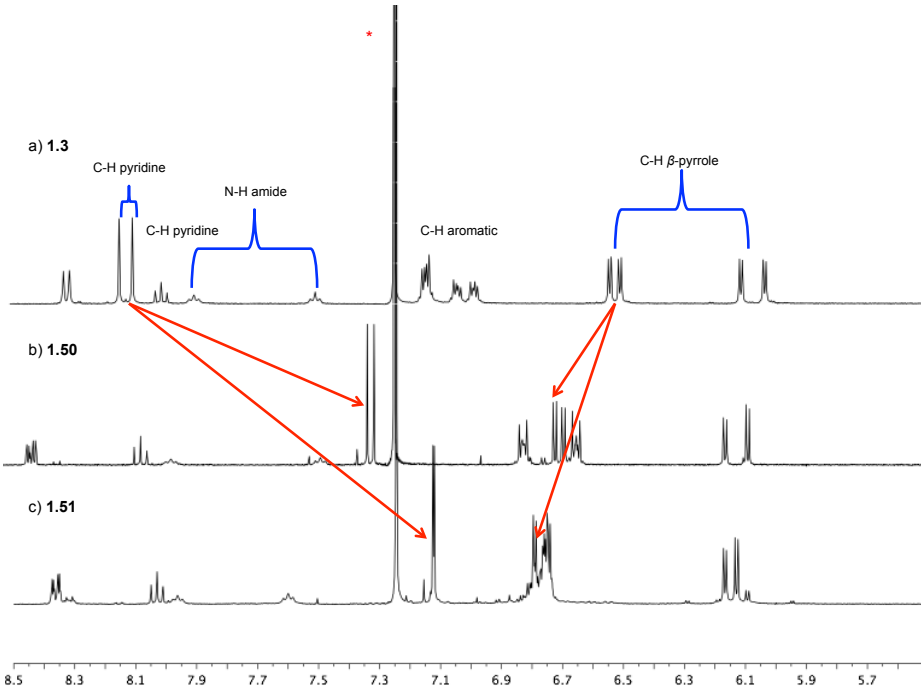

Figure 1.24: ^{1}H NMR spectra for a) compound **1.3**, b) Pd(II) complex **1.50**, and c) Ni(II) complex **1.51** in $CDCl_3$. * Denotes peaks ascribed to the NMR solvent.

A single crystal of **1.50** suitable for X-ray crystallographic analysis was obtained by slow evaporation of THF. As shown in Figure 1.25, the resulting structure revealed a bimetallic complex wherein the two metal centers (Pd1 and Pd2) reside in approximately square-planar N_4-pyrrole-imine donor environments. The sum of the angles are 224.27° and 298.01° at P1 and P2 respectively. These values stand in contrast to what has been observed in other Pd complexes of Schiff-base calix[4]pyrroles (sum of angles ≈ 359.9° at both Pd centers).[29] This difference is attributed to the inherent conformation of the macrocycle, which forces the metal complex to be twisted. This results in a smaller cavity in which the palladium centers reside. The individual N-Pd-N bond angles in complex **1.50** are between 79.75°-110.69°. Here the largest angles are between the palladium atom and two imine nitrogen atoms. These angles are comparable to what is observed for the

palladium(II) complexes of the unstrapped Schiff-base calixpyrrole.[29] Gross structural parameters including the Pd•••Pd separation (3.680 Å), Pd-N-imine, and Pd-N-pyrrole distances (for Pd1 and P2 Pd-Nimine = 2.029 and 2.071 Å, and 2.027 and 2.063 Å, respectively), and vertical bite angles, θ, between the PdN_4 planes (θ = 60.36º) for **1.3** can be compared to those of similar complexes described elsewhere for unstrapped Schiff-base calixpyrroles.[21, 29]

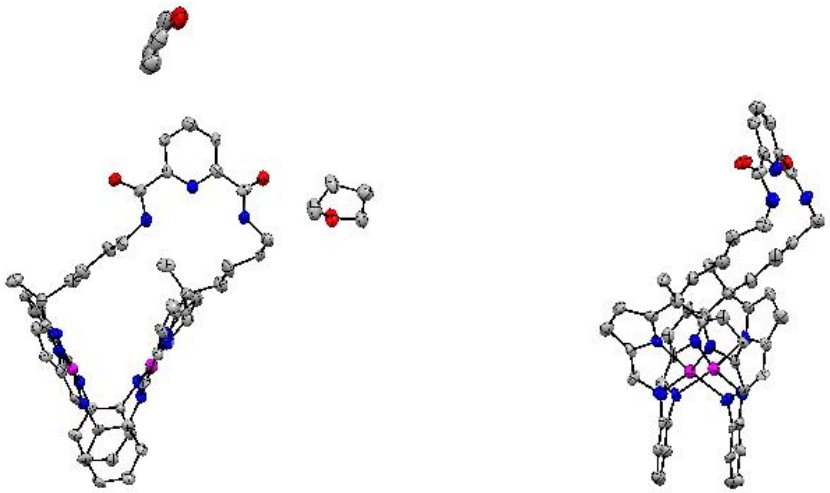

Figure 1.25: Two different views of the single crystal of **1.50•**$(THF)_2$. Displacement ellipsoids are scaled to the 50% probability level. Hydrogen atoms have been removed from both structures (front and side views) for clarity, as have molecules of tetrahydrofuran (THF). All solvent molecules have been removed from the side view.

Compound **1.52** was characterized by high-resolution mass spectrometry, infrared spectroscopy (IR), and magnetic measurements. A comparison of the IR spectrum of the free ligand **1.3** with that of the copper complex **1.52** revealed distinguishable differences ascribed to the coordination of the Cu(II) within the N_4-cavity. The shift in the imine

stretching bands ($\nu_{C=N}$) from 1666 cm^{-1} for **1.3** to 1599 cm^{-1} for the Cu(II) complex **1.52** can be explained by a "locking" of the conformation in the cavity after the complexation of the metal cation occurs. Differences are also seen in the modes corresponding to the amide groups in the strap in **1.3**, and **1.52**. The $\nu_{C=O}$ stretch shifts from 1610 cm^{-1} to 1561 cm^{-1}, on goinf from **1.3** to **1.52**. The corresponding amide bending mode signal shift from ν_{N-H} = 1539 cm^{-1} to 1467 cm^{-1}, in going from **1.3** to **1.52** (*cf*. Figure 1.26).

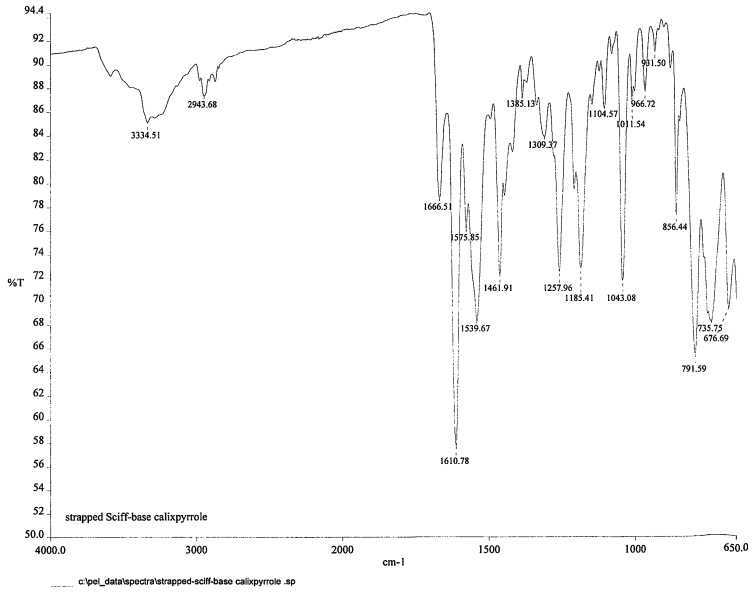

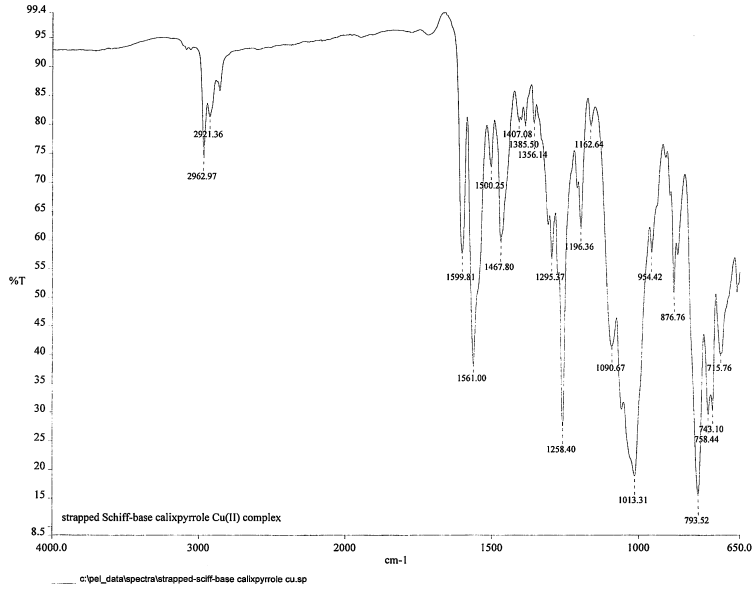

Figure 1.26: IR spectra of **1.3** (top) and **1.52** (bottom).

The magnetic moment (μ_{eff}) of **1.52** was determined at room temperature in deuterated chloroform using the Evans method as described in detailed in Apendix B.[30-32] The magnetic moment obtained at two different concentrations (10.3 and 20.6 mM) provided an average value of μ_{eff} = 2.12 μ_B. Compared with the value for two isolated Cu(II) metal center (S = ½) based on the literature (μ_{eff} = 2.45 μ_B),[30] the μ_{eff} value of **1.52** is lower. However, lower values of μ_{eff} similar to what was obtained for **1.52** have been reported for binuclear copper complexes of Schiff-base calixpyrrole (μ_{eff} = 2.45 μ_B).[21, 33] In this case, the relative low values of μ_{eff} (compared to two isolated Cu(II) centers) was ascribed to a weak antiferromagnetic coupling between the metal centers. This could be the reason why **1.52** displays a lower value of magnetic moment. However, studies of

magnetic susceptibility in the solid state need to be carried out to confirm this latter hypothesis.

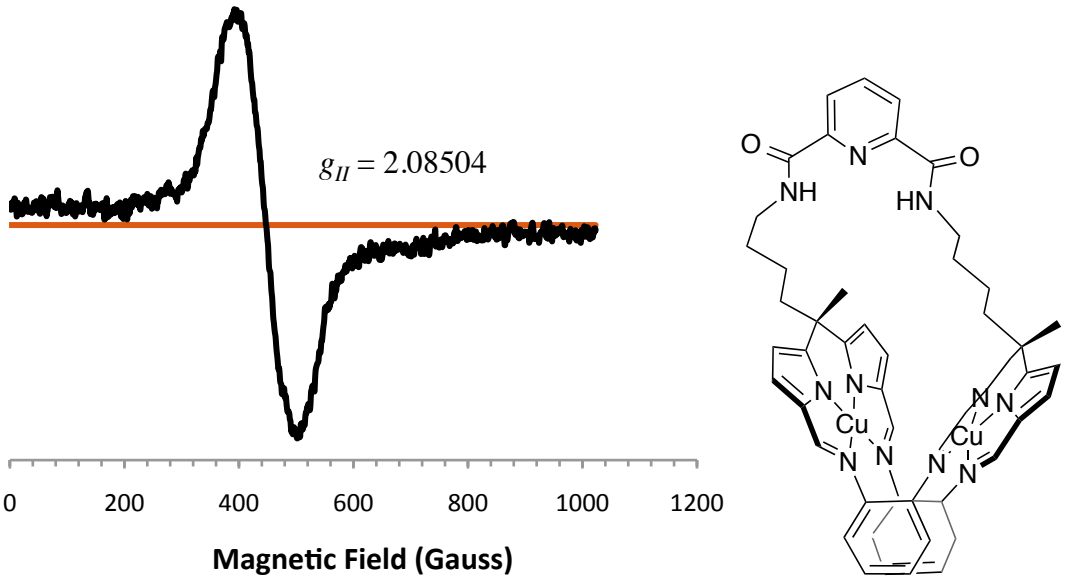

Figure 1.27: EPR spectrum of **1.52**. The spectrum was recorded at room temperature using a solution of the binuclear complex in CH_2Cl_2 (0.5 mM).

The EPR spectrum of **1.52** is shown in Figure 1.27. This spectrum was recorded in dichloromethane at room temperature on a Bruker EMX Plus spectrometer. The microwave frequency (~ 9.5 GHz) and magnetic fields were measured with a Gaussmeter Bruker ER083CS, and the magnetic fields were calibrated using a standard sample made of 2,2-diphenyl-1-picrylhydrzyl (DPP) that has a characteristic *g* value of 2.0036. As shown in Figure 1.27, the EPR spectrum of **1.52** is characterized by a slightly more positive deviation of *g* value (g = 2.08504) than that expected for species with one unpaired electron (S = ½, g = 2.0023).[36] However, the *g* value obtained was lower than that seen for typical square planar Cu(II) complexes (e.g., Cu(II)-etioporphyrin, g =

2.1693).[36, 37] This could be attributed to a non-perfect square planar coordination geometry in the case of **1.52**. Under the experimental conditions employed, no hyperfine values (*A*) could be measured. This lack of hyperfine features is attributed to two main factors: 1) the copper centers being coordinated in a distorted square geometry, and 2) the metal centers binding solvent molecules, such as, water molecules present as impurities in the solvent.

1.6.4 Anion Binding Studies of Compounds 1.50 and 1.52

Metal-containing anion receptors have been a subject of interest in recent years. This is due to the advantage that the metal center provides in the binding of anionic species. First, the metal center organizes anion binding groups in a specific geometry for the recognition of a specific anion. And second, the elestrostatic interactions between the Lewis acidic metal center and the anionic species can promote the binding event.[33-35] Considering this principle, anion binding studies of the bimetallic compounds **1.50** and **1.52** were carried out using ^{1}H NMR and UV-Vis spectroscopy, as well as isothermal titration calorimetry (ITC).

The ^{1}H NMR spectroscopic studies of **1.50** were performed by adding increasing quantities of different anions, such as, Cl^-, CN^-, and $H_2PO_4^-$ in the form of their tetrabutylammonium (TBA) salts. As shown if Figure 1.28, upon the addition of the Cl^-, CN^-, and $H_2PO_4^-$ anions no chemical shift was observed. This is taken as evidence that neither the strap nor the Pd metal centers interacts appreciably with the anions. This could reflect the lack of sufficient space in the twisted strap to accommodate an anion in the case of this metal complex. In the case of the ^{1}H NMR spectrum, the amide N-H protons in **1.50** disappeared upon the addition of CN^- anions (*cf*. Figure 1.26). This was attributed to either a deprotonation of the amide in the presence of this anion, or proton exchange in the solvent used ($CDCl_3$).

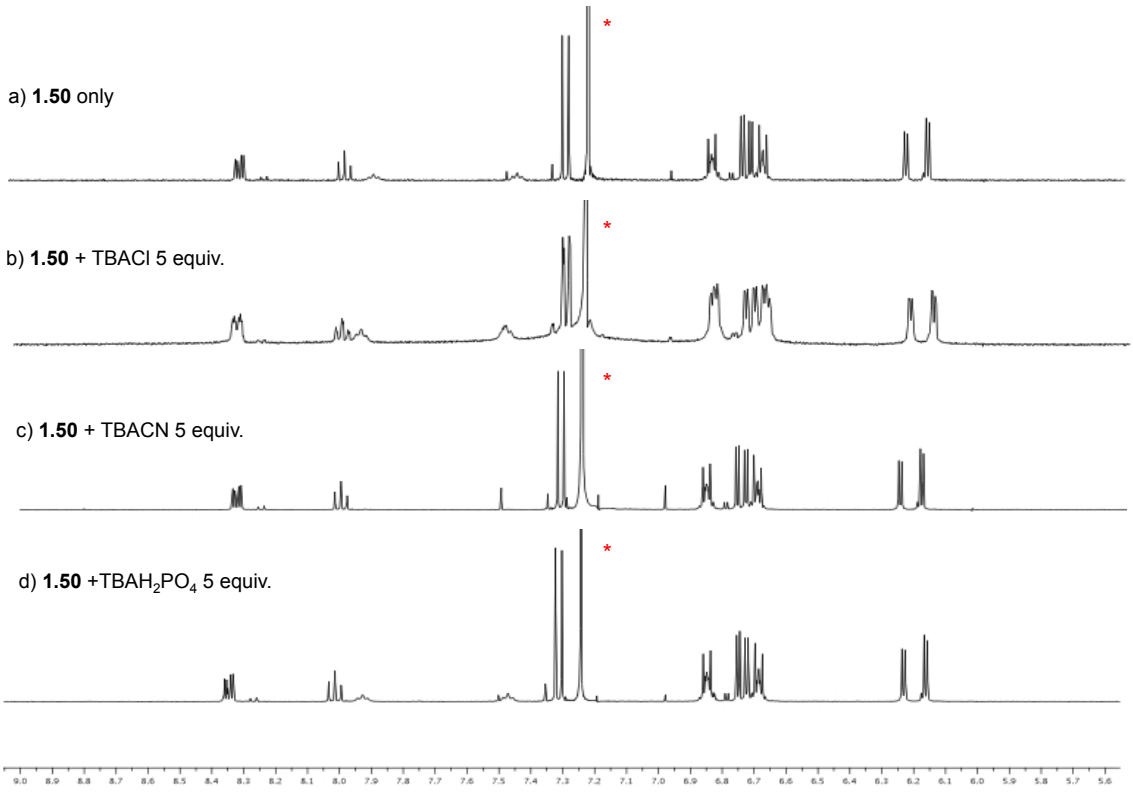

Figure 1.28: Partial ^{1}H NMR spectra of **1.51** recorded in the presence of TBACl, TBACN, and TBANO$_3$ in CDCl$_3$. The solution was prepared by mixing **1.51** (2.15×10^{-3} M) dissolved in CDCl$_3$ with 5 equiv of Cl^-, CN^-, and NO_3^- as their correspondingTBA salts dissolved in CDCl$_3$. * Denotes peaks ascribed to the NMR solvent.

^{1}H NMR spectroscopy did not give any conclusive evidence as to whether the cyanide anion interacts with the Pd metal centers. To obtain further insights, ^{105}Pd NMR analysis was introduced. Unfortunately, due to the low frequency of ^{105}Pd relative to ^{1}H (100 MHz),[38] the NMR facilities at The University of Texas at Austin proved inadequate to the task. An alternative means of assessing whether there is a deprotonation of the amide protons in the palladium complex or a proton exchange in deuterated chloroform involves the use of ^{13}C NMR spectroscopy. In this case, it was proposed that the carbon of the amide group would experience a chemical shift change, if deprotonation of the

amide group were taking place upon the addition of the CN^- anion. The ^{13}C NMR spectra, the signals of **1.50** and **1.50** in the presence of CN^- anions, the carbons peaks of the amide do not display any chemical shift change, which provides support for the proposition that a proton exchange took place. Furthermore, addition of H_2O to the tube containing **1.50** and CN^- in deuterated chloroform restored the amide N-H protons signals at δ = 7.93 and 7.47 ppm (*cf*. Figure 1.29).

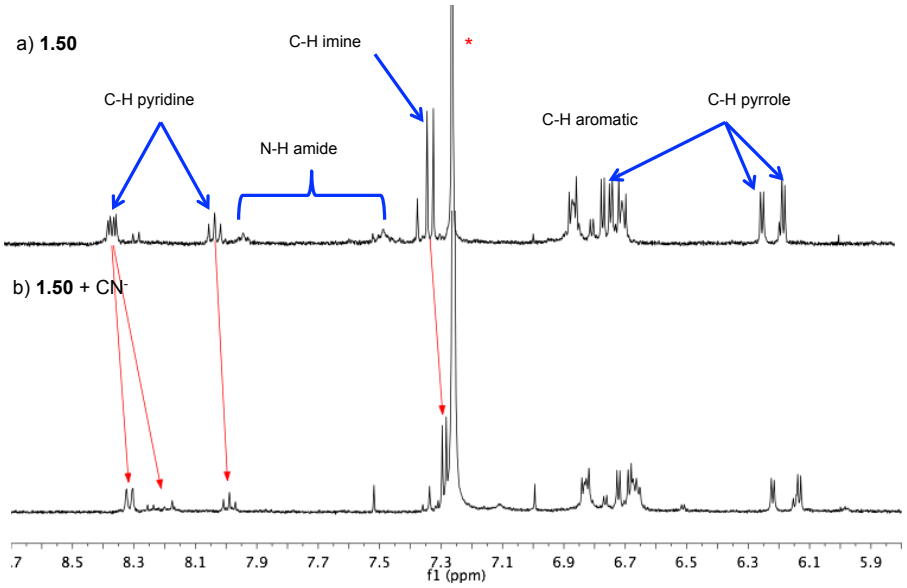

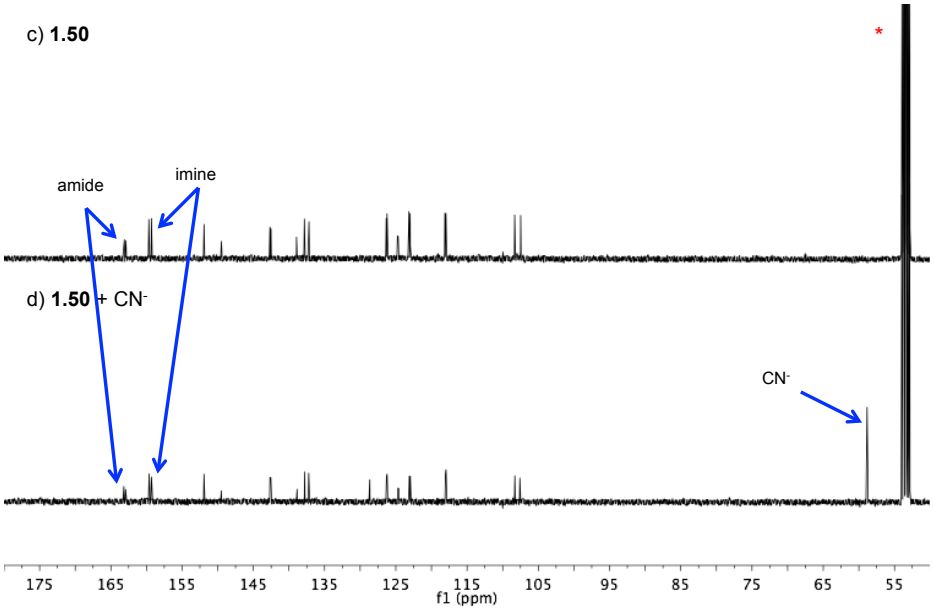

Figure 1.29: Partial NMR spectra of **1.50**, and **1.50** + CN^- (TBA salt). ^1H NMR spectra in $CDCl_3$ of a) **1.50**, and b) **1.50** after the addition of CN^- anions in the form of tetrabutylammonium salt (TBA). ^{13}C NMR spectra in $CDCl_3$ of c) **1.50**, and d) **1.50** after the addition of CN^- anions. The solution was prepared by mixing **1.50** (2.21 mM) dissolved in $CDCl_3$ with 2 equiv of TBA salt in $CDCl_3$. * Denotes peaks ascribed to the NMR solvent.

The idea that the cyanide anion interacts with the Pd metal centers was discarded on basis of the NMR spectral analysis (^1H and ^{13}C). For instance, the ^1H and ^{13}C NMR spectra of **1.50** and **1.50** + CN^- were essentially identical. Specifically, the signals corresponding to the carbon adjacent to the imine –CH=N- that would be more susceptible to the interaction of cyanide anions resonated at δ = 7.33 and 7.31, and 7.32 and 7.30 ppm, respectively (^1H NMR spectra in $CDCl_3$), and δ = 159.6 and 159.3, 159.7 and 159.3 ppm, respectively (^{13}C NMR spectra in CD_2Cl_2) remained unchanged (*cf.* Figure 1.29).

IR spectroscopy performed on **1.50**, shown in Figure 1.30, revealed that upon addition of CN^- anions the signals ascribed to the imine stretching ($\nu_{C=N}$) showed an appreciable shift, from 1666 cm^{-1} to 1661 cm^{-1}. The carbonyl stretching signals ($\nu_{C=O}$) of

the amide groups in the strap shifted from $\nu_{C=O}$ = 1541 cm^{-1} to 1612 cm^{-1}. The bands corresponding to the N-H bending frequencies (ν_{N-H}) shifted from 1470 cm^{-1} to 1556 cm^{-1}. These observations lead to the conclusion that there is an interaction between the **1.50** and CN^- anions. We assume that these interactions could be between the strap and the metal centers.

a)

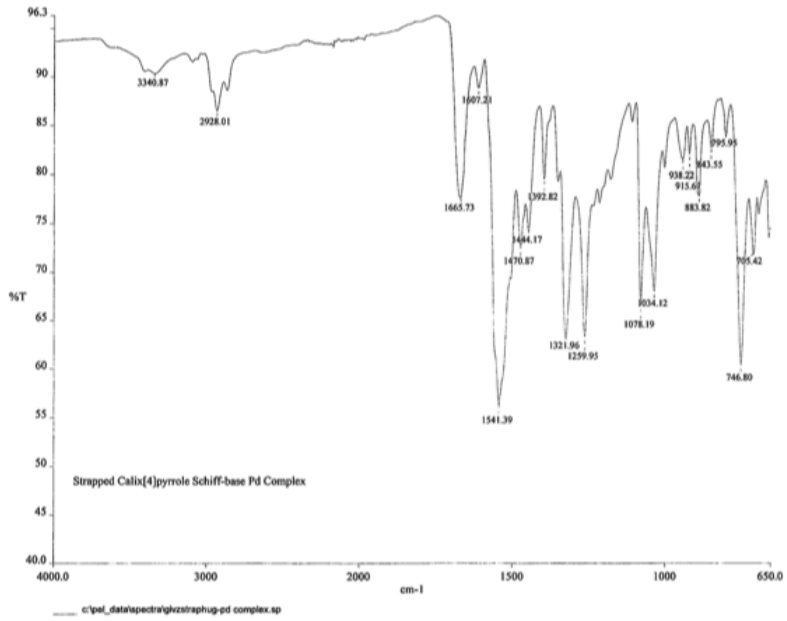

b)

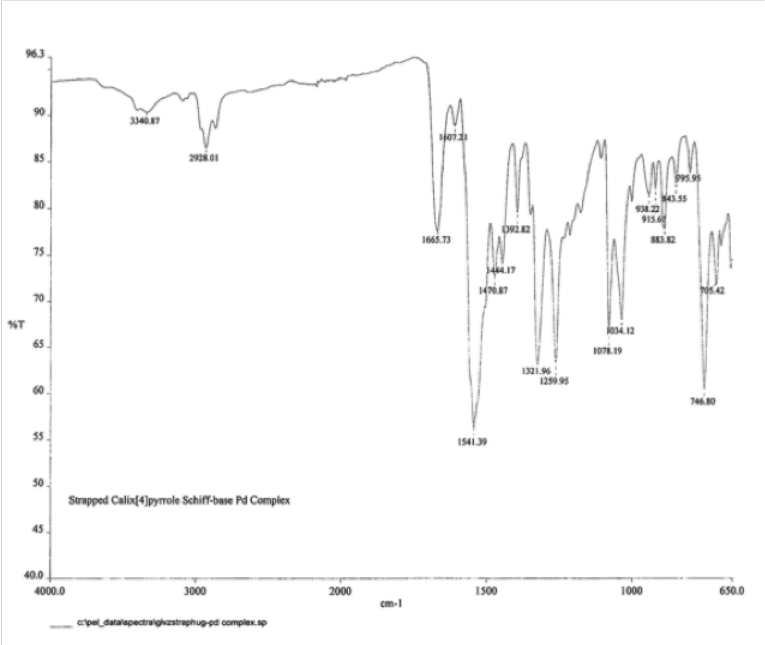

c)

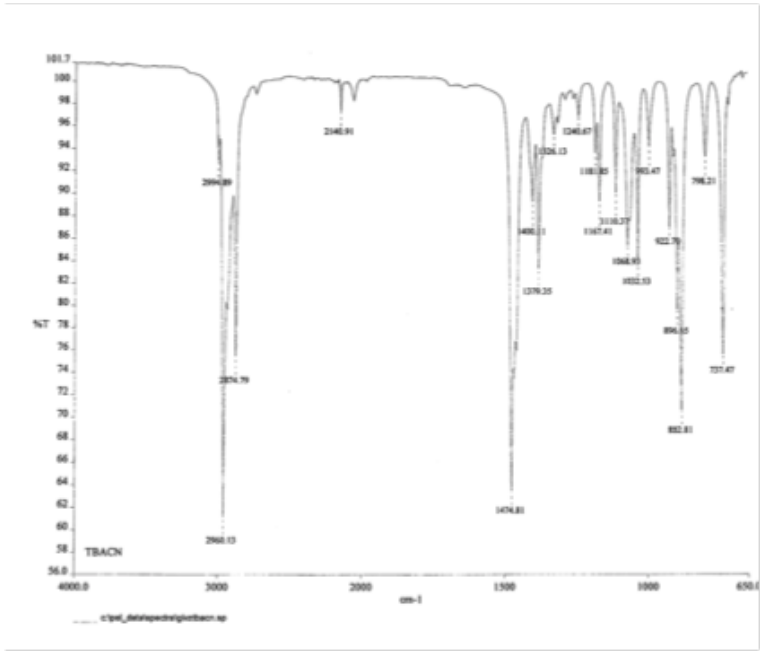

Figure 1.30: IR spectra of a) **1.50**, b) **1.50** upon addition of TBACN, and c) TBACN.

ITC analysis in acetonitrile revealed that upon addition of CN^- ions to **1.50** the isotherm obtained fitted to a 1:1 receptor-to-anion binding profile, with an association constant $K_a = 3.65 \times 10^5\ M^{-1}$. To determine if the binding takes place primarily on the strap or within the macrocycle, control studies using unstrapped calixpyrrole Schiff-base palladium(II) complex **1.50** and a strap fragment (Bis-dipyrromethane tetraaldehyde) **1.46** were carried out. In this case, the ITC isotherm obtained for compound **1.54** displayed a fit corresponding to a 1:1 receptor-to-anion binding profile. As shown in Figure 1.31, the association constant obtained for the unstrapped Schiff-base palladium complex, $K_a = 9.36 \times 10^3\ M^{-1}$, revealed that **1.54** binds cyanide anions; however, the introduction of the strap to the Schiff-base calixpyrrole enhances the binding of cyanide anions more than two orders of magnitude. ITC studies using the calixpyrrole-free strap **1.46** also revealed an interaction with CN^-. Unfortunately, the ITC traces could not be fitted using the 1:1 or 1:2 receptor-to-anion profile. On the other hand, titrations of **1.52** with TBACN in acetonitrile resulted in an isotherm that is consistent with some modest interaction with cyanide anions. However, the ITC profiles proved to complex to be fitted using either 1:1 or a 1:2 receptor-to-anion model (*cf.* Figure 1.31). Anion binding properties of compounds **1.51** and **1.53** could not be performed due to instability of the componds in acetonitrile.

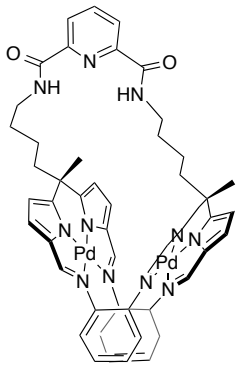

1.50

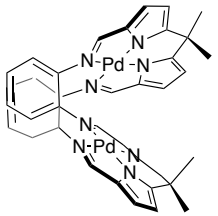

1.54

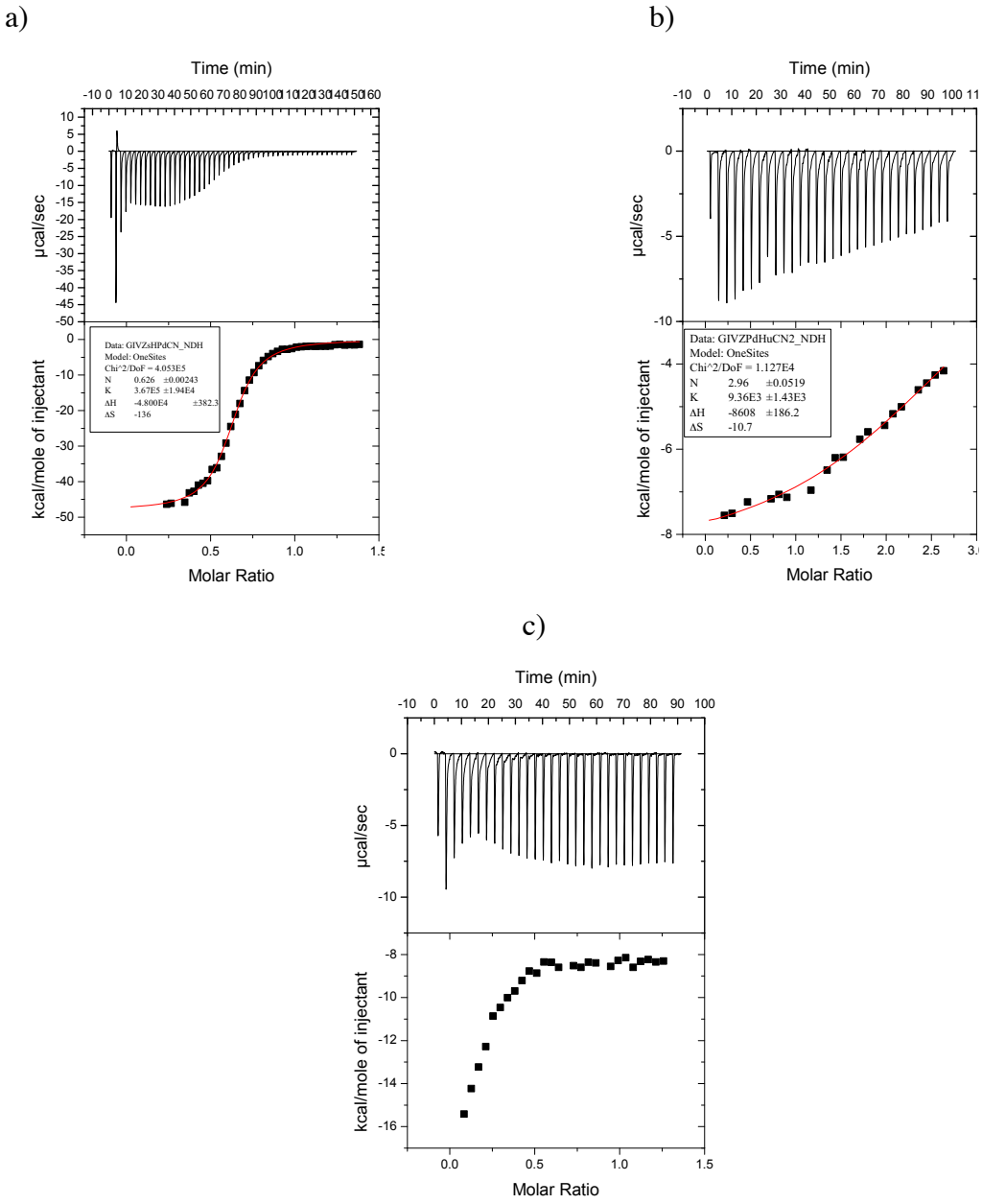

Figure 1.31: ITC traces corresponding to the addition of TBACN (3 mM) to a) **1.50** (0.35 mM), b) **1.54** (0.31 mM), and c) **1.52** (0.33 mM) in acetonitrile at 298 K.

1.7 CONCLUSIONS

The synthesis of strapped calix[4]pyrrole Schiff base macrocyles was presented. Macrocycle **1.2** proved to be unstable in acidic conditions. This macrocycle undergoes hydrolysis at low pH values as the result of protonation of the imine groups. The hydrolysis of **1.2** was followed by UV-Vis spectroscopy, HPLC, and mass spectrometry. It was proposed that the rigid strap induces strain in the macrocycle and promotes hydrolysis of **1.2**. Compound **1.2** showed a change in color upon contact with thorium salts, which was initially attributed to a possible interaction between the thorium salt and **1.2**. However, this suggestion was ultimately abbandoned due to a lack of overt evidence. In order to improve the stability of the macrocycle a flexible strap was introduced. The macrocycle **1.3** was obtained *via* the direct condensation of two equivalents of *o*-phenylenediamine with the α-strapped dipyrromethane under acidic conditions. Anion binding studies of **1.3** was limited by the conformation of the complex in which the twisted strap cannot favorably interact with anionic species. However, anion binding studies with cyanide revealed that the metal complex **1.50** displayed affinities for the cyanide anion that were more than than two orders of magnitude higher than the unstrapped palladium complex **1.54**. This finding could be rationalized in terms of the strap stabilizing a fixed conformation that serves to isolate the binding site from the medium. Thus increasing the anion binding affinity.

1.8 References

1. Lee, C.-H.; Miyaji, H.; Yoon, D.-W.; Sessler, J. L. *Chem. Commun.* **2008**, 24.

2. Gale, P. A.; Lee, C.-H. Anion Recognition in Supramolecular Chemistry: Topics in Heterocyclic Chemistry, ed. Maes, B. U. W. Vol. 24, Springer, 2010, pp. 54.

3. Baeyer, A. *Ber. Ctsch Chem. Ges.* **1886**, *19*, 2184.

4. Floriani, C.; Floriani-Moro, R. *Porphyrin Handbook* 2000, 3, 385.

5. Gale, P.A.; Sessler, J. L.; Král, V.; Lynch, V. *J. Am. Chem. Soc.* **1996**, *118*, 5184.

6. Lee, C.-H.; Mayaji, H.; Yoon, D.-W.; Sessler, J. L. *Chem. Commun.* **2008**, 24.

7. Yoon, D. W.; Hwang, H.; Lee, C.-H. *Angew. Chem. Int. Ed.* **2002**, *41*, 1757.

8. Lee, C. H.; Lee, J. S.; Na, H. K.; Yoon, D. W.; Miyaji, H.; Cho, W. S.; Sessler, J. L. *J. Org. Chem.* **2005**, *70*, 2067.

9. Miyaji, H.; Kim, H.-K.; Sim, E.-K.; Lee, C.-K.; Cho, W. S.; Sessler, J. L.; Lee, C.-H. *J. Am. Chem. Soc.* **2005**, *127*, 12510.

10. Jeong, S.-D.; Yoo, J.; Na, H. K.; Chi, D. Y.; Lee, C.-H. *Supramol. Chem.* **2007**, *19*, 271.
11. Miyaji, H.; Hong, S. J.; Jeong, S. D.; Yoon, D. W.; Na, H. K.; Hong, S. K.; Ham, S.; Sessler, J. L.; Lee, C. H. *Angew. Chem. Int. Ed.* **2007**, *47*, 2508.

12. Fisher, M. G.; Gale, P. A.; Hiscock, J. R.; Hursthouse, M. B.; Light, M. E.; Schmidtchen, F. P.; Tong, C. C. *Chem. Commun.* **2009**, 3017.

13. Yano, M.; Tong, C. C.; Light, M. E.; Schmidtchen, F. P.; Gale, P. A. *Org. Biomol. Chem.* **2010**, *8*, 4356.

14. Samanta, R.; Mahanta, S. P.; Choudri, S.; Panda, P. K.; Narahi, A. *Inorg. Chim. Acta* **2011**, *372*, 281.

15. Yoon, D. W.; Gross, D. E.; Lynch, V. M.; Sessler, J. L.; Hay, B.; Lee, C.-H. *Angew. Chem. Int. Ed.* **2008**, *47*, 5038.

16. Sessler, J. L.; Kim, S. K.; Gross, D. E.; Lee, C.-H.; Kim, J. S.; Lynch, V. M. *J. Am. Chem. Soc.* **2008**, *130*, 13162.

17. Kim, S. K.; Sessler, J. L.; Gross, D. E.; Lee, C.-H.; Kim, J. S.; Lynch, V. M.; Delmau, L. H.; Hay, B. P. *J. Am. Chem. Soc.* **2010**, *132*, 5827.

18. Kim. S. K.; Vargas-Zuniga, G. I.; Hay, B. P.; Young, N. J.; Delmau, L. M.; Moyer, B. A.; Sessler, J. L. *J. Am. Chem. Soc.* **2012**, *134*, 1782.

19. Park, I.-W.; Yoo, J.; Kim, B.; Adhikari, S.; Kim, S. K.; Yeon, Y.; Haynes, C. J. E.; Sutton, J. L.; Tong, C. C.; Lynch, V. M.; Sessler, J. L.; Gale, P. A.; Lee, C.-H. *Chem. Eur. J.* **2012**, *18*, 2514.

20. Sessler, J. L.; Cho, W.-S.; Dudek, S. P.; Hicks, L.; Lynch, V. M.; Huggins, M. T. *Journal of Porphyrins and Phthalocyanines* **2003**, *7*, 97.

21. Givaja, G.; Blake, A. J.; Wilson, C.; Schröder, M.; Love, J. B. *Chem. Commun.* **2003**, 12508. (b) Givanja, G.; Blake, A. J.; Wilson, C.; Schröder, M.; Love, J. B. *Chem. Commun.* **2005**, 4423. (c) Veauthier, J. M.; Tomat, E.; Lynch, V. M.; Sessler, J. L.; Mirsaidov, U.; Markert, J. T. *Inorg. Chem.* **2005**, *44*, 6736. (d) Tomat, E.; Cuesta, L.; Lynch. V. M.; Sessler, J. L. *Inorg. Chem.* **2007**, *46*, 6224. (e) Givaja, G.; Volpe, M.; Leeland, J. W.; Edwards, M. A.; Young, T. K.; Darby, S. B.; Reid, S. D.; Blake, A. J.; Wilson, C.; Wolowska, J.; McInnes, E. J. L.; Schröder, M.; Love, J. B. *Chem.-Eur. J.* **2007**, *13*, 3707. (f) Cuesta, L.; Tomat, E.; Lynch, V. M.; Sessler, J. L. *Chem Commun.* **2008**, 3144. (g) Love, J. B. *Chem. Commun.* **2009**, 3154. (g) Veauthier, J. M.; Cho, W.-S.; Lynch, V. M.; Sessler, J. L. *Inorg. Chem.* **2004**, *43*, 1220. (h) Askarizadeh, E.; Yaghoob, S. B.; Boghaei, D. M.; Slawin, A. M. Z.; Love, J. B. *Chem. Commun.* **2010**, *46*, 710. (i) Givaja, G. Volpe, M.; Edwards, M. A.; Blake, A. J.; Wilson, C.; Schröder, Love, J. B. *Angew. Chem. Int. Ed.* **2007**, *46*, 584.

22. Collman, J. P.; Wagenknecht, P. S.; Hutchison, J. E. *Angew. Chem.* **1994**, *106*, 1620. (b) Dempsey, J. L.; Esswein, A. J.; Manke, D. R.; Rosental, J.; Soper, J. D.; Nocera, D. G. *Inorg. Chem.* **2005**, *44*, 6879. (c) Chang, C. J.; Loh, Z.-H.; Shi, C.; Anson, F. C.; Nocera, D. G. *J. Am. Chem. Soc.* **2004**, *126*, 10013. (d) Chang, C. J.; Deng, Y.; Shi, C.; Anson, F. C.; Nocera, D. G. *Chem. Commun.* **2000**, 1355. (e) Guilard, R.; Brandes, S.; Tardieux, C.; Tabard, A.; Loher, M.; Miry, C.; Goerec, P.; Knop, Y.; Collman, J. P. *J. Am. Chem. Soc.* **1995**, *117*, 11721. (f) Proniewicz, L. M.; Odo, J.; Goral, J.; Chang, C. K.; Nakamoto, C. K. *J. Am Chem. Soc.* **1989**, *111*, 2105. (g) Durand, R. R.; Bencosme, Jr., C. S.; Collamn, J. P.; Anson, F. C. *J. Am. Chem. Soc.* **1983**, *105*, 2710. (h) Collman, J. P.;

Denisevich, P.; Konai, Y. Marrocco, M.; Koval, C.; Anson, F. C. *J. Am. Chem. Soc*. **1980**, *102*, 6027. (i) Hodgkiss, J. M.; Chang, C. J.; Pistorio, B. J.; Nocera, D. G. *Inorg. Chem*. **2003**, *42*, 8270. (j) Pistorio, B. J.; Chang, C. J.; Nocera, D. G. *J. Am. Chem. Soc*. **2002**, *124*, 7884. (k) Rosenthal, J.; Luckett, T. D.; Hodgkiss, J. M.; Nocera, D. G. *J. Am. Chem. Soc*. **2006**, *128*, 6546. (l) Rosenthal, J.; Pistorio, B. J.; Chng. L. L.; Potter, N. A.; Carmichael, C. D.; Nocera D. G. *J. Org. Chem*. **2005**, *70*, 1885.

23. Ranold, P. L.; Potter, N. A.; Carmichael, C. D.; Slawin, A. M. Z., Roussel, P.; Love, J. B. *Chem. Commun*. **2010**, *46*, 1833.

24. Arnold, P. L.; Emmalina, H.; White, F. J.; Magnani, N.; Caciuffo, R.; Love, J. B. *Angew. Chem. Int. Ed*. **2011**, *50*, 887.

25. Arnold, P. L.; Blake, A. J.; Wilson, C.; Love, J. B. *Inorg. Chem*. **2004**, *43*, 8206. (b) Arnold, P. L.; Patel, D.; Pécharman, A.-F.; Wilson, C.; Love, J. B. *Dalton Trans*. **2010**,*39*, 3501. (c) Arnold. P. L; Patel, D.; Wilson, C.; Love, J. B. *Nature* **2008**, *451*, 315. (d) Arnold, P. L.; Pécharman, A.-F.; Hollis, E.; Yahia, A.; Maron, L.; Parsons, S.; Love, J. B. *Nat. Chem*. **2010**, *2*, 1056. (e) (f) Jones, G. M.; Arnold, P. L. *Chem.-Eur J*. **2013**, *19*, 10287. (g) Arnold. P. L.; Hollis, E.; Glichol, G. S.; Love, J. B.; Griveau, J.-C.; Caciuffo, R.; Magnani, N.; Maron, L.; Castro, L.; Yahia, A.; Odoh, S. O.; Schreckenbach, G. *J. Am. Chem. Soc*. **2013**, *135*, 3841.

26. Leeland, J. W.; White, F. J.; Love, J. B. *J. Am. Chem. Soc*. **2011**, *133*, 7320.

27. Bejger, C.; Davis, C. M.; Park, J. S.; Lynch, V. M.; Love, J. B.; Sessler, J. L. *Org. Lett.* **2011**, *13*, 4902.

28. Brown, W. H., Foote, C. S., Iverson, B. L., Anslyn, E. V., Novak, B. M. *Organic Chemistry*, 6th Edition; Brooks/Cole CENGAGE Learning: United States of America, pg. 606-609.

29. Askarizadeh, E.; Devoille, A. M.; Bogheaei, D. M.; Slawin, A. M. Z.; Love, J. B. *Inorg. Chem.* **2009**, *48*, 7491.

30. Evans, D. F. *J. Chem. Soc.* **1959**,2003.

31. Schubert, E. M. *J. Chem. Educ.* **1992**, *69*, 62.

32. Grant, D. H. *J. Chem. Educ.***1995**, *72*, 39.

33. Ballester, P. *Chem. Soc. Rev.* **2010**, *39*, 3810.

34. Beer, P. D.; Cormode, D. P.; Davis, J. J. *Chem. Commun.* **2004**, 414.

35. Amendola, V.; Fabrizzi, L.; Mangano, C.; Pallavicini, P.; Poggi, A.; Tagletti, A. *Coord. Chem. Rev.* **2001**, *219-221*, 821.

36. Lommens, P.; Feys, J.; Vrielinck, H.; De Buysser, K.; Herman, G.; Callens, F.; Van Driessche, I. *Dalton Trans.* **2012**, *41*, 3574.

37. Roberts, E. M.; Koski, W. S. *J. Am. Chem. Soc.* **1960**, *82*, 3006.

38. Harris, R. K. in *Encyclopedia of Nuclear Magnetic Resonance*, D. M. Granty and R. K. Harris, (eds.), vol. 5, John Wiley & Sons, Chichester, UK, 1996.

Chapter 2: *Meso* Substituted Etioporphycenes

2.1 Introduction

A number of porphycenes and their metal complexes have been synthesized since Vogel *et al*. published their seminal report on the synthesis of porphycene in 1986.[5] However, most of the synthetic efforts to create porphycene derivatives have involved functionalization of the β-positions of the pyrrole rings (*cf*. Figure 2.1). Porphycene derivatives with substitution on the four *meso* positions of the macrocycle, have been less well studied due to the more complex synthetic methods required to access this type of target. Moreover, the porphyrinogen precursor to *meso*-tetrasubstituted porphycenes display a lower propensity to undergo oxidation during the McMurry coupling reaction typically used to prepare porphycene. On the other hand, 9-substituted porphycenes (*cf*. Figure 2.1), wherein the functionalization occurs on only one *meso* position, provides another alternative to derivatization in which the introduction of the substituents is introduced in the last step of synthesis. In this chapter, the synthesis 9-substituted etioporphycenes **2.44**, **2.47**, **2.48**, and **2.49** is detailed. These functionalized porphycenes were found to display different features reflecting the macrocycle electronics. The synthesis of 9-substituted etioporphycenes presented in this chapter were analyzed by ^{1}H and ^{13}C NMR spectroscopy, UV-Vis spectroscopy, mass spectrometry, and electrochemical methods.

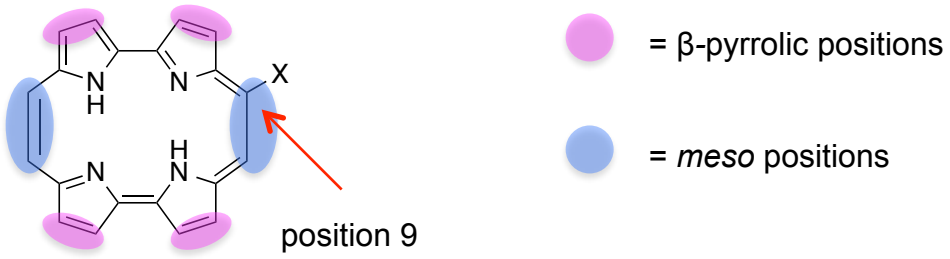

Figure 2.1: Porphycene framework showing substitution on position 9.

2.2 PORPHYCENES : CONSTITUTIONAL ISOMERS OF PORPHYRINS

Porphyrins have been recognized as distinct chemical entities for over a century.[1, 2] The basic structure and chemical features were elucidated by Hans Fischer in the early 20th century, work for which he was awarded the Nobel Prize in 1930. Since then, these tetrapyrrolic aromatic macrocycles have been widely studied by chemists. Inspiration for this effort comes from their role in biological processes, such as photosynthesis and respiration. In order to study develop the chemistry of these compounds further, researchers have focused on in the preparation of new porphyrin analogues. In this context, porphycene being one of the most studied and stable porphyrin isomers (*cf.* Figure 2.2), has central role to play.

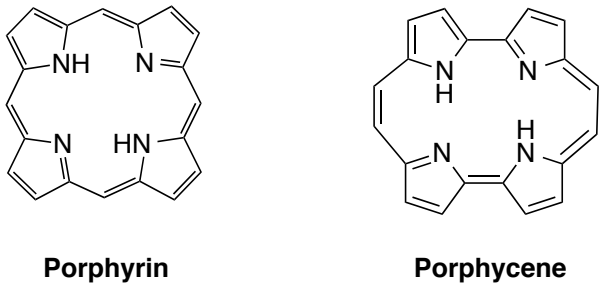

Figure 2.2: Basic structures of porphyrin and porphycene.

Porphycene dates to 1986. In that year, Vogel and coworkers prepared a [20]annulene from two 5,5'-diformyl-2,2'-bipyrrole subunits *via* reductive McMurry-type coupling in ca 3% yield (*cf*. Scheme 2.1).[2] This macrocycle was found to undergo spontaneous two-electron oxidation upon exposure to air. These species initially displayed features comparable to porphyrins and acenes. This led Vogel to propose the trivial name "porphycene" for this compound.[3] Porphycene is a tetratpyrrolic ring which contains two 2,2'-bipyrrole subunits linked by two double bonds to form a tetraaza central core.[3, 4] This macrocycle is formally known as [18]porphyrin-(2.0.2.0). It was first recognized constitutional isomer of porphyrin.[5]

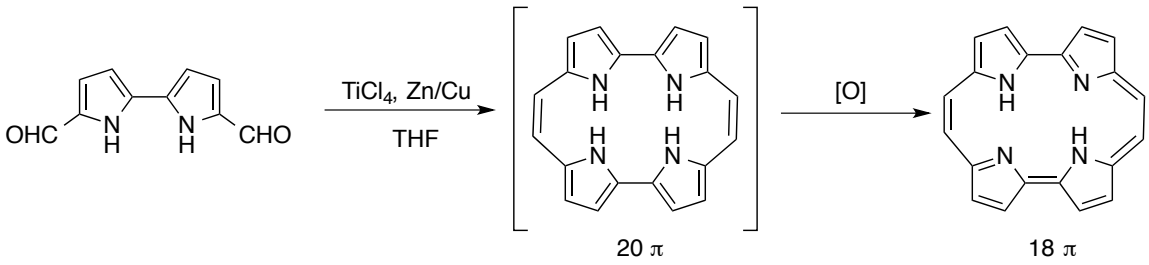

2.1

Scheme 2.1: Synthesis of porphycene **2.1** *via* the reductive coupling of 5,5'-diformyl-2,2'-bipyrrole under McMurry conditions.

Porphycenes pocess a less symmetric structure than porphyrins: Roughly, D_2h symmetry *vs*. D_4h symmetry of porphycene and porphyrin, respectively. Porphycene display different optical properties, such as strong absorption features in the red region of the UV-Vis spectrum and higher absortivity (ε) values (e.g., strong absorption between 620 to 760 nm) than the corresponding porphyrin. This enhancement in the absortivity for porphycenes was attributed to symmetry-allowed transitions that are forbidden in

porphyrin. These unique optical features have made porphycenes of interest in various biomedical applications, including photodynamic therapy (PDT) and the photoinactivation of viruses and bacteria, particularly in the area of blood purification.[6]

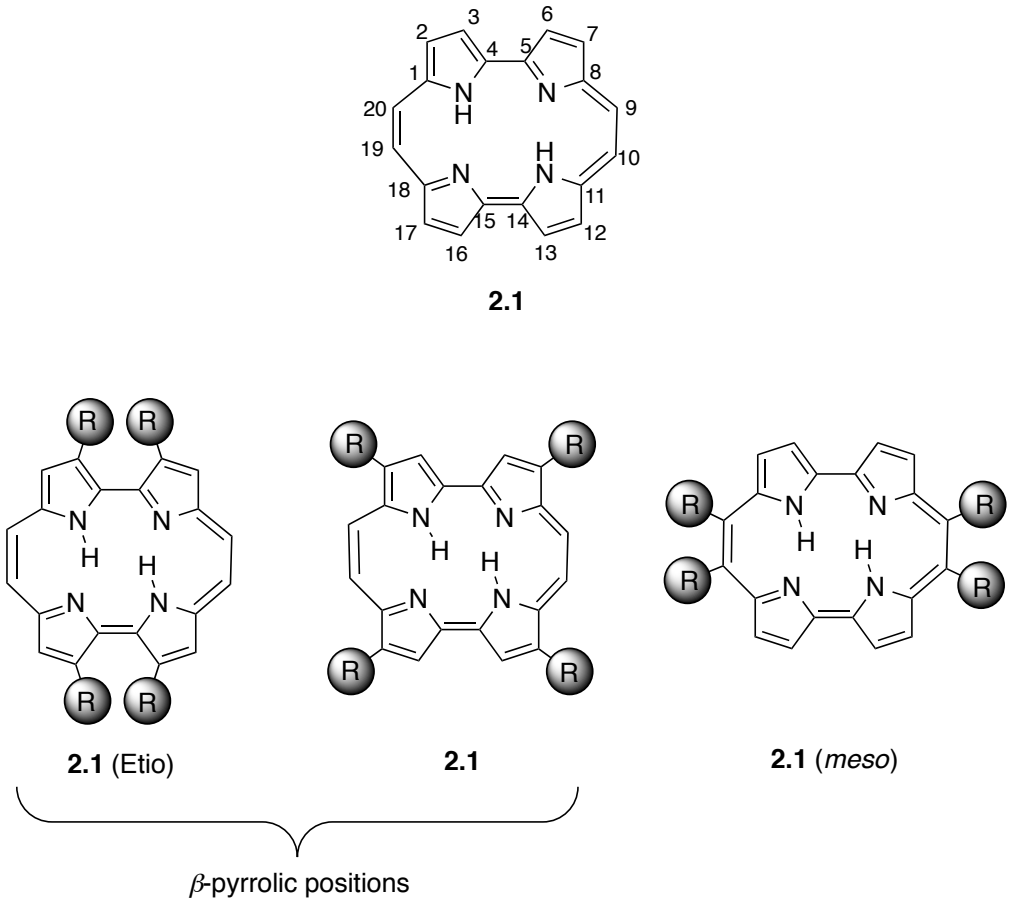

Figure 2.3: Porphycene framework showing different sites of substitution, namely in the β-pyrrolic positions (left) or *meso* positions (right).

Since the synthesis of the first porphycene was published, a number of porphycene derivatives have been reported.[4-7] In analogy to what is true for porphyrins, the basic optical properties of porphycenes can be modified by the attachement of

subtituents.[8] One approach involves functionalizing on the β-pyrrolic positions of the macrocycle (2, 7, 12, and 17 positions, and/or 3, 6, 13, and 16 positions in the macrocycle). Those bearing alkyl substituents on the 3, 6, 13, and 16 positions are called etioporphycenes (*cf*. Figure 2.3). These modifications can influence the shape and size of the cavity of the macrocycle. For instance, etioporphycenesare often characterized by deformations of the porphycene plane. This destabilizes the pyrrole NH-N-pyrrole hydrogen bonds in the cavity. As a consequence, etioporphycenes are able to accommodate bigger metal cations in their cavity than unsubstituted porphycenes.[9] Other types of functionalization are known. As shown in Figure 2.4, these include 1) the use of fused aromatic rings on the pyrroles, which produces, e.g., tetrabenzoporphycenes **2.2**, and 2) linkages between two adjacent pyrrolic rings, which produce, e.g., dibenzoporphycenes **2.3**[6] and dinaphthoporphycenes **2.4**.[7]

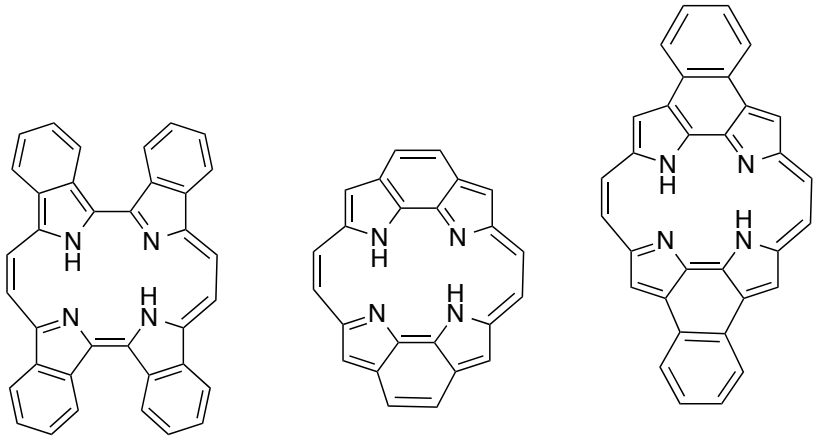

2.2 **2.3** **2.4**

Figure 2.4: Examples of tetrabenzoporphycene **2.2**, dibenzoporphycene **2.3**, and dinaphthoporphycene **2.4**.

In contrast to etioporphycenes, the insertion of substituents at the ethynyl bridges or so-called *meso* positions of the macrocycle (i.e., positions 9, 10, 19, and 20) tends to stabilize intramolecular hydrogen bonds. Functionalization of the *meso* positions can often be affected after the ring structure has been constructed. However, typically, only one substituent is added. This give rise to yielding asymmetric porphycenes, as will be detailed in the following section (*cf*. Figure 2.5).[10]

2.3 *MESO*- SUBSTITUTED PORPHYCENES

2.3.1 *Meso*-Tetrasubstituted Porphycenes

As described in the previous section, porphycenes are obtained by the reductive coupling of 5,5'-diformyl-2,2'-bipyrrole using McMurry reactants that include $TiCl_4$, Zn, and CuCl.[3, 5, 11] Although porphycenes are more soluble in organic solvents, the solubility of the unsubstituted porphycene and many of its derivatives is still limited.

Meso-tetrasubstituted porphycenes have been synthesized from 5,5'-acyl substituted bipyrroles using the reductive coupling conditions introduced by Vogel. For instance, the synthesis of porphycene **2.5** starts with the acylation of bipyrrole in analogy to what is done when effecting the formylation of bipyrrole. However, instead of using dimethylformamide (as needed for formylation), an alkyl *N,N'*-amide and phosphorous oxychloride ($POCl_3$) was employed.[9] The bipyrrole obtained was subjected to McMurry coupling,[11] followed by oxidation with 2,3-dichloro-5,6-dicyano-*p*-benzoquinone (DDQ), to give the corresponding porphycene **2.5** (*cf*. Figure 2.5).[12, 13] Catalytic hydrogenation with palladium/carbon in ethylacetate gave a colorless dihydro compound, **2.5**, which subsequently underwent oxidation by DDQ.[14] In 2011, Yamada and coworkers reported the synthesis of the pyrrolocyclophene **2.6**, which could not be oxidized to give the corresponding porphycene. This was attributed to steric repulsions between the alkyl substituents that are so severe that they preclude attaining the planar conformation

characteristic of porphycenes. Thus, intermediate **2.6** was isolated in the form of colorless crystrals (*cf*. Figure 2.5).[15] This lack of color stands in marked contrast to what is true for the blue-purple porphycenes.

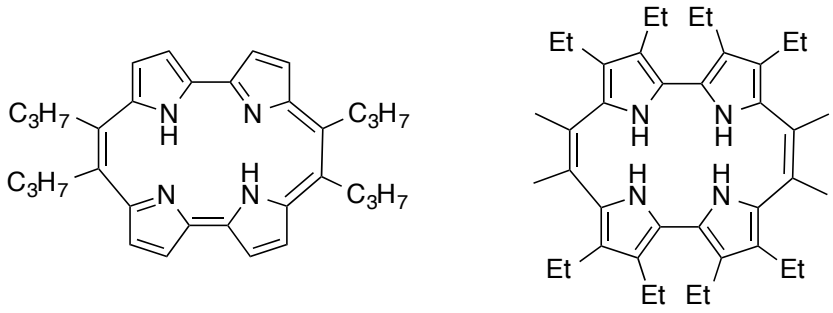

2.5 **2.6**

Figure 2.5: *Meso*-tetrapropylporphycene **2.5**, and pyrrolocyclophene **2.6**.

In 2008, Srinivasan and coworkers reported the synthesis of *meso*-tetrasubtituted porphycenes **2.7** and **2.8** using a different synthetic approach from the traditional McMurry coupling (*cf*. Scheme 2.2).[9] In this case, **2.7** and **2.8** were prepared in 5% yield *via* an acid-catalyzed oxidative coupling involving 5,6-diphenyl or ditolyl dipyrromethanes **2.9** and **2.10,** respectively.[9]

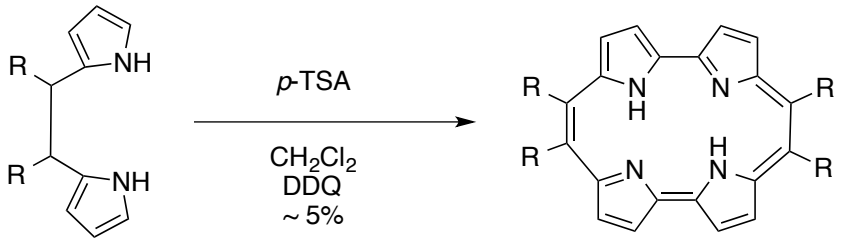

2.9 R = Ph
2.10 R = Tolyl

2.7 R = Ph
2.8 R = Tolyl

Scheme 2.2: Synthesis of *meso*-tetraphenylporhycene **2.7** and *meso*-tetratolylporphycene **2.8** *via* acid-catalyzed oxidative coupling.

2.3.2 Porphycenes Bearing Substituents on Position 9

Porphycenes bearing only one substituent in a *meso* position (position 9), were reported by Vogel in a series of patents dating from the 1990s.[16-20] This method of functionalization offers the advantage that the substituent is inserted in the last step of the synthesis. Also, the inherent regioselectivity of this method allows asymmetric porphycene derivatives using relatively easily. Exclusive 9-substitution is ascribed in the reactivity of the macrocycle, which has aromatic character. In 1997, Vogel reported that the treatment of porphycenes with fuming nitric acid produces the 9-nitro substituted porphycene **2.11**.[21] Silver nitrate in acetic acid and dichloromethane provides an alternative to access the nitration and leads to *meso*-nitration in the case of porphycenes bearing substituents in the β-pyrrolic positions. The porphycenes may reduced using the Zinin reduction,[22] or by treatment with Raney Ni and hydrazine. This affords the 9-amino derivative **2.12** (*cf*. Scheme 2.3). In 1996, Kadish and coworkers reported the synthesis of 9-formyletioporphycene **2.13** using the Vielsmeier Haack reagent ($POCl_3$ in DMF).[23] A different method developed for the functionalization of the 9 position involves acylation followed by the treatment with a Pb(IV) salt (PbO_2 or $Pb(OAc)_4$) in the presence of a

carboxylic acid. This yields 9-acetoxyporphycene **2.14**. Further hydrolysis of **2.14** in basic media affords the free 9-hydroxyporphycene **2.15**.[20]

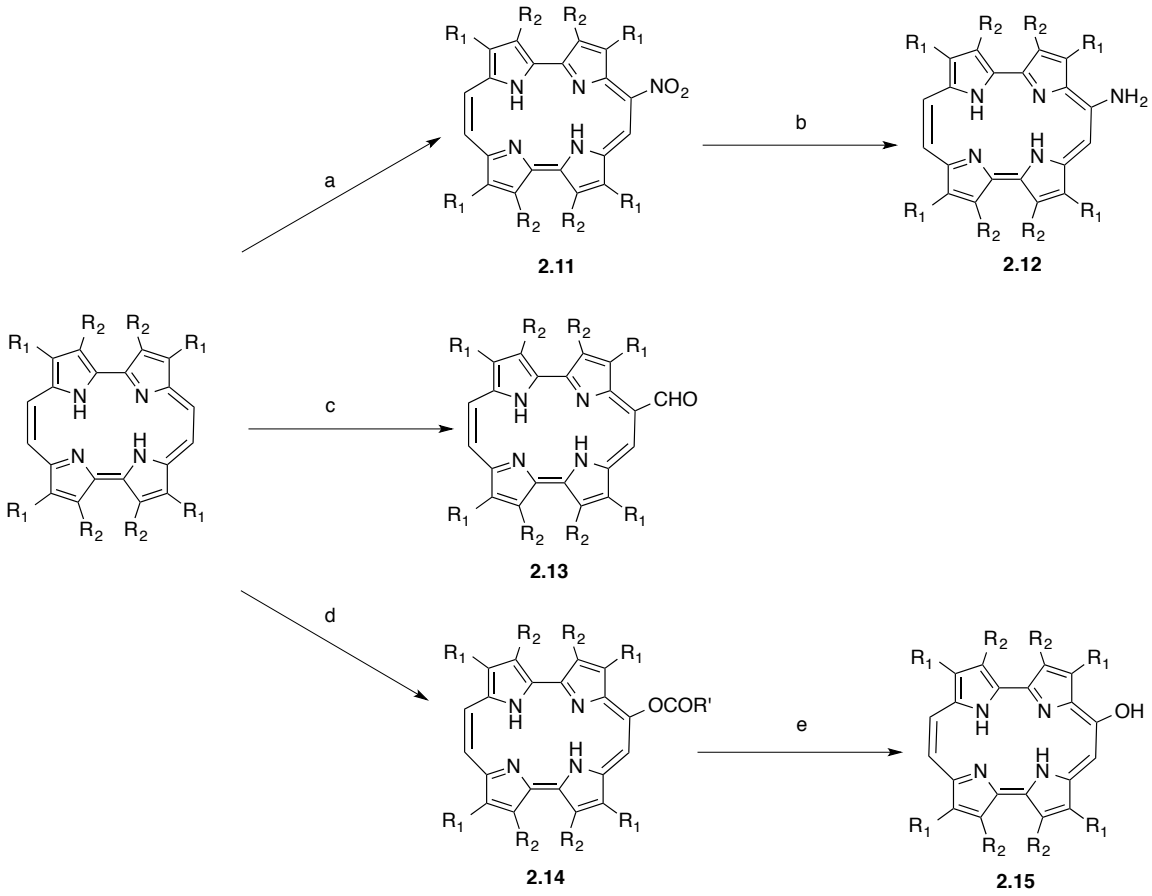

Scheme 2.3: Synthesis of 9-substituted porphycenes **2.11-2.15**. Reaction conditions: (R_1 = C_3H_7, R_2 = H) a) HNO_3 or $AgNO_3$/HOAc in CH_2Cl_2, b) $Na_2S_2O_4$, $NaOH_{(aq)}$, (R_1 = C_2H_5, R_2 = CH_3) c) $POCl_3$, DMF, $C_2H_4Cl_2$, (R_1 = C_3H_7, R_2 = H, R' = $(CH_2)_3CO_2t$-Bu) d) PbO_2, $HO_2C(CH_2)_3CO_2t$-Bu, CH_2Cl_2, e) NaOMe, MeOH.

In fact, these 9-subtituted porphycenes have been used as building blocks for the preparation of more complex systems (*cf*. Figure 2.6). For instance, 9-hydroxy substituted porphycenes can be used to prepare ethers, such as **2.16**, or esters, such as **2.17**-**2.9**, whereas the amino derivatives have been used for the synthesis of amide-substituted porphycenes, such as **2.20**-**2.22**.[23, 24 6] Recently, Guldi and coworkers reported the synthesis of compound **2.23** for the subsequent functionaliztion of graphene.[24]

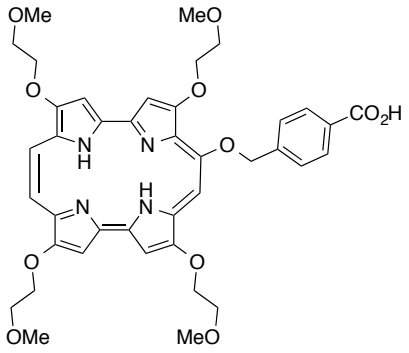

2.16

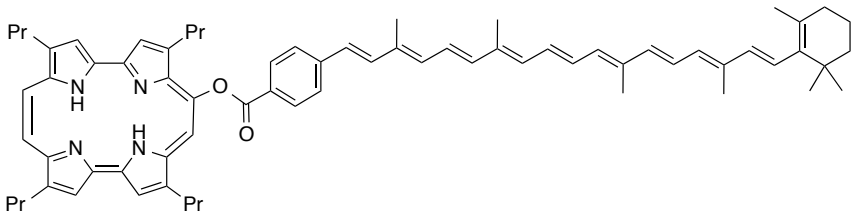

2.17

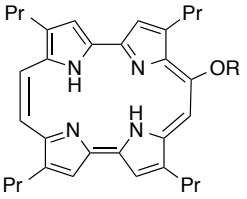

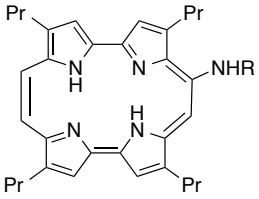

2.18 R = CO-Glu-CO_2tBu
2.19 R = CO-$(CH_2)_3$-NBOC

2.20 R = CO-$(CH_2)_3$-CO_2H
2.21 R = CO-$(CH_2)_3$-CO(poly-lysine)
2.22 R = (C_4H_8)-CONH$(C_3H_5(CCOH)_2)$)

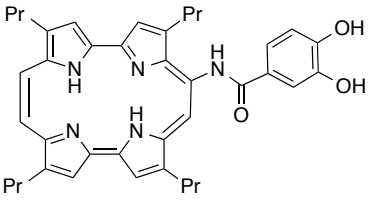

2.23

Figure 2.6: Porphycene derivatives generated from 9-amino and 9-hydroxy substituted porphycenes.

The goal of this project was to obtain a ferrocene-substituted porphycene. As detailed below, this objective was not successfully met. Nevertheless, it is appropriate to detail the rationale for this effort.

2.4 *MESO*-LINKED FERROCENE PORPHYRINS

The donor-acceptor properties of ferrocene and porphyrins along with their electrochemical features have been extensively explored in the context of understanding photoinduced electron transfer processes and as mimics photosynthetic active sites.[25,26] These features have been of fundamental importance for the development of molecular-based electronic devices,[27,28] as well as multielectron redox catalysis.[29] Due to their unique structural and electronic properties, a variety of ferrocene-appended porphyrins can be found in literature. These systems involve ferrocne moieties attached to porphyrins directly or through spacers linked to the *meso* or β-pyrrolic positions of the porphyrirn.[30] The following sections summarize the synthesis and properties of various *meso*-linked ferrocene-porphyrins. This overview is designed to set the stage for work with *meso*-ferrocene substituted porphycenes. However, as noted above these latter targets were not successfully attained.

2.4.1 Direct Connection

Meso-linked ferrocene-porphyrins have been synthesized by reacting ferrocene-carboxaldehyde with pyrrole in the presence of a Lewis acid followed by oxidation with *p*-chloranyl (TCQ).[31-33] This afforded the 5,10,15,20-tetrakis(ferrocenyl)porphyrin **2.24** in 40% yield (*cf*. Figure 2.7). Nadtochenko *et al*. reported that the presence of ferrocene substituents in the *meso* positions resulted in quenching of the porphyrin fluorsescence quantum yield, by 10^5 fold relative to 5,10,15,20-tetrakis(phenyl)porphyrin **2.25** (*cf*. Figure 2.7).[30] In addition, the absorption spectrum of **2.24** revealed a significant red shift in the Soret ($\Delta\lambda \sim 15$ nm) and Q bands. This was ascribed to the strong electronic coupling between the porphyrin π system and the ferrocenyl moieties. The redox

properties of **2.24** revealed not only positive potential shifts, due to electronic effects of both the ferrocene and the porphyrin-based redox couples in **2.24**, but also, a communication between the ferrocene groups mediated by the conjugated porphyrin backbone, as inferred from the observation of multiple redox waves corresponding to the successive oxidations of interacting ferrocenes. This coupling and the presence of multiple redox states was confimed by Nemykin *et al*. who characterized mixed valence (MV) species using Mössbauer spectroscopy and spectroelectorchemical methods.[34]

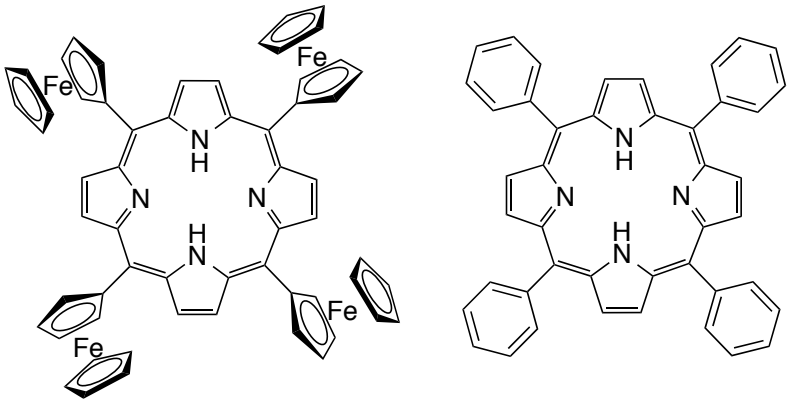

2.24 **2.25**

Figure 2.7: 5,10,15,20-Tetrakis(ferrocenyl)porphyrin **2.24** and 5,10,15,20-tetrakis(phenyl)porphyrin **2.25**.

These results motivated the synthesis of the partially *meso*-substituted ferrocene porphyrins (mono- and bis-ferrocenyl derivatives) shown in Figure 2.8.[35] In the case of the bis(ferrocenyl)porphyrin **2.26**, one-electron electrochemical oxidation produced a red shift in the Soret band from 426 to 452 nm. Also, the Q bands were seen to dissappear, along with the appearance of band at 803 nm. This new band was attributed to an intervalence charge transfer (IVCT) process involving a mixed valence Fe(II)-Fe(III) species.[30, 34] On the other hand, the "communication" between the porphyrin and

ferrocene subunits in mono(ferrocenyl)porhyrin **2.27** and its zinc complex **2.28**, makes the porphyrin core azamacrocycle harder to oxidize and reduce. This resultes in a widening of the HOMO-LUMO gap (HLG), an effect ascribed to the electron donating properties of the ferrocene moiety. As expected, the ferrocinium group had the opposite effect (*cf*. Figure 2.8).[30]

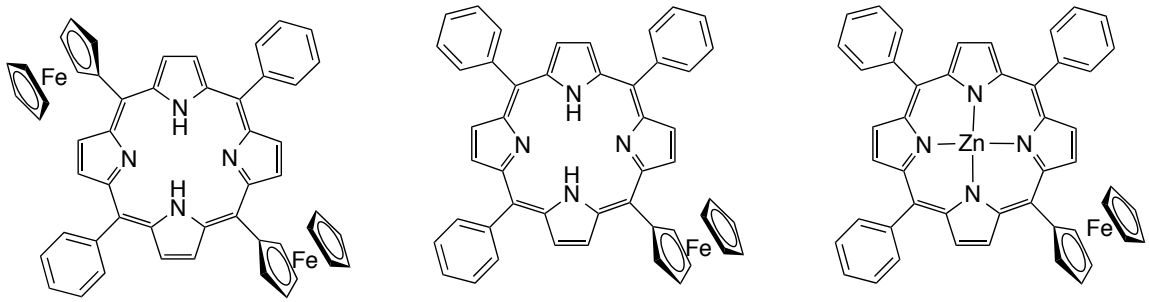

2.26 **2.27** **2.28**

Figure 2.8: 5,15-Diferrocenyl-10,20-diphenylporphyrin **2.26** and 5-ferrocenyl-10,15,20-triphenylporphyrin **2.27**, and its zinc(II) complex **2.28**.

The introduction of two ferrocene groups on the *meso* positions of β-alkylated porphyrins afforded compound **2.29** as a single isomer with both ferrocenyl fragments in *syn* configuration with respect to the porphyrin ring (*cf*. Figure 2.9).[36, 38] In this case, the alkyl groups in the β-pyrrolic positions prevent trotation of the metallocenyl, which results in a ruffled porphyrin core. The electrochemical properties of compound **2.29** revealed two successive, ferrocene-centered, one electron tranfers separated by 0.19 V. This latter finding was attributed to the presence of unusually strong electronic interactions between both ferrocenyl substituents. As a result the oxidation of the first metallocene makes oxidation of the seconf Fe(II) center correspondingly more difficult. The analogous nickel(II) complex **2.30** displayed even more pronounced splittings of the

half wave potentials (i.e., by of 0.41 V). Absorption analyses of **2.29** and **2.30** revealed electrochemically driven formation of mixed valence species, as inferred from the appearance of absorption bands in the near infrared region between 950 and 1100 nm. Studies of porphyrin **2.31** revealed similar tendencies. In fact, in this case the ferrocene-redox couples could be tuned *via* insertion of selected metal cations (*cf*. Figure 2.9).[37, 38]

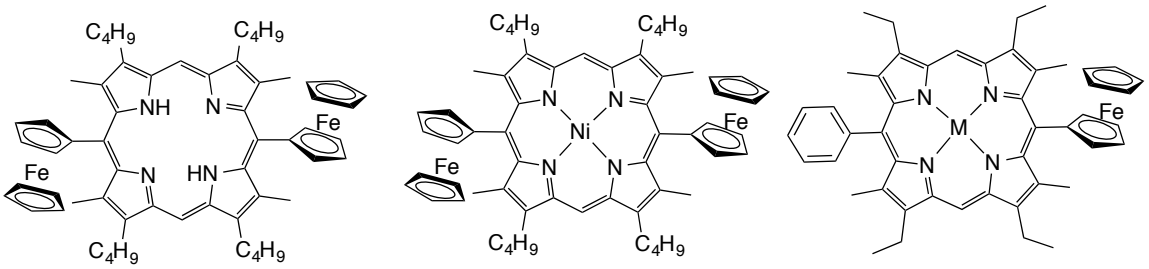

Figure 2.9: Ferrocenylporphyrins **2.29**, **2.30**, and **2.31**.

2.4.2 Linkage Through Conjugated Spacers

Another method utilized to obtain ferrocenylporphyrins has involved introduction of a conjugated spacer between the ferrocene groups and the porphyrin core. In 1967 Adler and Longo reported the synthesis of compound **2.32** in 5% yield by refluxing pyrrole and 4-ferrocenylbenzaldehyde in propionic acid (*cf*. Figure 2.10).[39] Surprisingly, electrochemical and UV-Vis analysis of **2.32** revealed the absence of communication between the ferrocene subunits and the porphyrin ring. In this case, electrochemical analysis of **2.32** revealed that all four ferrocenes oxidized at the same apparent potential. Moreover, the UV-Vis spectrum of **2.32** was found to be similar to that of 5,10,15,20-tetraphenylporphyrin **2.25**.[35, 40, 41]

Another strategy to introduce ferrocene fragments at the periphery of a porphyrin has involved the use of Sonogashira coupling. Ethynyl bridged ferrocene-porphyrin **2.33** was developed by Lindsey, Ng and coworkers as a potentially "push-pull" nonlinear optically active (NLO) chomophore (*cf*. Figure 2.10).[42, 43] However, a lack of redox interaction between the metallocene groups in the bisferrocenyl **2.33** was noted, as inferred from the observation of only a single oxidation wave corresponding to the oxidation of borth iron centers. This result was rationalized in terms of the large distance between each iron center, which was thought to hamper the electronic communication between the ferrocene subunits.

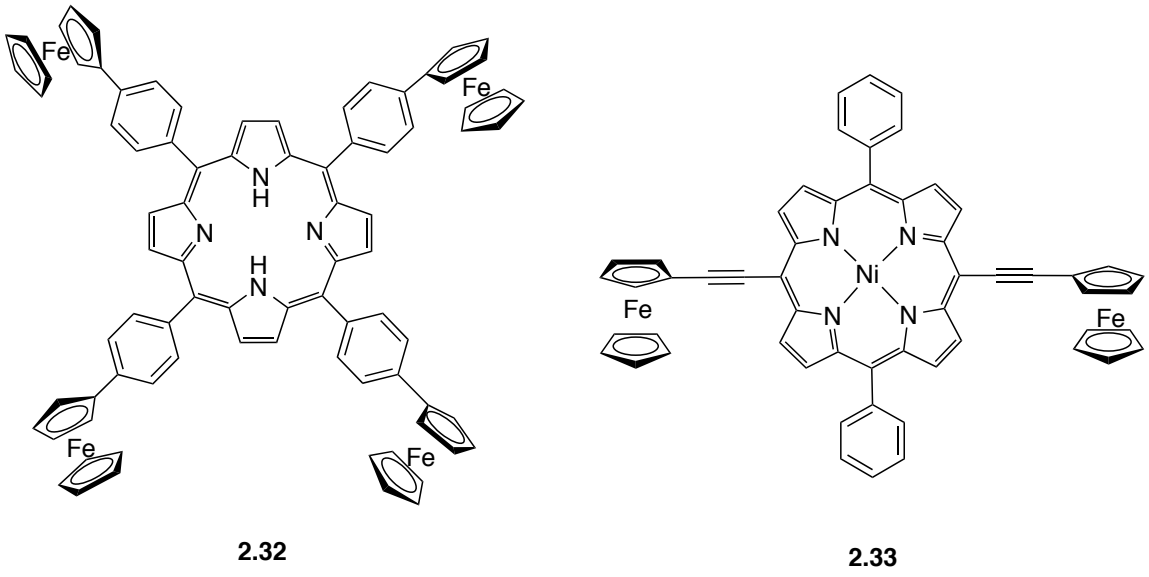

2.32 **2.33**

Figure 2.10: Ferrocenylphenyl porphyrin **2.32**, and ethynyl bridged ferrocene-porphyrin **2.33**.

Another strategy, introduced by Wrighton and coworkers relied on the condensation between a ferrocene ylide and an aldehyde-containing porphyrin to produce

2.34 and its reduced analogue **2.35** as shown in Scheme 2.4.[44] In this case, steady state emission spectroscopy and Stern-Volmer analysis revealed that the quenching of the ethyl linked derivative **2.35** was half as fast as the vinyl trans-linked analogue **2.34**. These results were explained in terms of the ferrocene center in both componds serving to quench the single excited state of the porphyrin core through an electron transfer mechanism.

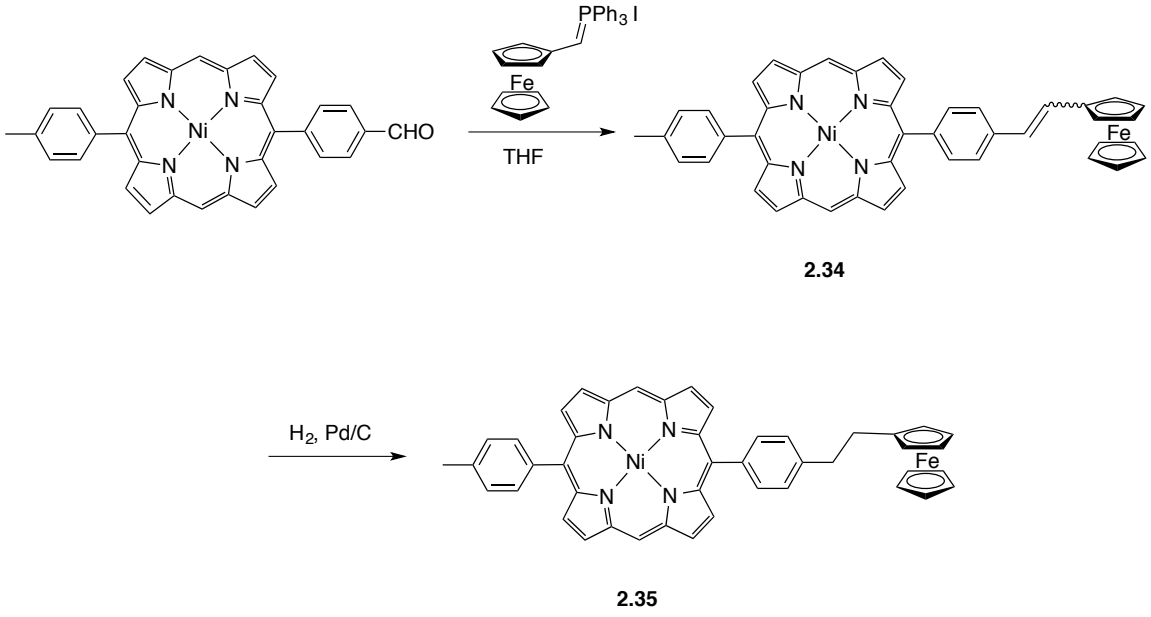

Scheme 2.4: Synthesis of ferrocenyvinylporphyrin **2.34** and ferrocenyethylporphyrin **2.35**.

In 2004, Fukuzumi and coworkers reported the ferrocene-porphyrin trimer-fullerene sequence **2.36**, a system prepared with the goal of achieving a long-lived charge separated states (*cf*. Figure 2.11).[45] This system displayed electron transfer features that reflected the presence of a ferrocene subunit as electron donor, and a fullerene as an electron acceptor. Irradiation in the near-IR region (~ 1000 nm) of **2.36** in benzonitrile at

163 K resulted in intermolecular photoinduced electron transfer from the singlet and triplet excited states of the central porphyrin trimer to the fullerene fragment. This afforded the charge separated species that in the limit consist of a ferrocene-porphyrin$^{\bullet+}$ and a fullerene$^{\bullet-}$. Electron transfer from the ferrocene moiety to the porphyrin radical cation in **2.36** led to formation of the separated charged species ferrocene^{+}-porphyrin timer-fullerene$^{\bullet-}$. On this basis, it was suggested that compound **2.36** could be used as a light harvesting system.[45]

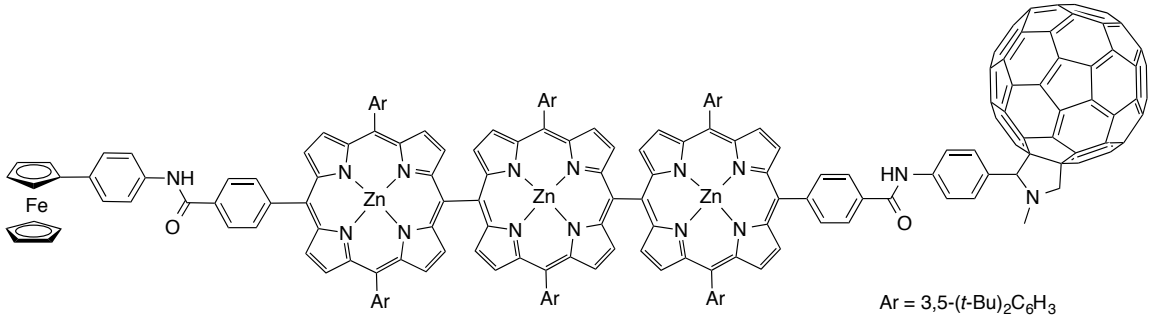

2.36

Figure 2.11: Ferrocene-porphyrin trimer-fullerene **2.36**.

2.5 SYNTHESIS AND CHARACTERIZATION

The synthesis of the etioporphycene **2.37** is outlined in Scheme 2.5. It was prepared by the author following Vogel's method.[50] This synthesis starts with the preparation of the β,β'-substituted pyrrole **2.39**, a precursor obtained *via* the Zard-Barton reaction.[46-48] This latter reaction involves the condensation of ethyl isocyanoacetate with a nitro compound **2.38** in the presence of tetrabutylammonium bromide (TBABr), afforded compound **2.39** in 40% yield.[48] Iodination of **2.39** followed by N-protection of the iodopyrrole using *tert*-butyloxycarbonyl (BOC) affordes **2.40** in quantitative yield. Ullman coupling of **2.40** produced the tetra-β-substituted bipyrrole **2.41** in 25% yield. Reaction with DMF and $POCl_3$ produces α,α'-diformyl bipyrrole **2.33** in near quantitative yield.[49] Bipyrrole **2.33** was subjected to McMurry coupling conditions ($TiCl_4$, Zn, and CuCl) in THF, which afforded etioporphycene **2.37** in 6% yield.[49] The etioporphycene nickel(II) complex **2.43** was obtained in 90% yield by adding four equivalents of nickel(II) acetate salt in boiling acetic acid.[22] Etioporphycene **2.37** and the corresponding etioporphycene nickel(II) complex **2.43** were characterized by standard spectroscopic techniques. The results from the spectroscopic analyses were in accord with what is reported in the literature.[50, 22]

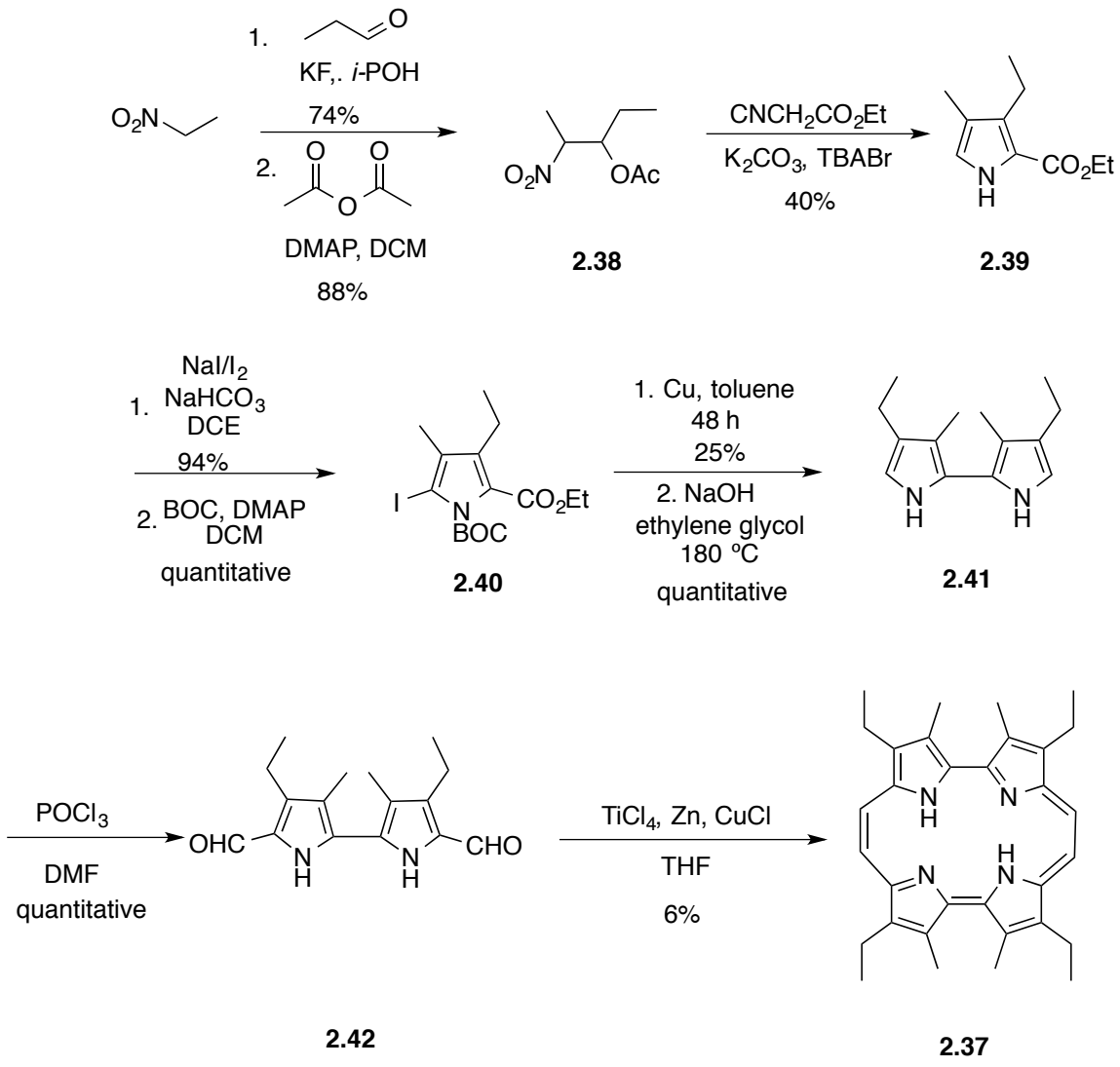

Scheme 2.5: Synthesis of *β*-*β'*-substituted bipyrrole **2.41**[49] and etioporphycene **2.37**.[50]

Attempts to functionalize the etioporphycene nickel(II) complex **2.43** by acylation of the *meso* position (position 9) with ferrocenecarboxamide under Vielsmeier Haack conditions ($POCl_3$ and *N*,*N'*-dimethylferrocenecarboxamide,[52] in 1,2-dichloroethane, or dichlorobenzene at 82 and 118 °C, respectively). Unfortunately, under all the attempted

conditions, only starting material was recovered. This failure was attributed to steric repulsions between the ferrocene derivative and the ethyl groups present on the β-pyrrolic positions in porphycene **2.43**. However, a successful strategy was found that involved reacting compound **2.43** with dimethyl forrmamide (DMF) in the presence of phosphorous oxychloride ($POCl_3$) in 1,2-dicloroethane at 50 ºC.[22] This afforded 9-formyl etioporphycene in 36% yield. As shown in Figure 2.12, the ^{1}H NMR of **2.44** spectrum revealed the appearance of a sharp singlet at δ = 11.62 ppm corresponding to the hydrogen in the aldehyde group, as well as splitting of the porphycene peaks due to the loss of symmetry in the macrocycle. This spectrum was in accordance with what was reported by Kadish and coworkers.[22]

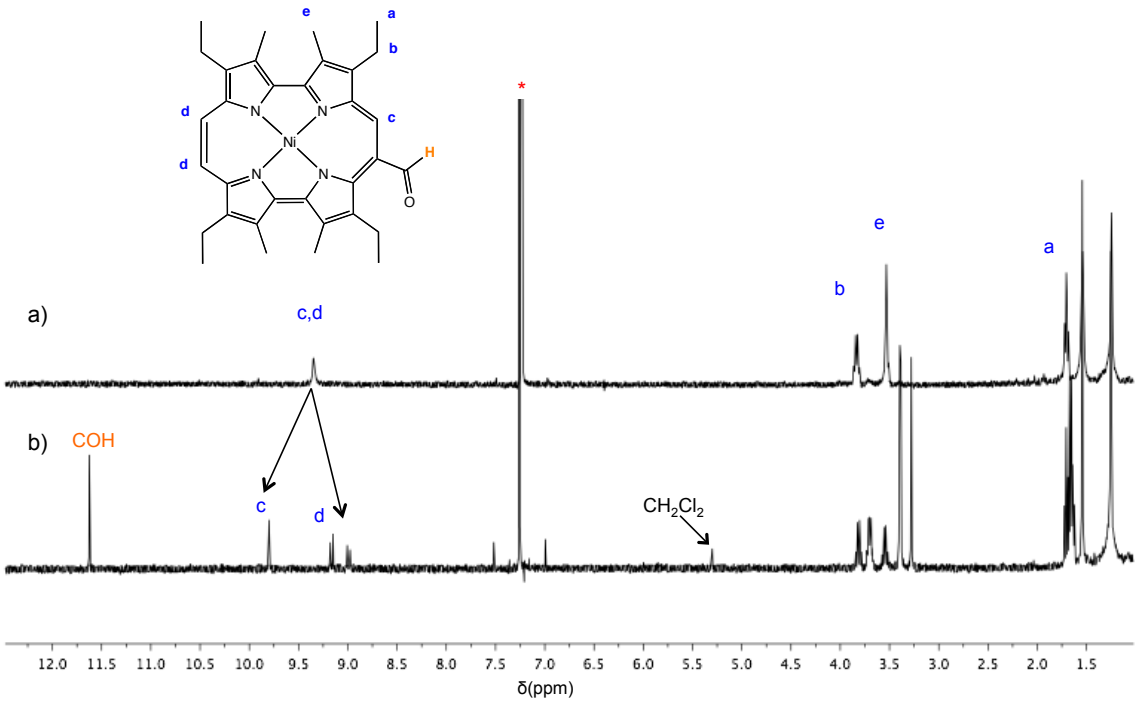

Figure 2.12: ^{1}H NMR spectra of a) etioporphycene-Ni(II) complex, **2.43**, b) 9-formyletioporphycene-Ni(II) complex, **2.44**. * Denotes peaks ascribed to the NMR solvent.

A single crystal of 9-formyletioporphycene-Ni(II) **2.44** was obtained by slow evaporation of CH_2Cl_2. The crystals corresponding to **2.44** grew as clusters of thin, dark green needles. X-ray crystallographic analysis revealed that in **2.44** the Ni cation resides on a position with site symmetry 2/m. This characteristic imparts a loss of symmetry of the ligand. The aldehyde group is disordered about four equivalent positions in the crystal and the atoms of the aldehyde group were assigned site occupancy factors of ¼. To the best of our knowledge, this is the first X-ray structure for a of 9-formyletioporphycene-Ni(II) complex (*cf*. Figure 2.13).

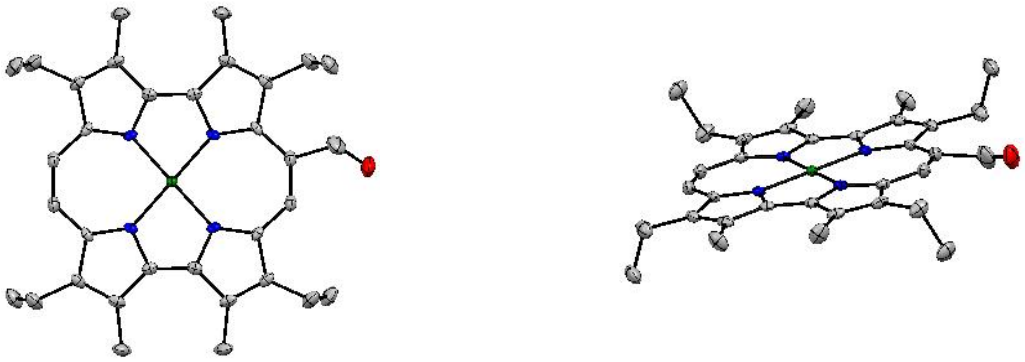

Figure 2.13: Two different views of **2.44**. Displacement ellipsoids are scaled to the 50% probability level. The Ni cation resides within the cavity on a position with crystallographic site symmetry of 2/m at ½, ½, ½. The crystallographic symmetry imposes a disorder on the aldehyde group around four equivalent positions on the ligand.

2.6 Synthesis of 9-Substituted Etioporhycenes Through an Ethenyl Spacer

Compound **2.44** was envisioned as a good building block for the synthesis of ferrocenyletioporphycenes. In this case, a ferrocene ylide could be attached to **2.44** *via* Wittig condensation using a similar synthetic route similar to that described by Wrighton

for the synthesis of ferrocenylvinylporphyrins **2.34** and **2.35** (*cf*. Scheme 2.4 in Section 2.5.2).[44] As shown in Scheme 2.6, (ferrocenylmethyl)-triphenylphosphonium iodide **2.46** was synthesized according to the synthetic route described by Pauson and Watts.[53] Compound **2.46** was deprotonated with either *n*-butyl lithium (n-BuLi) or potassium *t*-butoxide (K*t*BuO) under air and moisture free conditions in tetrahydrofuran (THF) at -78 ºC. Once the ylide **2.46** was formed, it was added to the solution containing porphycene **2.44** in THF to obtain dark purple solution, which changed to blue-green color after quenching with small quantities of methanol.

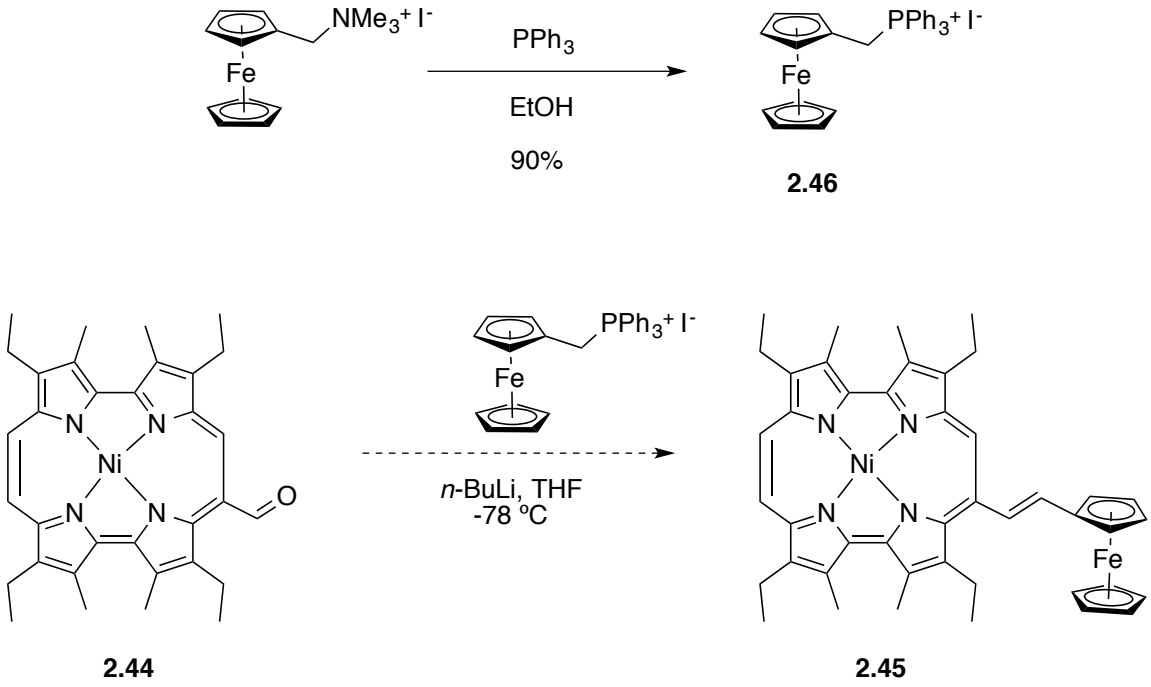

Scheme 2.6: Synthesis of (ferrocenylmethyl)triphenylphosphonium iodide **2.46** and attempted synthesis of 9-ferrocenylvinyletioporphycene **2.45**.

As shown in Figure 2.14, ^{1}H NMR spectroscopic analysis of the blue-green product obtained after chromatography purification provided initial support for the assumption that compound **2.45** had been obtained. The NMR spectrum of **2.45** displayed two new signals at δ = 8.44 to 6.57 ppm, respectively that were assigned to the ethenyl group. Also, a set of multiplets at δ = 7.70 and 7.54, and 5.22, 4.93, and 4.43 ppm that were seen that were ascribed to the ferrocenyl group. However, no satisfactory analysis of this putative product could be obtained *via* high-resolution spectrometry (i.e., (CI+) m/z found 603.3).

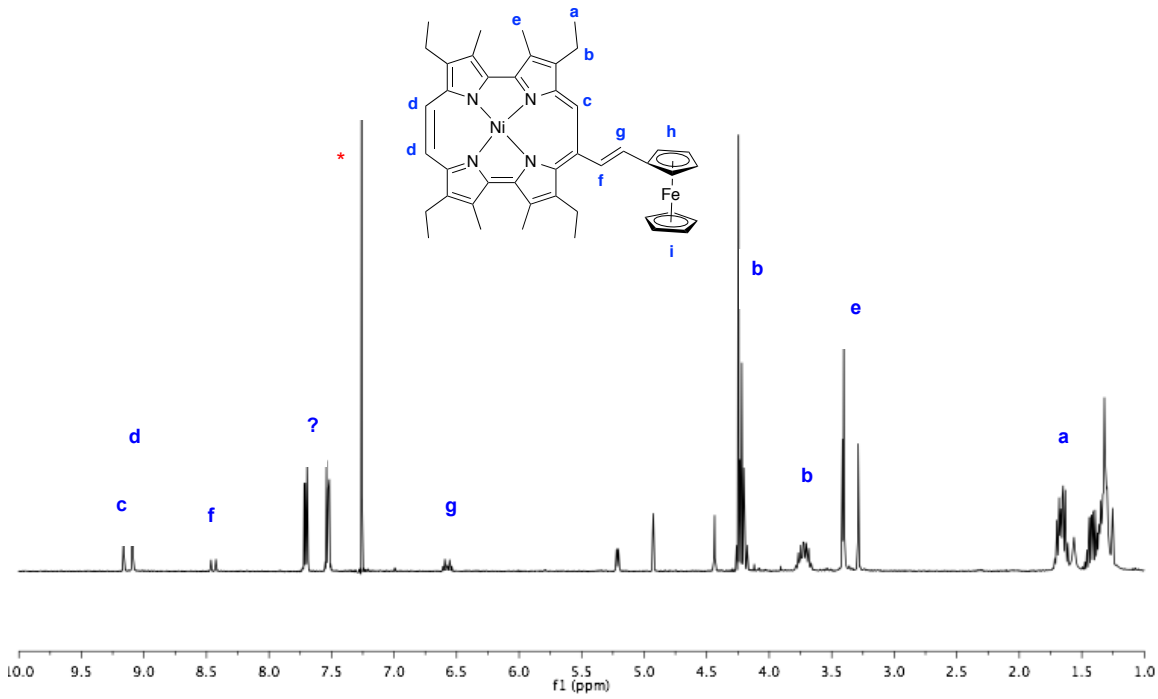

Figure 2.14: ^{1}H NMR spectra of the product from Scheme 2.6 that was tentatively considered to be 9-ferrocenylvinylporphycene **2.45**. The spectrum was recorded in $CDCl_3$. * Denotes peak ascribed to the NMR solvent.

The above results provided a motivation to explore whether the methyl subtituents on the β-pyrrolic positions in **2.44** were preventing reaction with the ylide due to steric hindrance. Thus, *meso* substituted porphycenes **2.47** and **2.48**, with ethenyl bridges were synthesized. As shown in Scheme 2.7, the ylide **2.49** was obtained by deprotonation of the benzyltriphenylphosphonium chloride with lithium bis(trimethylsilyl)amide (LHMDS) in dry THF at -78ºC. The resulting yellow solution was added to a solution of **2.44** in THF to give 9-benzylethenyletioporphycene **2.47** in 31% yield. The synthesis of porphycene **2.48** was achieved by reacting formylporphycene **2.44** with carbethoxymethylene triphenyl phoshorane in xylenes at 144 ºC to afford 9-(propenoate)etioporphcene **2.48** in 44% yield.

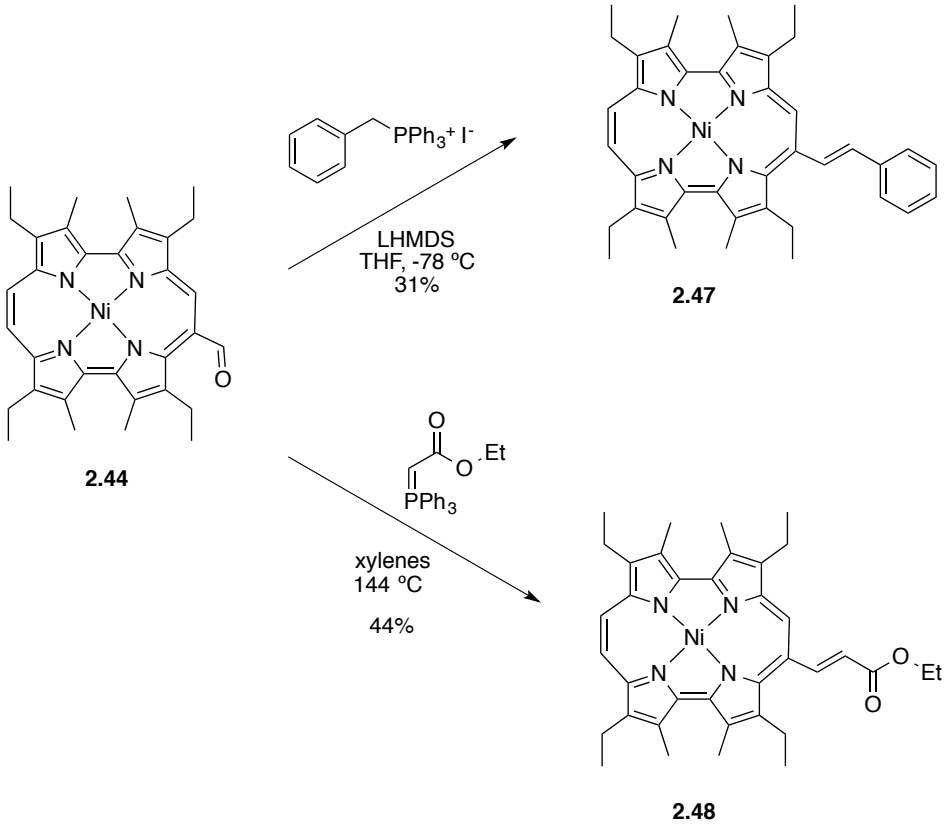

Scheme 2.7: Synthesis of 9-benzyethenylletioporphycene **2.47** and 9-(propenoate)etioporphycene **2.48**.

^{1}H NMR spectroscopic analysis of porphycene **2.47** carried out in $CDCl_3$ at RT, revealed the appearance of two new doublets at δ = 8.76 and 7.16 ppm, which were assigned to the –CH= of the ethenyl group on the *meso* position of the macrocycle. Also, a set of multiples at δ = 7.74-7.33 ppm, corresponding to the benzyl group were identified (*cf*. Figure 2.15). The ^{1}H NMR spectrum of porphycene **2.48** recorded in $CDCl_3$ also displayed new doublets at δ = 9.42 ppm and 6.74 ppm. These doublets were ascribed to the ethenyl group linking the ester group to the macrocyclic core. A new set of signals at δ = 4.43 and 1.43 ppm, corresponding to the ethyl group in the ester was seen (*cf*. Figure 2.15).

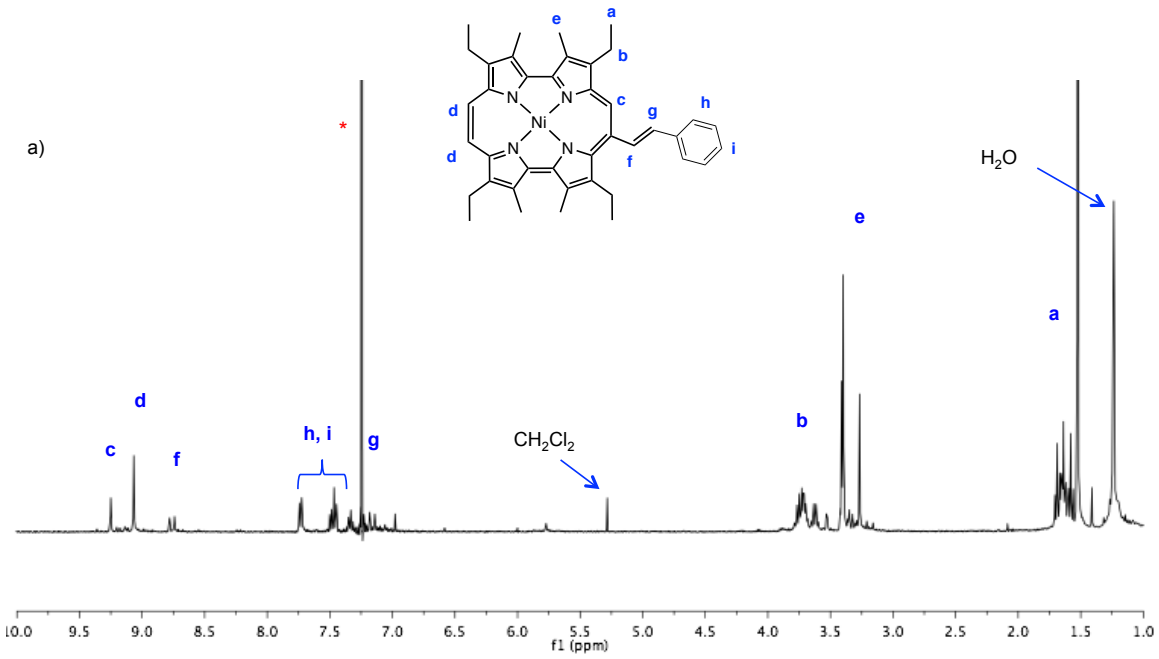

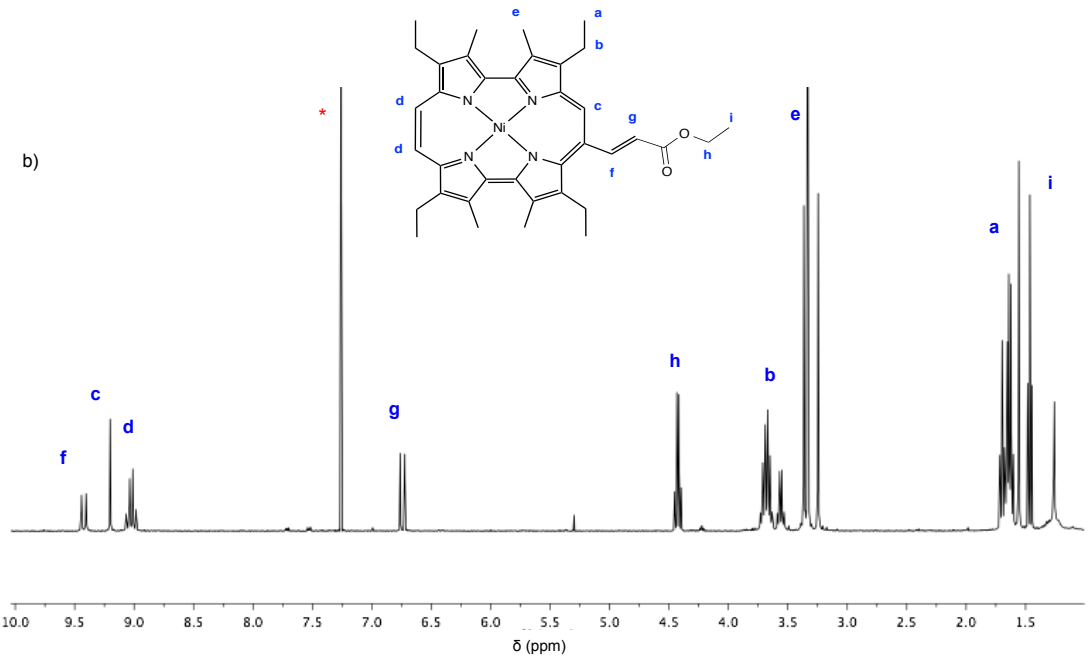

Figure 2.15: ^{1}H NMR spectra of porphycenes a) **2.47** and b) **2.48** recorded in $CDCl_3$. * Denotes peak ascribed to the NMR solvent.

Compound **2.49** was obtained by the reduction of porphycene **2.48** using diisobutyl aluminium hydride (DIBALH) in CH_2Cl_2. This treatment yielded **2.49** in 86% yield after chromatographic purification. Upon the reduction of the ester group to the corresponding alcohol **2.49**, the ^{1}H NMR spectrum of compound **2.49** recorded in $CDCl_3$, revealed the appeareance a new set of signals at δ = 9.12 and 6.56 ppm in the form of a doublet and a multiplet, respectively. These peaks were assigned to –CH= of the ethenyl group on the *meso* position of the porphycene. Additionally, a broad doublet at δ = 4.56 ppm was identified and assigned to the corresponding to the $–CH_2-$ subunit bound to the alcohol group (marked as "h" in Figure 2.16). A broad singlet at δ = 1.55 ppm corresponding to the OH group (*cf*. Figure 2.16).

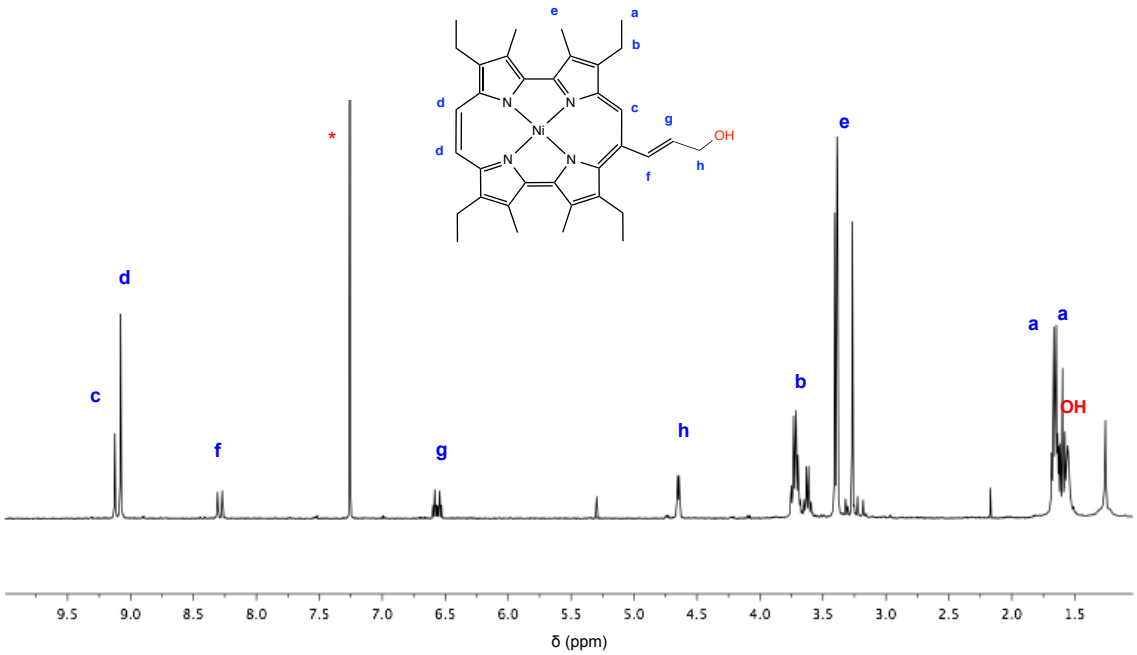

Figure 2.16: ^{1}H NMR spectrum of porphycene **2.49** recorded in $CDCl_3$. * Denotes peak ascribed to the NMR solvent.

Countless efforts using various conditions were made to obtain single crystals of porphycene **2.48** suitable for X-ray diffraction analyses. Unfortunately, under all the attempted crystallization conditions (i.e., slow diffusion of hexanes, pentane, or diethyl ether into CH_2Cl_2, 1,2-dichloroethane, chloroform, THF, benzene, acetonitrile, or dichlorobenzene, or slow evaporation of the same solvents mentioned before), only amorphous solids were obtained. On the other hand, a single crystal of compound **2.49** was obtained as dark blue squares, and these crystals were analyzed by X-ray diffraction. However, the crystals obtained did not refract with a good refinement. Nevertheless, for the sake of completeness, the crystal structure of compound **2.49** is presented in Figure 2.17. The insertion of a propenol group induces a distortion from planarity leading to

ruffled porphycene core. Presumably, this is the result of steric congestion between the ethyl groups on the β-pyrrolic position and the propenol group.

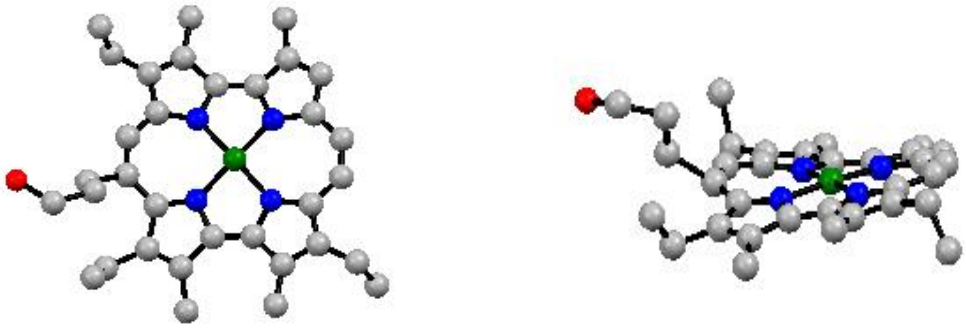

Figure 2.17: Two different views of the low resolution X-ray structure of **2.49**. Hydrogen atoms have been removed from both views for clarity.

2.7 Spectral Features

The absorption spectra of 9-substituted etioporphycenes depend largely on the nature of the specific substituent.[54] In fact, relative to the etioporphycene nickel(II) complex **2.43**, 9-substitution with an aldehyde, a ethenylbenzene, and a propeonate groups, induce significant perturbations. As shown in Figure 2.18 and Table 2.1, for porphycenes **2.44**, **2.47**, and **2.48**, the presence of a substituent in the *meso* position is reflected in a clear broadening of the visible spectral features (Soret and Q-like bands). In the case of **2.44** and **2.48** the introduction of an electron withdrawing group on the *meso* position induces a red shift, as well as a reduction in the relative intensities of both the Soret and Q bands. For instance, the absorption spectrum of **2.44** is characterized a red shift the Soret band (by 25 nm) as compared to the absorption spectrum of **2.43** (i.e., from 389 and 414 nm, for **2.43** and **2.44**, respectively). This shift is attributed to the stronger absorption of blue light by porphycenes **2.44** and **2.48** (*cf*. Table 2.1 and Figure 2.18). The peak at the longest wavelength in all the porphycenes absortion spectra is red-shifted.

In fact, a larger hypsochromic effect was observed for 9-formyletioporphycene **2.44** and 9-benzylethenyletioporphycene **2.47**. Here, the longest wavelength spectral feature is shifted by 53 and 35 nm, respectively, in comparison to **2.43** (i.e., from 604 to 657 nm for **2.43** and **2.44**, and 604 to 639 nm for **2.43** and **2.47**, respectively). Since these absorption bands are attributed to the transition from the HOMO to the LUMO energy level,[6, 52, 54-56] the observed red shift in the absoption spectra provides evidence for a decreasing HOMO-LUMO energy gap as a consequence of the 9-susbtituent.

Analysis of the absorption spectral features of porphycene **2.49** revealed that *meso* substitution with a propenol group induces a more modest red shift (ca. 10nm) in the Soret band than those observed for porphycenes **2.44**, **2.47**, and **2.48**, in comparison to **2.43**. In the case of porphycenes **2.47** and **2.49**, the relative intensity of all the bands is enhanced (*cf*. Tale 2.1). None of the 9-substituted macrocycles displayed appreciable fluorescence intensity when excited at λ = 600 and 400 nm

Compd	**Macrocycle ID**	**λ_{max} (nm) ($\varepsilon \times 10^{-3}$ M^{-1} cm^{-1})**				
2.37	EtioPc	359sh	382	570	617	657
			(144.3)	(32.2)	(18.4)	(30.0)
2.43	EtioPc-Ni	364sh	389	604	-	-
		(450.0)	(138.0)	(13.9)		
2.44	EtioPc-Ni-CHO	-	414	615	657	
			(134.0)	(4.2)	(35.0)	
2.47	EtioPc-Ni-Bz	-	412	639		
			(340.2)	(155.5)		
2.48	EtioPc-Ni-ester	-	419	636		
			(198.9)	(46.0)		
2.49	EtioPc-Ni-COH	-	399	629		
			(289.0)	(117.5)		

Table 2.1: UV-vis data for compounds **2.37**-**2.49** in CH_2Cl_2.

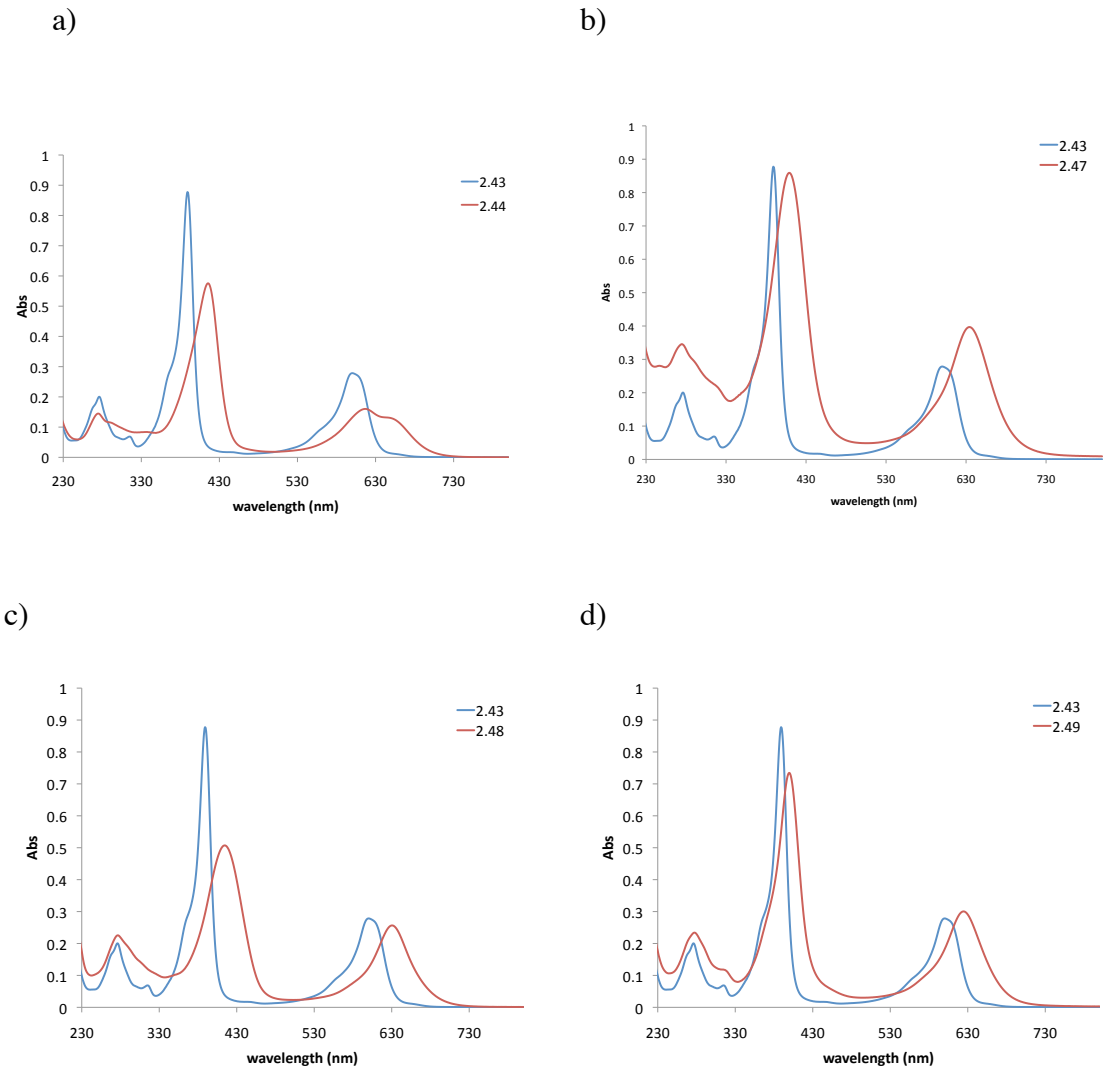

Figure 2.18: Absorption spectra of porphycenes **2.43** (blue) and: a) **2.44** (red), b) **2.47** (red), c) **2.48** (red), and d) **2.49** (red). All the solutions had a concentration of 2.5×10^{-6} M in dry CH_2Cl_2 at 298 K.

2.8 Electrochemistry

The redox properties of the 9-susbtituted porphycenes obtained were analyzed by ciclyc voltametry. In agreement to earlier studies,[22] the electrochemistry of porphycenes **2.43** and **2.44**, were characterized by the presence of two well-defined oxidation and two reduction waves (*cf*. Table 2.2 and Figure 2.19). Cyclic voltamograms of porphycenes **2.37**, **2.43**, **2.44**, **2.48**, and **2.49** were recorded in anhydrous benzonitrile, using 0.1 M $TBAPF_6$ as the supporting electrolyte. These analyses revealed the presence of redox waves similar to those of the unsubstituted nickel(II) complex **2.43**, Table 2.3. However, the oxidation potential peaks of the 9-substituted porphycenes appeared to be broader. In fact, this effect is enhanced when an ethenyl spacer was introduced. The absolute potential separation ($\Delta E_{1/2}$) between these two reductions of the 9-substituted porphycenes varies between 200 and 340 mV. Compound **2.47** could not be studied by electrochemical methods due to the small amount of sample obtained.

In addition, easier reductions and harder oxidations were observed for 9-formylporphycene **2.44** relative to **2.43**. Particularly, the direct substitution of a formyl group on the porphycene **2.44** produced a system that was easier to reduce than the unsubtituted porphycenes **2.37** and **2.43**. Shifts of 14 and 27 mV, respectively in the corresponding waves were observed. Compared with other 9-subtituted porphycenes containing an ethenyl spacer (e.g., porphycenes **2.48** and **2.49**), porphycene **2.44** proved harder to oxidize but easier to reduce. For instance, compound **2.44** is reduced at –0.86 V in benzonitrile as compared to compound **2.48** and **2.49** where the electroreduction occurs at –1.08, and –1.15 V, respectively, under the same conditions (*cf*. Table 2.2 and Figure 2.19). The lower reduction potential values and the decrease in the electrochemical HUMO-LUMO gap (HLG) of 9-formyletioporphycene **2.44** with respect to **2.43**, is evidence for a higher level of electron acceptor character arising through direct substitution with an electron withdrawing group (formyl group) in the *meso* position.

This effect may reflect a redistribution of the electron density present in the macrocyclic core.

		$E_{1/2}$, V *vs* SCE					
		Ring oxidation		Ring reduction			
Compd	**Macrocycle ID**	**2nd**	**1st**	**1st**	**2nd**	**HLG (V)**	**$\Delta E_{1/2}$ (mV)**
2.37	EtioPc	-	-	-1.00	-1.20	-	200
2.43	EtioPc-Ni	-	0.76	-1.13	-1.40	1.89	270
2.44	EtioPc-Ni-CHO	-	0.95	-0.86	-1.20	1.81	340
2.48	EtioPc-Ni-ester	-	-	-1.10	-1.35	-	220
2.49	EtioPc-Ni-COH	-	-	-1.15	-1.45	-	300

Table 2.2: Potentials (V *vs* SCE) for the oxidation and reduction of investigated etioporphycene, **2.37**, and the 9-substituted porphycenes **2.43**, **2.44**, **2.48**, and **2.49** in benzonitrile containing 0.1 M $TBAPF_6$. The absolute potential difference ($\Delta E_{1/2}$) was calculated between the two reduction peaks. HOMO-LUMO gap (HLG) was calculated between the first reduction potential and the first oxidation potential. Peak potentials at 50 mV/s.

The functionalization of etioporphycene with a propenol group on the *meso* position (compound **2.49**), leads not only to a loss of symmetry but also an electron donating inductive effect. These factors are thought to affect the electronics of the porphycene. Evidence for this perturbation is seen when the electrochemistry of the 9-propenoletioporphycene **2.49** is compared with that of the etioporphycene-Ni(II) complex **2.43**. Under the same electrochemical conditions **2.49** proved harder to reduce. For instance, two reductions at $E_{1/2}$ = –1.15 and –1.45 V for **2.49**, and – 1.13 and – 1.40 V for **2.43**. Unfortunately, the HUMO-LUMO gap of **2.49** could not be calculated due to irreversible nature of the oxidation processes (*cf*. Table 2.2).

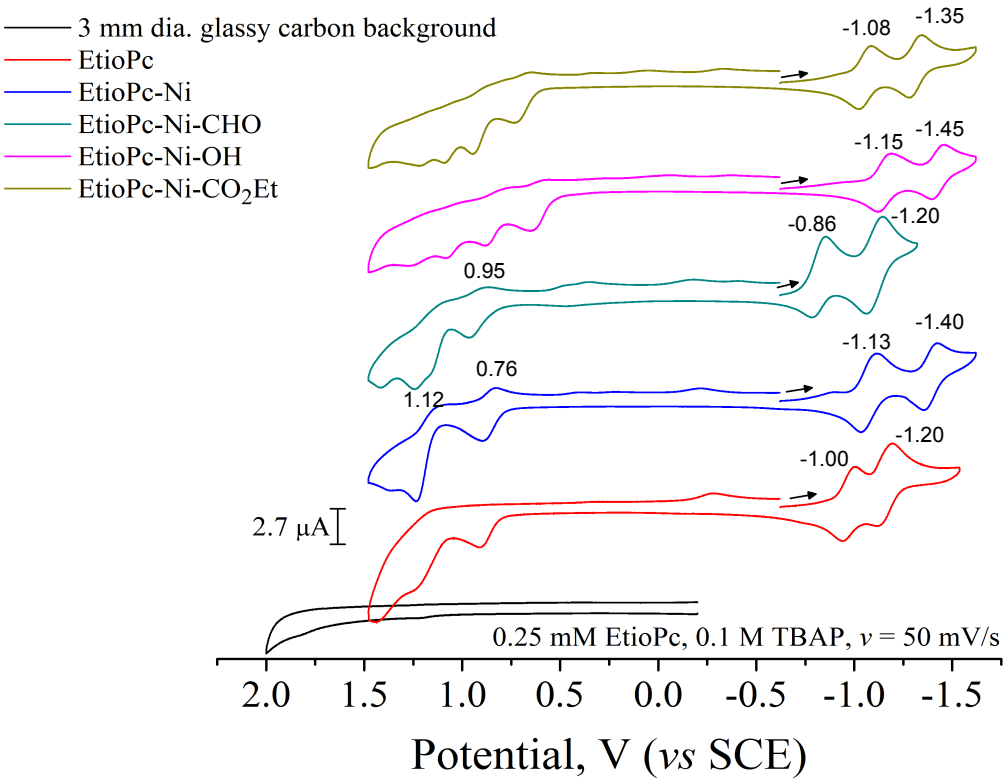

Figure 2.19: Cyclic voltammograms recorded at 298 K for 0.25 mM solutions of etioporphycenes **2.37**, **2.43**, **2.44**, **2.48**, and **2.49**. All voltammograms were recorded using anhydrous benzonitrile. The electrodes were a glassy carbon (Ø = 3 mm^2) for the working electrode, a Pt wire as the counter electrode and a saturated calomel electrode, employed as the reference electrode (SCE). The supporting electrolyte was $TBAPF_6$ (0.1 M).

2.9 Conclusions

The synthesis of several 9-substituted porphycenes was successfully accomplished. 9-substituted porphycenes **2.44**, **2.47**, **2.48**, and **2.49** were obtained either by direct formylation of the porphycene-Ni(II) complex or *via* use of a Wittig reaction between **2.44** and the corresponding ylide. These porphycenes were characterized by optical spectroscopy, ^{1}H and ^{13}C NMR spectroscopy, and electrochemical analysis. In the case of compounds **2.44** and **2.49**, the characterization also included single crystal analysis. Porphycene **2.44** was found to be easier to reduce and harder to oxidize than the initial nickel complex **2.43**. This finding was considered to reflect a negative inductive effect produced by the formyl group on the macrocyclic core. Conversely, 9-substitution of etioporphycenes through a conjugated spacer group (ethenyl) resulted in macrocycles that are harder to reduce but easier to oxidized. However, these systems did not display reversible electrooxidation features in the cyclic voltammogram. Wittig coupling between porphycene **2.44** and the ferrocenyl ylide **2.46** was explored. Unfortunately, the resulting product, tentatively asigned as porphycene **2.45** could not be charcatrized in a definite manner. For instance, no satisfactory mass spectromatogram was otained. Nor were the characteristic ferrocene features seen by cyclic voltametry. These results, taken in concert, led to the conclusion that the target sought in the context of this project, namely the 9-ferroceneethenyletioporphycene **2.45**, was simply not obtained.

2.10 References

1. Milgrom, L. R. *The Colours of Life: An Introduction to the Chemistry of Porphyrins and Related Compounds*, Oxford University Press, Oxford, **1997**.

2. *The Porphyrin Handbook*, Vol. 6, Academic Press, San Diego, **2000**, pp. 157-168, 196-198.

3. Sessler, J. L.; Weghorn, S. J. *Expanded, Contracted & Isomeric Porphyrins*, Tetrahedron Organic Chemistry Series, Vol. 15. Pergamon, Great Britain, **1997**, pp. 127-177.

4. Grosmann, M.; Franck, B. *Angew. Chem. Int. Ed. Engl.* **1986**, *25*, 1100.

5. Vogel, E.; Köcher, M.; Schmickler, H.; Lex, J. *Angew. Chem. Int. Ed. Engl.* **1986**, *25*, 257.

6. Sánchez-García, D.; Sessler, J. L. *Chem. Soc. Rev.* **2008**, *37*, 215.

7. D'Souza, F.; Boulas, P.; Aukauloo, A. M.; Guilard, R.; Kisters, M.; Vogel, E.; Kadish, K. M. *J. Phys. Chem.* **1994**, *98*, 11885.

8. Vogel, E.; Kocher, M.; Lex, J.; Ermer, O. *Isr. J. Chem.* **1989**, *29*, 257.

9. Anju, K. S.; Ramakrishnan, S.; Thomas, A. P.; Suresh, E.; Srinivasan, A. *Org. Lett.* **2008**, *10*, 5545.

10. McMurry, J. E.; Fleming, M. P. *J. Am. Chem. Soc.* **1974**, *96*, 4708.

11. Vogel, E.; Grigat, I.; Köcher, M.; Lex, J. *Angew. Chem.* **1989**, *101*, 1687.

12. Vogel, E.; Grigat, I.; Köcher, M.; Lex, J. *Angew. Chem. Int. Ed. Engl.* **1989**, *28*, 1655.

13. Vogel, E. *Pure & Appl. Chem.* **1990**, *62*, 557.

14. Kuzuhara, D.; Yamada, H.; Yano, K.; Okujima, T.; Mori, S.; Uno, H. *Chem. Eur. J.* **2011**, *17*, 3376.

15. Vogel, E.; Koch, P. A.; Rahbar, A.; Cross, A. D. *US. Pat.,* 5 262 401, 1992.

16. Vogel, E.; Benninghaus, T.; Richert, C.; Müller, M.; Cross, A. D. *US. Pat.,* 5 179 120, 1992.

17. Vogel, E.; Clemens, R.; Benninghaus, T.; Müller, M.; Cross, A. D. *US. Pat.*, 5 409 900, 1996.

18. Vogel, E.; Müller, M.; Halpern, O.; Cross, A. D. *US. Pat.*, 5 409 900, 1996.

19. Vogel, E.; Müller, M.; Halpern, O.; Cross, A. D. *US. Pat.*, 5 610 175, 1997.

20. Vogel, E.; Müller, M.; Halpern, O.; Cross, A. D. *US. Pat.*, 5 637 608, 1997.

21. Porter, H. K. *Org. React.* **1973**, *20*, 455.

22. D'Souza, F.; Boulas, P. L.; Kristers, M.; Sambrotta, L.; Aukauloo, A. M.; Guilard, R.; Kadish, K. M. *Inorg. Chem.* **1996**, *35*, 5743.

23. Braslavsky, S. E.; Müller, M.; Mártire, D. O.; Pörting, S.; Bertolotti, S. G.; Chakravorti, S.; Koç-Weier, G.; Knipp, B.; Schaffner, K. *J. Photochem. Photobiol., B.* **1997**, *40*, 191.

24. Costa, R. D.; Malig, J.; Brenner, W.; Jux, N.; Guldi, D. M. *Adv. Mater.* **2013**, 1.

25. Wasielewski, M. R. *Chem. Rev.* **1992**, *92*, 435.

26. Gust, D.; Moore, T. A.; Moore, A. L. *Acc. Chem. Res.* **1993**, *26*, 198.

27. Health, J. R.; Kuekes, P. J.; Snider, G. S.; Williams, R. S. *Science* **1998**, *280*, 1716.

28. Beer, P. D.; Gale, P. A.; Chen, G. Z. *Coord. Chem. Rev.* **1999**, *185/186*, 3.

29. Bard, A. J. *Nature* **1995**, *374*, 13.

30. Bucher, C.; Devillers, C. H.; Moutet, J.-C.; Royal, G.; Saint-Aman, E. *Coord. Chem. Rev.* **2009**, *253*, 21.

31. Narayan, S. J.; Venkatraman, S.; Dey, S. R.; Sridevi, B.; Anand, V. R. G.; Chandrashekar, T. K. *Synlett.* **2000**, *12*, 1834.

32. Lindsey, J. S.; Schreiman, I. C.; Hsu, H. C.; Kearney, P. C.; Marguerettaz, A. M. *J. Org. Chem.* **1987**, *52*, 827.

33. Lindsey, J. S.; Hsu, H. C.; Schreiman, I. C. *Tetrahedron Lett.* **1986**, *41*, 1900.

34. Nemykin, V. N.; Barrett, C. D.; Hadt, R. G.; Subbotin, R. I.; Maximov, A. Y.; Plshin, E. V.; Koposcov, A. Y. *Dalton Trans.* **2007**, *31*, 3378.

35. Gryko, D. T.; Zhao, F.; Yasseri, A. A.; Roth, K. M.; Bocian, D. F.; Kuhr, W. G.; Lindsey, J. S. *J. Org. Chem.* **2000**, *65*, 7356.

36. Boyd, P. D. W.; Burrell, A. K.; Campbell, W. M.; Cocks, P. A.; Gordon, K. C.; Jameson, G. B.; Officer, D. L.; Zhao, Z. *Chem. Commun.* **1999**, 637.

37. Rhee, S. W.; Na, Y. H.; Do, Y.; Kim, J. *Inorg. Chim. Acta* **2000**, *49*, 309.

38. Rhee, S. W.; Park, B. B.; Do, Y.; Kim, J. *Polyhedron* **2000**, *19*, 1961.

39. Adler, A. D.; Longo, F. R.; Finarelli, J. D.; Goldmacher, J.; Assour, J. Korsakoff, L. *J. Org. Chem.* **1967**, *32*, 467.

40. Wei, L.; Padmaja, K.; Youngblood, W. J.; Lysenko, A. B.; Lindsey, J. S.; Bocian, D. F. *J. Org. Chem.* **2004**, *69*, 1461.

41. Kalita, D.; Morise, M.; Kobuke, Y. *New J. Chem.* **2006**, *30*, 77.

42. Ambroise, A.; Wagner, R. W.; Rao, P. D.; Riggs, J. A.; Hascoat, P.; Diers, J. R.; Seth, J.; Lammi, R. K.; Bocian, D. F.; Holten, D.; Lindsey, J. S. *Chem. Mater.* **2001**, *13*, 1023.

43. Poon, K.-W.; Liu, W.; Chan, P.-K.; Yang, Q.; Chan T.-W. D.; Mak, T. C. W.; Ng, D. K. P. *J. Org. Chem.* **2001**, *66*, 1553.

44. Giasson, R.; Lee, E. J.; Zhao, X.; Wrighton, M. *J. Phys. Chem.* **1993**, *97*, 2596.

45. a) Imohori, H.; Kimura, M.; Hosomizu, K.; Sato, T.; Ahn, T. K.; Kim, S. K.; Kim, D.; Nishimura, Y.; Yamazaki, I.; Araki, Y.; Ito, O.; Fukuzumi, S. *Chem. Eur. J.* **2004**, *10*, 5111. b) Imahori, H.; Sekiguchi, Y.; Kashiwagi, Y.; Sato, T.; Araki, Y.; Ito, O.; Yamada, H.; Fukuzumi, S. *Chem. Eur. J.* **2004**, *10*, 3184.

46. Barton, D. H. R.; Zard, S. Z. *J. Chem. Soc., Chem Commun.* **1985**, 1098.

47. Barton, D. H. R.; Kervagoret, J.; Zard, S. Z. *Tetrahedron* **1990**, *46*, 7585.

48. Sessler. J. L.; Cyr, M. J.; Burrell, A. K. *Synlett.* **1991**, 127.

49. Bobál, P.; Lightner, D. A. *J. Heterocyclic Chem.* **2001**, *38*, 527.

50. Sessler, J. L.; Hoehner, M. C. *Synlett.* **1994**, *3*, 211.

51. Guilard, R.; Aukauloo, M. A.; Tardieux, C.; Vogel, E. *Synthesis* **1995**, 1480.

52. Hu, J.; Barbour, L. J.; Gokel, G. W. *New. J. Chem.* **2004**, *28*, 907.

53. Pauson, P. L.; Watts, W. E. *J. Chem. Soc.* **1963**, 2990.

54. Vogel, E.; Balci, M.; Pramod, K.; Koch, P.; Lex, J.; Ermer, O. *Angew. Chem. Int. Ed. Engl.* **1987**, *26*, 928.

55. Vogel, E.; Koch, P.; Hou, X.-L.; Lex, J.; Lausmann, M.; Kisters, M.; Aukauloo, M. A.; Richard, P.; Guilard, R. *Angew. Chem. Int. Ed. Engl.* **1993**, *32*, 1600.

56. Arad, O.; Rubio, N.; Sánchez-García, D.; Borrell, J. I.; Nonell, S. *J. Porphyrins Phthalocyanines* **2009**, *13*, 376.

Chapter 3: Experimental Procedures

Prior to use, all glassware was soaked in KOH-saturated isopropyl alcohol overnight, then washed with water and acetone, and dried for ca. 12 h at 120 °C. Tetrahydrofuran (THF) was dried by passage through two columns of activated alumina. Acetonitrile (MeCN), methanol (MeOH), and dimethylformamide (DMF) were dried by passage through two columns of molecular sieves. When used as the reaction medium, dichloromethane (CH_2Cl_2) was freshly distilled from CaH_2. CH_2Cl_2 used for chromatographic purifications was used as received from Fisher Scientific. Triethyl amine (TEA) was distilled from BaO. Hexanes were purchased from Fisher Scientific and used as received. All other chemicals used were purchased from Aldrich, TCI, Acros, or Strem and used without further purification.

TLC analyses were carried out using Sorbent Technologies silica gel (200 mm) sheets. Column chromatography was performed on Sorbent silica gel 60 O (40-60 mm) or neutral alumina (50-200 mm, Brockman grade II). The purification of compound **1.2** was carried out using a Teledyne CombiFlash Companion with a neutral alumina column. High Performance Liquid Chromatography (HPLC) analyses were performed on a Shimadzu Analytical/Preparative HPLC system equipped with PDA detector and a Nova-Pak® silica 4 μm 3.9 × 150 mm cartridge. A TRIS buffer (pH = 9)/MeCN gradient (10-99% TRIS over 20 minutes) was used for the analysis of **1.2**. A 1% TFA/MeCN gradient (10-99% over 20 minutes) was used to follow the hydrolysis of this compound.

pH values were obtained using an ORION SA pH/ISE meter model 720. The calibrations were performed using buffer standard solutions (pH 4, 7, and 10). These buffer solutions were obtained form Fischer Scientific and used as received.

Nuclear magnetic resonance (NMR). NMR spectra were recorded on a Varian Mercury 400 MHz, a Variant MR 400 MHz, or a Agilent MR 400 MHz instrument. The NMR spectra were referenced to solvent and all the solvents were purchased from Cambridge Isotope Laboratories. All chemical shifts (δ) are reported in ppm and

referenced to the solvent. Chemical ionization (CI) and electrospray ionization (ESI) mass spectrograms, were recorded using a VG ZAB-2E instrument and a VG AutoSpec apparatus, respectively.

Electronic parmagnetic resonance spectra (EPR). Spectra were recorded by the author on a Bruker EMX Plus spectrometer at 298 K using CH_2Cl_2 as solvent.

Absorption spectra. UV-Vis absorption spectra were recorded on a Varian Cary 5000 spectrophotometer. All the spectra were measured in dry CH_2Cl_2, which was purchased commercially and distilled from CaH_2.

Electrochemistry. The electrochemical measurements were carried out by Netzahualcoyotl Arroyo and the author in the group of Prof. Alan J. Bard at the University of Texas at Austin. Tetra-*n*-butylammonium hexafluorophosphate ($TBAPF_6$) was used as the supporting electrolyte and it was recrystallized from ethanol/water (4:1) twice and dried at 100 °C before use. Benzonitrile (Aldrich, anhydrous, UV grade) was used as received after being transported unopened into an inert atmosphere drybox (Bosch). Cyclic voltammetry was carried out in a three-electrode cell, which consisted of a glassy carbon bottom used as working electrode, a platinum-wire counter electrode, and a saturated calomel electrode (SCE) used as a reference electrode. A model 660 electrochemical workstation (CH instruments, Austin, TX) was used for these measurements with a scan rate of 0.1 V/s. A glassy carbon electrode with area of 3 mm^2 was used for all experiments.

Isothermal titration calorimetry (ITC). Microcalorimetric calculations were carried out using an Isothermal Titration Calorimeter (ITC) purchased from Microcal Inc., MA. Solutions were prepared using spectral grade acetonitrile in the concentration range ~ 0.3 mM. These solutions were added to the calorimetry cell and 3 mM solutions of the tetraalkylammonium anion salt under consideration were introduced in the form of 50-30 (3-6 μL) injections at 30 and 25 ± 0.01 ºC. The original heat pulses were normalized using reference titrations carried out using the same salts solution but pure

solvent, as opposed to a solution containing the receptor. Binding constants were calculated by applying either one-site or two-site models using ORIGIN software provided by Microcal Inc.

3.1 Synthetic Details and Characterization Data

β-Bromoethyl acetophenone (1.38). A mixture of 3-hydroxyacetophenone (5g, 36 mmol), dibromoethane (68.97 g, 0.36 mol), potassium carbonate (10.15 g, 73 mmol) and acetonitrile (150 mL) was warmed at 60 °C for 7 days. After cooling, the mixture was filtered through a pad of celite and concentrated under reduced pressure. The oily residue was purified by column chromatography over silica gel (hexanes / EtOAc = 7:3, v/v), yielding the compound **1.38** (7.5 g, 84.3%). ^{1}H NMR ($CDCl_3$): δ (ppm) = 7.53 (dd, *J* = 8 Hz, Ar-H, 1H), 7.44 (bs, Ar-H, 1H), 7.32 (t, *J* = 4 Hz, Ar-H, 1H), 7.08 (dd, *J* = 11.2 Hz, Ar-H, 1H), 4.29 (t, *J* = 6 Hz, -O-$\mathbf{CH_2}CH_2$-Br, 2H), 3.63 (t, *J* = 6 Hz, -O-$CH_2\mathbf{CH_2}$-Br, 2H), 3.60 (s, C(O)$\mathbf{CH_3}$, 3H). ^{13}C NMR ($CDCl_3$): δ (ppm) = 202.0, 167.4, 140.3, 130.6, 122.7, 118.8, 66.3, 29.9, 27.4. HRMS (CI+) m/z calculated for ($C_{10}H_{11}O_2Br$) 241.9942, found 241.9944.

***N*-(3-Phenoxyethyl-one)phthalimide (1.39).** A mixture of **(1.38)** (7.32 g, 0.030 mol), potassium phthalimide (6.69 g, 36 mmol), and 100 mL of anhydrous dimethylformamide (100 mL) was warmed at 85°C for 12 h. After cooling, dichloromethane was added and the resulting mixture was washed with 0.2 M aqueous sodium hydroxide, dried over sodium sulfate, and concentrated under reduced pressure. The oily residue was purified by column chromatography over silica gel (hexanes/EtOAc = 6:4, v/v), yielding compound **1.39** (4.5 g, 46.8%) as a white solid. ^{1}H NMR ($CDCl_3$): δ (ppm) = 7.85 (m, phthalimide Ar-H, 2H), 7.71 (m, phthalimide Ar-H, 2H), 7.51 (dd, *J* = 7.2 Hz, Ar-H, 1H), 7.49 (s, Ar-H, 1H), 7.32 (t, *J* = 8 Hz, Ar-H, 1H), 7.06 (dd, *J* = 12 Hz, Ar-H, 1H), 4.27 (t, *J* = 5.6 Hz, -O$\mathbf{CH_2}CH_2$N-, 2H), 4.11 (t, *J* = 5.6 Hz, -$OCH_2\mathbf{CH_2}$N-, 2H), 2.55 (s, C(O)$\mathbf{CH_3}$, 3H). ^{13}C NMR ($CDCl_3$): δ (ppm) = 134.1, 132.0, 129.6, 123.4, 121.4, 120.0, 113.3, 64.9, 37.2, 26.7. HRMS (CI+) m/z calculated for ($C_{18}H_{15}NO_4$) 309.1239, found ($C_{18}H_{15}NO_4$) 309.1241.

2-(2-(3-(1,1-Di(1 *H* pyrrol-2-yl)ethyl)phenoxy)ethyl)isoindoline-1,3-dione (1.40). A solution of **(1.39)** (4.4 g, 14 mmol) was dissolved in pyrrole (28.8 g, 0.43 mol) and a catalytic amount of trifluoroacetic acid (4.5 mL) was added dropwise for 15 min. The mixture was heated at 60°C for 12 h. The crude product was obtained by dilution with dichloromethane, washing with 2 M aqueous sodium hydroxide. The organic fractions were collected and concentrated under reduced pressure. Vacuum distillation was then used to remove excess of pyrrole affording a brownish solid, which was purified by column chromatography over silica gel (hexanes/EtOAc = 8:2, v/v), yielding the compound **1.40** (2.15 g, 35.5%) as a pale yellow solid. ^{1}H NMR ($CDCl_3$): δ (ppm) = 7.83 (m, phthalimide Ar-H, 2H), 7.81 (bs, N-H, 2H), 7.70 (m, phthalimide Ar-H, 2H), 7.12 (t, *J* = 8 Hz, Ar-H, 1H), 6.67 (dd, *J* = 8 Hz, Ar-H, 1H), 6.66 (m, Ar-H and CH-pyrrole, 3H), 6.13 (m, CH-pyrrole, 2H), 5.95 (m, CH-pyrrole, 2H), 4.15 (t, *J* = 5.6 Hz, -O**C**$\mathbf{H_2}$$CH_2$N-, 2H), 4.04 (t, *J* = 5.6 Hz, -OCH_2**C**$\mathbf{H_2}$N-, 2H), 1.99 (s, **C**$\mathbf{H_3}$, 3H). ^{13}C NMR ($CDCl_3$): δ (ppm) = 160.9, 159.5, 145.6, 130.2, 131.2, 129.7, 125.7, 122.3, 118.1, 110.0, 108.8, 107.9, 66.7, 50.2, 25.6. HRMS (CI+) m/z calculated for ($C_{26}H_{23}N_3O_3$) 425.1739, found ($C_{26}H_{23}N_3O_3$) 425.1827.

***meso-N*-(3-Phenoxyethylamine)-3-one (1.41).** A mixture of **1.40** (1 g, 2 mmol), hydrazine hydrate (0.19 g, 2.4 mmol) was dissolved in methanol (15 mL). The mixture was heated at reflux for 2 h. The cooled mixture was filtered and the filtrate was concentrated under reduced pressure to obtain a white solid. The solid obtained was suspended in diethyl ether and treated with 40% w/w aqueous potassium hydroxide. The compound was extracted into diethyl ether (3 × 50 mL). The combined organics were dried over Na_2SO_4 and concentrated under reduced pressure to give a light yellow oil **1.41** (0.62 g, 89.9%). ^{1}H NMR ($CDCl_3$): δ (ppm) = 7.83 (bs, N-H, 2H), 7.17 (t, *J* = 8 Hz, Ar-H, 1H), 6.75-6.67 (m, Ar-H, 3H), 6.64 (m, C-H pyrrole, 2H), 6.15 (m, C-H pyrrole, 2H), 5.96 (m, C-H pyrrole, 2H), 3.88 (t, *J* = 4.8 Hz, -O**C**$\mathbf{H_2}$$CH_2$N-, 2H), 3.00 (t, *J* = 5.2 Hz, -OCH_2**C**$\mathbf{H_2}$N-, 2H), 2.02 (s, **C**$\mathbf{H_3}$, 3H). No ^{13}C NMR data were obtained for this sample. HRMS (CI+) m/z calculated for ($C_{18}H_{21}N_3O$) 295.1685, found ($C_{18}H_{21}N_3O$) 295.1718.

Bis-dipyrromethane (1.41a). 2,6-Pyridinecarbonyl dichloride (1.24 g, 6 mmol) and the compound **1.41** (3.6 g, 1.2 mmol) were dissolved in THF (200 mL), TEA (1.2 g, 1.2 mmol) was added to the mixture, which was let stir for 3 h. The solution was then washed with a saturated solution of $NaHCO_3$ (100 mL), and extracted with CH_2Cl_2 (4 × 50 mL). The combined organic layers were dried over Na_2SO_4 and concentrated under reduced pressure. The crude materials obtained in this way was purified by column chromatography over silica gel (CH_2Cl_2/MeOH = 98:2, v/v), yielding the compound **1.41a** (0.82**,** 18.7%). ^{1}H NMR ($CDCl_3$): δ (ppm) = 8.35 (t, *J* = 6 Hz, C(O)N-**H**, 2H), 8.23 (dd, *J* = 8 Hz, C-**H** pyridine, 2H), 8.08 (bs, N-**H**, 4H), 7.92 (t, *J* = 8 Hz, C-**H** pyridine, 1H), 7.09 (t, *J* = 7.6 Hz, Ar-**H**, 1H), 6.71-6.64 (m, Ar-**H**, 6H), 6.59 (m, C-**H** pyrrole, 4H), 6.11 (m, C-**H** pyrrole, 4H), 5.93 (m, C-**H** pyrrole, 4H), 3.98 (t, *J* = 4.8 Hz, -O**CH$_2$**CH$_2$N-, 4H), 3.72 (q, *J* = 5.6 Hz, -OCH$_2$**CH$_2$**N-, 4H), 1.98 (s, **CH$_3$**, 6H). No ^{13}C NMR data were obtained for this sample. HRMS (ESI+) m/z calculated for ($C_{43}H_{43}N_7O_4$) 721.8577, found ($C_{43}H_{43}N_7O_4Na$) 744.3271.

Bis-dipyrromethane tetraaldehyde (1.42). To a solution of **1.41a** (0.5 g 0.69 mmol) in DMF (5 mL), phosphorous oxychloride ($POCl_3$) (0.43 g, 2 mmol) was added dropwise for 15 min. The reaction mixture was stirred for 1 h. Water was added to the mixture and 2 M potassium hydroxide was added until the pH was strongly basic to give a yellow solid, which was collected by filtration and washed with plenty of water. This yielded the compound **1.42** (0.3 g, 52%) as a pale yellow solid. ^{1}H NMR (DMSO-d_6): δ (ppm) = 11.98 (bs, N-**H**, 4H), 9.51 (m, C(O)N-**H**, 2H), 8.39 (s, C**H**O, 4H), 8.17 (m, C-**H** pyridine, 3H), 7.22 (t, *J* = 8.4 Hz, Ar-**H**, 2H), 6.92 (s, Ar-**H**, 2H), 6.89 (m, C-**H** pyrrole, 4H), 6. 54 (d, *J* = 7.2 Hz, Ar-**H**, 2H), 5.89 (m, C-**H** pyrrole, 4H), 4.07 (t, *J* = 6 Hz, -O**CH$_2$**CH$_2$N-, 4H), 3.70 (q, *J* = 5.6 Hz, -OCH$_2$**CH$_2$**N-, 4H), 2.05 (s, **CH$_3$**, 6H). ^{13}C NMR (DMSO_d_6): δ (ppm) = 184.7, 179.5, 163.9, 158.5, 148.3, 146.0, 133.6, 114.7, 110.7, 88.6, 55.7, 45.7, 27.8. HMRS (ESI+) m/z calculated for ($C_{43}H_{43}N_7O_8$) 833.3932, found ($C_{43}H_{43}N_7O_8Na$) 856.3076.

Strapped calixpyrrole Schiff-base macrocycle (1.2). To a solution of **1.42** (0.1 g, 0.12 mmol) in a mixture CH_2Cl_2/MeOH (1:9, v/v, 150 mL) was added *o*-

phenyldiamine (0.025 g, 0.24 mmol), and *p*-toluensulfonic acid (0.091 g, 0.48 mmol). The reaction mixture was then stirred at room temperature for 18 h. After the reaction deemed was completed (as judged by TLC, neutral alumina, CH_2Cl_2/MeOH, 9:1, v/v) the CH_2Cl_2 was removed under reduced pressure. Triethylamine was added dropwise until an orange precipitate was formed. The orange powder was collected by filtration, dissolved in CH_2Cl_2 (1 mL), and purified using a Teledyne CombiFlash Companion with a neutral alumina column (CH_2Cl_2/MeOH = 9.9:0.1, v/v), yielding compound **1.2** (0.012g, 10.3%) as a pale yellow solid. ^{1}H NMR (CD_2Cl_2): δ (ppm) = 8.34 (d, *J* = 7.6 Hz, C(O)N-**H**, 2H), 8.14 (s, C-**H** imine, 4H), 7.99 (t, *J* = 7.2 Hz, C-**H** pyridine, 2H), 7.87 (t, *J* = 7.2 Hz, Ar-**H**, 2H), 7.19-7.07 (m, Ar-**H**, 8H), 7.04 (s, Ar-**H**, 2H), 6.89 (d, *J* = 7.2 Hz, Ar-**H**, 2H) 6.83 (d, *J* = 7.2 Hz, Ar-**H**, 2H), 6.50 (d, *J* = 4 Hz, C-**H** pyrrole, 4H), 5.76 (d, *J* = 3.6 Hz, C-**H** pyrrole, 4H), 4.15 (t, *J* = 6 Hz, -O**CH$_2$**CH$_2$N-, 4H), 3.93 (q, *J* = 6.4 Hz, -OCH$_2$**CH$_2$**N-, 4H), 2.48 (s, **CH$_3$**, 6H). HMRS (ESI+) m/z calculated for ($C_{59}H_{51}N_{11}O_4$) 978.41949, found ($C_{59}H_{52}N_{11}O_4$) 978.41983.

2-(5,5-Di(1H-pyrrol-2-yl)hexyl)isoindoline-1,3-dione (1.48). A solution of **1.47** (10 g, 43 mmol) was dissolved in pyrrole (28.8 g, 1.297 mol) and catalytic amount of trifluoroacetic acid (1.5 mL) was added dropwise for 15 min in an ice bath. The mixture was stirred at room temperature for 2 h. The crude product was obtained by dilution with dichloromethane and washing with 2 M aqueous sodium hydroxide. The organic fractions were collected, washed with water (60 mL), saturated sodium chloride solution (60 mL), dried over Na_2SO_4, and concentrated under reduced pressure. Removal of excess of pyrrole *via* vacuum distillation afforded a brownish solid, which was purified by column chromatography over silica gel (hexanes/EtOAc = 8:2, v/v). This yielded compound **1.48** (12.39 g, 84.1%) as a pale yellow solid. ^{1}H NMR ($CDCl_3$): δ (ppm) = 7.83 (m, phthalimide Ar-**H**, 2H), 7.71 (m, phthalimide Ar-**H**, 2H), 6.61 (s, C-**H** pyrrole, 2H), 6.10 (m, C-**H** pyrrole, 2H), 6.05 (m, C-**H** pyrrole, 2 H), 3.65 (t, *J* = 6 Hz, -CH$_2$CH$_2$CH$_2$C**H$_2$**N-, 2H), 2.02 (m, -CH$_2$CH$_2$C**H$_2$**CH$_2$N-, 2H), 1.66 (m, -CH$_2$C**H$_2$**CH$_2$CH$_2$N-, 2H), 1.57 (s, **CH$_3$**, 3H), 1.29 (m, -C**H$_2$**CH$_2$CH$_2$CH$_2$N-, 2H). ^{13}C NMR (CD_2Cl_2): δ(ppm) = 168.5, 137.8, 133.9, 133.8, 133.7, 132. 1, 123.1, 123.1, 117.7, 116.9, 108.1, 107.7, 104.5, 40.3, 38.9,

38.7, 37.5, 28.7, 26.4, 21.4. HMRS (CI+) m/z calculated for ($C_{22}H_{23}N_3O_2$) 361.4450, found ($C_{22}H_{24}N_3O_2$) 362.4490.

5,5-Di(1H-pyrrol-2-yl)hexan-1-amine (1.49). A mixture of **1.48** (10 g, 29 mmol) and hydrazine hydrate (2.37 g, 30.2 mmol) were dissolved in ethanol (200 mL). The mixture was refluxed for 2 h. The cooled mixture was filtered and the filtrate was concentrated under reduced pressure to obtain a white solid. The solid obtained was suspended in diethyl ether (10 mL) and treated with 40% w/w aqueous potassium hydroxide to dissolve the solid in the ethereal fraction. The compound was extracted into diethyl ether (3 × 50 mL). The combined organic fractions were dried over Na_2SO_4 and concentrated under reduced pressure to give a light yellow oil **1.49** (6.16 g, 98.5%). ^{1}H NMR ($CDCl_3$): δ (ppm) = 8.07 (bs, N-**H**, 2H), 6.59 (bs, C-**H** pyrrole, 2H), 6.12 (bs, C-**H** pyrrole, 2H), 6.06 (bs, C-**H** pyrrole, 2H), 3.68 (t, *J* = 7.2 Hz, -$CH_2CH_2CH_2C\mathbf{H}_2N$-, 2H), 2.63 (bs, $\mathbf{NH_2}$, 2H), 1.97 (m, -$CH_2CH_2C\mathbf{H}_2CH_2N$-, 2H), 1.56 (s, $\mathbf{CH_3}$, 3H), 1.40 (m, -$CH_2C\mathbf{H}_2CH_2CH_2N$-, 2H), 1.25 (m, -$C\mathbf{H}_2CH_2CH_2CH_2N$-, 2H). ^{13}C NMR ($CDCl_3$): δ (ppm) = 161.5, 142.9, 122.0, 115.4, 107.4, 60.1, 40.1, 21.9, 14.4. HRMS (CI+) m/z calculated for ($C_{14}H_{21}N_3$) 231.3430, found ($C_{14}H_{22}N_2$) 332.3335.

Bis-dipyrromethane (1.49a). 2,6-Pyridinecarbonyl dichloride (3.27 g, 16 mmol) and compound **1.49** (6.96 g, 32 mmol) were dissolved in dry THF (200 mL). TEA (3.27 g, 14 mmol) was added to the mixture, which was stirred for 3 h in an ice bath. The solution was washed with a saturated solution of $NaHCO_3$ (100 mL) and then extracted into CH_2Cl_2 (4 × 50 mL). The combined organic layers were dried over Na_2SO_4 and concentrated under reduced pressure. The crude product obtained in this way was purified by column chromatography over silica gel (DCM/ MeOH = 98:2, v/v), yielding the compound **1.49a** (5 g**,** 26.3%). ^{1}H NMR ($CDCl_3$): δ (ppm) = 8.36 (d, *J* = 7.6 Hz, C-**H** pyridine, 2H), 8.04 (t, *J* = 8 Hz, C-**H** pyridine, 1H), 7.92 (bs, N-**H**, 2H), 7.60 (t, *J* = 7.2 Hz, C(O)N-**H**, 2H), 6.59 (m, C-**H** pyrrole, 4H), 6.10 (m, C-**H** pyrrole, 4H), 6.05 (m, C-**H** pyrrole, 4H), 3.50 (m, -$CH_2CH_2CH_2C\mathbf{H}_2N$-, 4H), 2.07 (m, -$CH_2CH_2C\mathbf{H}_2CH_2N$-, 4H), 1.65 (m, -$CH_2C\mathbf{H}_2CH_2CH_2N$-, 2H), 1.57 (s, $\mathbf{CH_3}$, 6H), 1.29 (m, -$C\mathbf{H}_2CH_2CH_2CH_2N$-, H). ^{13}C NMR ($CDCl_3$): δ (ppm) = 163.6, 148.8, 139.0, 137.9, 124.9, 116.9, 107.6, 104.4, 40.5,

38.9, 30.0, 26.5, 21.5. HRMS (ESI+) m/z calculated for ($C_{35}H_{43}N_7O_2$) 593.7760, found ($C_{35}H_{43}N_7O_2Na$) 616.7668.

Bis-dipyrromethane tetraaldehyde (1.46). To a solution of **1.49a** (g 0.69 mmol) in DMF (5 mL), phosphorous oxychloride ($POCl_3$) (0.43 g, 2 mmol) was added dropwise for 15 min and stirred for 1 h. Water was added to the mixture along with 2 M potassium hydroxide until the pH was strongly basic. This gives a yellow solid, which was collected by filtration and washed with plenty of water, yielding the compound **1.46** (0.3 g, 52%) as a pale yellow solid. ^{1}H NMR (DMSO-d_6): δ (ppm) = 11.77 (bs, N-**H**, 4H), 9.34 (s, C**H**O, 4H), 9.24 (t, J = 6 Hz, C(O)N-**H**, 2H), 8.13 (m, -$CH_2CH_2CH_2CH_2$N-, 4H), 6.85 (d, J = 4 Hz, C-**H** pyrrole 4H), 6.04 (d, J = 3.6 Hz, C-**H** pyrrole, 4H), 2.18 (m, -$CH_2CH_2CH_2CH_2$N-, 4H), 1.65 (s, **C**H_3, 6H), 1.54 (m, -$CH_2CH_2CH_2CH_2$N-, 4H), 1.12 (m, -$CH_2CH_2CH_2CH_2$N-, 4H). ^{13}C NMR (DMSO_d_6): δ (ppm) = 179.1, 163.3, 149.1, 147.2, 133.2, 124.5, 108.8, 30.2, 22.1. HMRS (ESI+) m/z calculated for ($C_{43}H_{43}N_7O_8$) 833.3932, found ($C_{43}H_{43}N_7O_8Na$) 856.3076.

Strapped calixpyrrole Schiff-base macrocycle (1.3). To a solution of **1.46** (0.02 g, 0.028 mmol) in a mixture of CH_2Cl_2/MeOH (1:9, v/v, 50 mL) was added *o*-phenyldiamine (0.0061 g, 0.057 mmol) and *p*-toluensulfonic acid (0.02 g, 0.11 mmol). The mixture was stirred at room temperature for 18 h. After the reaction was deemed complete (TLC neutral alumina CH_2Cl_2/MeOH = 9:1, v/v), the CH_2Cl_2 was removed under reduced pressure. Triethylamine was added dropwise until an dark yellow precipitate was formed. The dark yellow powder was collected by filtration to give **1.3** (0.0097g, 40%) as a yellow powder. ^{1}H NMR (CD_2Cl_2): δ (ppm) = 8.27 (d, J = 7.6 Hz, C-**H** pyridine, 2H), 8.26 (s, C-**H** imine, 2H), 8.05 (s, C-**H** imine, 2H), 7.95 (t, J = 6 Hz, C-**H** pyridine, 1H), 7.85 (t, J = 4.4 Hz, C(O)N-**H**, 1H), 7.44 (t, J = 4.4 Hz, C(O)N-**H**, 1H), 7.08 (m, Ar-**H**, 4H), 7.00 (m, Ar-**H**, 4H), 6.95 (m, Ar-**H**, 4H), 6.49 (d, J = 3.6 Hz, C-**H** pyrrole, 2H), 6.45 (d, J = 3.6 Hz, C-**H** pyrrole, 2H), 6.06 (d, J = 3.6 Hz, C-**H** pyrrole, 2H), 5.98 (d, J = 3.6 Hz, C-**H**, 2H), 3.60 (m, -C**H**$_2$ alkyl, 2H), 2.23 (m, -C**H**$_2$ alkyl, 2H), 1.91 (s, -**C**H_3, 3H), 1.73 (s, **C**H_3, 3H), 1.64 (m, -C**H**$_2$ alkyl, 4H), 1.52 (m, -C**H**$_2$ alkyl -, 4H),1.30 (m, -C**H**$_2$ alkyl, 2H), 1.19 (m, -C**H**$_2$ alkyl, 2H). ^{13}C NMR ($CDCl_3$): δ (ppm) =

215.0, 163.0, 148.3, 145.8, 144.7, 130.7, 130.5, 126.4, 126.3, 124.6, 118.1, 117.8, 117.3, 107.8, 106.5, 39.5. HMRS (ESI+) m/z calculated for ($C_{51}H_{52}N_{11}O_2$) 854.0440, found ($C_{51}H_{52}N_{11}O_2$+1) 850.4300. Anal. Calc. for $C_{55}H_{65}Cl_2N_{11}O_5$ [**1.3**·$(CH_3OH)_3CH_2Cl_2$]: C, 64.04; H, 6.35; N, 15.49. Found: C, 64.38; H, 6.37; N, 15.89.

Strapped calixpyrrole Schiff-base macrocycle-Pd complex (1.50). To a solution of **1.3** (0.026 g, 0.12 mmol) in CH_2Cl_2 (5 mL) was added palladium(II) acetate (0.05 g, 0.059 mmol). The mixture was stirred at room temperature for 30 min. After this time, triethylamine (TEA) was added (1 mL) and the compound was precipitated with pentane. The resulting brown solid was collected by filtration, dissolved in CH_2Cl_2 (1 mL), and purified by column chromatography, silica gel (CH_2Cl_2/MeOH = 98:2, v/v), yielding the compound **1.50** (0.017 g, 27.3%) as a dark orange solid. ^{1}H NMR ($CDCl_3$): δ (ppm) = 8.36 (m, C-**H** pyridine, 2H), 7.99 (t, *J* = 7.6 Hz, C-**H** pyridine, 1H), 7.92 (t, *J* = 6.8 Hz, C(O)N-**H** 1H), 7.47 (t, *J* = 7.6 Hz, C(O)N-**H**, 1H), 7.32 (s, C-**H** imine, 2H), 7.30 (s, C-**H** imine, 2H), 6.85 (m, Ar-**H**, 4H), 6.75-6.69 (m, C-**H** pyrrole, 4H), 6.68 (m, Ar-**H**, 4H), 6.23 (d, *J* = 4 Hz, C-**H** pyrrole, 2H), 6.17 (d, *J* = 4 Hz, C-**H** pyrrole, 2H), 3.61 (m, -C**H**$_2$ alkyl -, 2H), 3.06 (m, -C**H**$_2$ alkyl -, 2H), 2.25 (m, -C**H**$_2$ alkyl -, 2H), 1.72 (m, -C**H**$_2$ alkyl -, 2H), 1.67 (s, **CH$_3$**, 3H), 1.32 (s, **CH$_3$**, 3H), 1.23 (m, -C**H**$_2$ alkyl, 2H), 1.12 (m, -C**H**$_2$ alkyl -, 2H), 0.86 (t, *J* = 7.6 Hz, -C**H**$_2$ alkyl, 2H), 0.73 (m, -C**H**$_2$ alkyl, 2H). ^{13}C NMR (CD_2Cl_2): δ (ppm) = 163.1, 162.9, 159.7, 159.3, 151.9, 149.5, 142.7, 142.5, 138.9, 137.8, 137.2, 126.4, 126.2, 124.8, 124.7, 123.2, 122.9, 118.1, 117.9, 108.3, 107.48, 47.7, 46.9, 46.8, 39.7, 39.5, 38.2, 35.4, 29.7, 28.5, 24.0, 23.9, 22.9. HMRS (ESI+) m/z calculated for ($C_{51}H_{47}N_{11}O_2Pd_2$) 1057.1984, found ($C_{51}H_{47}N_{11}O_2NaPd_2$) 1082.1908. Anal. Calc. for $C_{53}H_{55}Cl_2N_{11}O_4Pd_2$ [**1.50**·$(CH_3OH)_2$]: C, 56.69; H, 4.94; N, 13.72. Found: C, 56.72; H, 4.56; N, 13.75.

Strapped calixpyrrole Schiff-base macrocycle-Ni complex (1.51). To a solution of **1.3** (0.027 g, 0.032 mmol) in 1,2-dichloroethane (5 mL) was added a solution of nickel(II) acetylacetonate (0.016 g, 0.063 mmol). The mixture was stirred at room

temperature for 30 min. After this time, triethylamine (TEA) was added (1 mL) and the mixture was sirred at 50 ºC for 18 h. The solvent was reduced to 1 mL under reduced pressure. The material obtained in this way was purified by column chromatography over neutral alumina grade III (CH_2Cl_2/MeOH = 95:5, v/v), yielding the compound **1.51** (0.007 g, 22.9%) as a dark brown solid. ^{1}H NMR ($CDCl_3$): δ (ppm) = 8.37 (m, C-**H** pyridine, 2H), 8.03 (t, *J* = 7.6 Hz, C-**H** pyridine, 1H), 7.96 (t, *J* = 4 Hz, C(O)N-**H**, 1H), 7.60 (t, *J* = 4 Hz, C(O)N-**H**, 1H), 7.13 (s, C-**H** imine, 2H), 7.12 (s, C-**H** imine, 2H), 6.80-6.70 (m, Ar-**H** and C-**H** pyrrole, 12 H), 6.17 (d, *J* = 4 Hz, C-**H** pyrrole, 2H), 6.13 (d, *J* = 4 Hz, C-**H** pyrrole, 2 H), 3.59 (m, -C**H**$_2$ alkyl, 2H), 3.14 (m, -C**H**$_2$ alkyl, 2H), 2.20 (m, -C**H**$_2$ alkyl, 2H), 1.67 (m, -C**H**$_2$ alkyl, 4H), 1.36 (m, -C**H**$_2$ alkyl, 2H), 1.24 (s, **CH$_3$**, 3H), 1.21 (s, **CH$_3$**, 3H), 0.84 (m, -C**H**$_2$ alkyl, 2H), 0.65 (m, -C**H**$_2$ alkyl, 2H). No ^{13}C NMR data were obtained for this sample due to the lack of stability of the product. HMRS (ESI+) m/z clacd for ($C_{51}H_{48}N_{11}Ni_2O_2$) 962.2694, found ($C_{51}H_{48}N_{11}Ni_2O_2$) 962.2665.

Strapped calixpyrrole Schiff-base macrocycle-Cu complex (1.52). To a solution of **1.3** (0.05 g, 0.059 mmol) in CH_2Cl_2 (5 mL) was added a solution of copper(II) tetrafluoroborate in 2 mL of methanol (0.081 g, 0.23 mmol). The mixture was stirred at room temperature for 1 h. After this time, triethylamine (TEA) was added (0.2 mL) and the compound was precipitated with pentane. The brown solid was collected by filtration, dissolved in DCM (1 mL), and purified by column chromatography, silica gel (CH_2Cl_2/ MeOH = 95:5, v/v), yielding the compound **1.52** (0.033 g, 57.9%) as dark brown-green solid. HMRS (ESI+) m/z calculated for ($C_{51}H_{47}$ $Cu_2N_{11}O_2$) 971.2506, found ($C_{51}H_{47}$ $Cu_2N_{11}O_2Na$) 996.2392. μ_{eff} = 2.12 μ_B Anal. Calc. for $C_{52}H_{51}Cu_2N_{11}O_3$ [**1.52**·CH_3OH]: C, 62.14; H, 5.11; N, 15.33. Found: C, 62.33; H, 5.52; N, 15.67.

Strapped calixpyrrole Schiff-base acrocycle-Ru complex (1.53). To a solution of **1.3** (0.03 g, 0.035 mmol) in dry DCM (2 mL) was added a solution of [Ru(Cp*)($NCCH_3$)$_3$]PF_6 (0.071 g, 0.14 mmol). The mixture was stirred at room temperature for 18 h. The solvent was reduced to 1 mL under reduced pressure. The compound obtained was purified by column chromatography, neutral alumina grade III

(CH_2Cl_2/ MeOH = 9:1, v/v), yielding the compound **1.53** (0.002 g, 4.3%) as a dark brown solid. HMRS (ESI+) m/z calculated for ($C_{71}H_{79}N_{11}O_2Ru_2$) 1321.4532, found ($C_{71}H_{79}N_{11}O_2Ru_2$) 1321.4511.

Etioporphycene (2.37). To solution of activated zinc dust (21 g, 0.33 mol), CuCl (3.2 g, 32 mmol), and dry THF (1 L) were added dropwise $TiCl_4$ (18.4 mL, 0.160 mol) under an argon atmosphere. The resulting mixture was heated at reflux for 2 h, giving a black solution. At this time, a solution of bipyrroledialdehyde **2.42** (300 mL) in boiling THF was added in small aliquots. The mixture was heated at reflux for 2 min. The cooled mixture was transferred to an ice bath at -10 ºC and 200 mL of a saturated aqueous solution of Na_2CO_3 was added slowly. The dark green solution obtained in this way was filtered through a pad of celite, which was washed thoroughly with plenty of CH_2Cl_2. The filtrate was washed with water (2 × 100 mL) and the combined organic fractions were evaporated under reduced pressure. The black solid obtained as a result was purified by column chromatography over silica gel using CH_2Cl_2 as the eluent. The product obtained in this way was recrystallized from the mixture CH_2Cl_2 and MeOH (0.5:3.5, v/v), yielding compound **2.37** as violet needles (0.2 g, 5.69%). ^{1}H NMR ($CDCl_3$): δ (ppm) = 9.55 (s, *meso*-**H**, 4H), 3.86 (m, C**H$_2$**CH$_3$, 8H), 3.57 (s, C**H$_3$**, 12H), 1.71 (t, *J* = 8 Hz, CH_2C**H$_3$**, 12H). ^{13}C NMR ($CDCl_3$): δ (ppm) = 143.8, 142.0, 137.2, 130.5, 109.9, 19.9, 17.3, 16.2. UV-Vis (CH_2Cl_2), λ_{max}, nm (ε × 10^{-3} M^{-1} cm^{-1}) = 359sh, 382 (144.3), 570 (32.2), 617 (18.4), 657 (30.0). HMRS (CI+) m/z calculated for ($C_{32}H_{40}N_4$) 478.3253, found ($C_{32}H_{40}N_4$) 480.3247.

Etioporphycene-Ni(II) (2.43). Etioporphycene **2.37** (0.00031 mol, 0.15 g) and $Ni(OAc)_2$•$4H_2O$ (31 g, 0.12 mmol,) were heated at reflux in 25 mL of glacial acetic acid for 2 h. The resulting nickel(II) complex was obtained as a precipitate on cooling the reaction and adding 5 mL of water. The solid was collected by filtration and washed several times with water to afford **2.43** as dark blue needles (0.152 g, 90%). ^{1}H NMR ($CDCl_3$): δ (ppm) = 9.35 (s, *meso*-**H**, 4H), 3.83 (q, *J* = 8 Hz, -C**H$_2$**CH$_3$, 8H), 3.52 (s, -C**H$_3$**, 12H), 1.69 (t, *J* = 8 Hz, -CH_2C**H$_3$**, 12H). ^{13}C NMR ($CDCl_3$): δ (ppm) = 140.8, 138.2, 134.2, 127.3, 105.8, 14.0, 15.3, 14.9. UV-Vis (CH_2Cl_2), λ_{max}, nm (ε × 10^{-3} M^{-1} cm^{-}

[1]) = 364 (45.0), 389 (138.0), 604 (13.9). HMRS (CI+) m/z calculated for ($C_{32}H_{36}N_4Ni$) 534.2293, found ($C_{32}H_{36}N_4Ni$) 534.2327.

(Ferrocenylmethyl)triphenyl phosphonium iodide (2.46). (Ferrocenylmethyl)trimethylammonium iodide (1 g, 2.6 mmol,) and triphenylphosphine (0.13 g, 0.5 mmol) were heated at reflux in ethanol (100 mL) for 2 h. The solution was then cooled and poured slowly into diethylether (300 mL) with vigourous stirring. The yellow precipitate that resulted was collected by filtration and washed with diethyl ether (500 mL). The salt was recrystallized from ethanol to obtain yellow leaflets. This afforded compound **2.46** (1.37 g, 89.7%). ^{1}H NMR ($CDCl_3$): δ (ppm) = 7.81-7.69 (m, phosphine, 15H), 4.36 (bs, cyclopentadienyl, 5H), 4.29 (s, cyclopentadienyl, 2H), 4.06 (s, cyclopentadienyl, 2H), 2.84 (bs, methyl, 2H). ^{13}C NMR ($CDCl_3$): δ (ppm) = 1.35.0, 134.4, 134.3, 130.2, 130.1, 118.2, 117.4, 70.5, 69.98, 68.8. HMRS (CI+) m/z calculated for ($C_{29}H_{26}FeP$) 461.11270, found ($C_{29}H_{26}FeP$) 461.11160.

9-Formyletioporphycene (2.44). Etioporphycene nickel complex **2.43** (0.1 g, 0.19 mmol) and dry DMF (0.26 mL, 3.4 mmol) were dissolved in 5 mL of dry 1,2-dichloroethane at 0 ºC under nitrogen. $POCl_3$ (0.31 mL, 3.4 mmol) was added dropwise to the reaction mixture, which was stirred at 50 ºC for 3 h. After this time, 15 mL of saturated aqueous sodium acetate was added slowly and stirred for 30 min at 50 ºC. The green solution was cooled and washed with water (5 × 50 mL) and the organic fractions were taken to dryness under reduced pressure. The black solid was purified by column chromatography over silica gel (CH_2Cl_2/Hexanes = 1:1, v/v), yielding compound **2.44** as green powder and recrystallized in CH_2Cl_2/MeOH afforded green needles (0.060g, 64%). ^{1}H NMR ($CDCl_3$): δ (ppm) = 11.62 (s, -C**H**O, 1H), 9.80 (s, *meso*-**H**, 1H), 9.16 (d, *J* = 12 Hz, *meso*-**H**, 1H), 8.99 (d, *J* = 16 Hz, *meso*-**H**, 1H), 3.81 (q, *J* = 8 Hz, -C**H$_2$**CH$_3$, 2H), 3.73-3.66 (m, -C**H$_2$**CH$_3$, 4H), 3.53 (q, *J* = 8 Hz, -C**H$_2$**CH$_3$, 2H), 3.40 (s, -C**H$_3$**, 3H), 3.38 (s, -C**H$_3$**, 6H), 2.28 (s, -C**H$_3$**, 3H), 1.73-1.62 (m, -CH$_2$C**H$_3$**, 12H). ^{13}C NMR ($CDCl_3$): δ (ppm) = 192.9, 150.5, 150.3, 149.2, 148.7, 147.4, 146.4, 145.2, 144.9, 143.9, 143.2, 140.8, 132.3, 130.1, 129.1, 129.0, 115.4, 109.3, 106.5, 105.1, 29.7, 23.3, 19.9, 19.8, 17.8, 17.5, 17.3, 15.9, 15.7, 15.3, 15.3, 15.1. UV-Vis (CH_2Cl_2), λ_{max}, nm (ε × 10^{-3} M^{-1} cm^{-1}) =

414 (13.4), 604 (4.2). HMRS (ESI+) m/z clacd for ($C_{33}H_{26}N_4NiO$ + Na) 585.21348, found ($C_{33}H_{26}N_4NiO$ + Na) 585.21260.

9-Benzylethenyletioporphycene (2.47). Lithium bis(trimetylsilyl)amide (0.018 g, 0.11 mmol) was dissolved in dry THF and added dropwise through a cannula to a solution of benzyltriphenylphosphonium chloride (0.041g, 0.11 mmol) in THF at -78 ºC. The mixture was stirred for 30 min. A yellow solution formed, which was transferred with a cannula to a solution containing 9-formyletioporphycene **2.44** (0.01 g, 0.018 mmol) in dry THF at -78 ºC, stirring was continued for 3 h. The reaction was quenched *via* the addition of small amounts of methanol and the organic solvent was evaporated off under reduced pressure. The resulting dark green solid was purified by column chromatography over silica gel using CH_2Cl_2/Hexanes = 1:1, v/v as the eluent. This afforded compound **2.47** (0.008 g, 30.9%) as an emerald green solid. ^{1}H NMR ($CDCl_3$): δ (ppm) = 9.25 (s, *meso*-**H**, 1H), 9.07 (s, *meso*-**H**, 2H), 9.76 (d, *J* = 16 Hz, ethenyl -C**H**, 1H), 7.73 (d, *J* = 4 Hz, ar-**H**, 2H), 7.48 (t, *J* = 4 Hz, ar-**H**, 2H), 7.34 (t, *J* = 4 Hz, ar-**H**, 1H), 7.16 (d, *J* = 16 Hz, ethenyl –C**H**=, 1H), 3.77-3.70 (m, -C**H$_2$**CH_3, 6H), 3.62 (t, *J* = 8 Hz, -C**H$_2$**CH_3, 2H), 3.41 (s, -C**H$_3$**, 3H), 3.40 (s, -C**H$_3$**, 6H), 3.27 (s, -C**H$_3$**, 3H), 1.71-1.62 (m, -CH_2C**H$_3$**, 9H), 1.58 (t, *J* = 8 Hz, -CH_2C**H$_3$**, 3H). ^{13}C NMR ($CDCl_3$): δ (ppm) = 165.5, 150.3, 150.5, 147.4, 149.5, 148.2, 147.5, 146.4, 145.2, 144.7, 144.0, 143.3, 140.3, 132.5, 133.9, 133.5, 132.9, 130.3, 129.4, 129.0, 115.2, 109.2, 106.7, 105.7, 29.7, 23.3, 19.8, 19.7, 17.6, 17.5, 17.3, 15.4, 15.5, 15.3, 15.2, 15.1. UV-Vis (CH_2Cl_2), λ_{max}, nm (ε × 10^{-3} M^{-1} cm^{-1}) = 412 (340.2), 639 (155.5). HMRS (CI+) m/z calculated for ($C_{40}H_{42}$ $N_4$58Ni) 636.2763, found ($C_{40}H_{42}N_4$58Ni) 636.2772.

9-(Propenoate)etioporphycene (2.48). 9-Formyletioporphycene **2.44** (0.02 g, 0.035 mmol) and (carboxymethoxymethylene)triphenyl phosphorane (0.066 mol, 0.022 g) were dissolved in 5 mL of xylenes and heated at reflux under nitrogen for 4 h. At this time, the solvent was removed under reduced pressure and the green residue was purified by column chromatography over silica gel (CH_2Cl_2/Hexanes = 3.5:1.5, v/v). This yielded **2.48** (0.01 g, 44.4%) as a dark green solid. ^{1}H NMR ($CDCl_3$): δ (ppm) = 9.42 (d, *J* = 16 Hz, ethenyl –C**H**=, 1H), 9.20 (s, *meso*-**H**, 1H), 9.03 (q, *J* = 12 Hz, *meso*-**H**, 2H), 6.74 (d,

J = 16 Hz, ethenyl –C**H**=, 1H), 4.43 (q, *J* = 4 Hz, ester-C**H**$_2$CH$_3$, 2H), 3.73-3.63 (m, -C**H**$_2$CH$_3$, 6H), 3.56 (q, *J* = 8 Hz, -C**H**$_2$CH$_3$, 2H), 3.36 (s, -C**H**$_3$, 3H), 3.36 (s, -C**H**$_3$, 6H), 3.25 (s, -C**H**$_3$, 3H), 1.72-1.60 (m, -CH$_2$C**H**$_3$, 12H), 1.46 (t, *J* = 4 Hz, ester –CH$_2$C**H**$_3$, 3H). ^{13}C NMR ($CDCl_3$): δ (ppm) = 167.4, 151.3, 151.5, 149.5, 148.3, 147.6, 146.4, 145.2, 144.4, 144.0, 143.3, 140.3, 135. 5, 132.5, 132.2, 130.3, 129.4, 129.0, 123.7, 115.5, 109.7, 106.5, 105.3, 30.7, 24.3, 20.8, 19.7, 18.6, 17.9, 17.5, 15.5, 15.7, 15.3, 15.2, 15.1. UV-Vis (CH_2Cl_2), λ_{max}, nm (ε × 10^{-3} M^{-1} cm^{-1}) = 419 (198.9), 636 (95.6). HMRS (ESI+) m/z calculated for ($C_{37}H_{42}N_4NiO_2$) 627.25535, found ($C_{37}H_{42}N_4NiO_2$ + Na)$^+$ 655.25453. Anal. Calc. for $C_{43}H_{54}N_4O_2$ [**2.48**·C_6H_{12}]: C, 71.97; H, 7.58; N, 7.81. Found: C, 71.84; H, 7.13; N, 7.48.

9-(propenol)etioporphycene (2.49). Diisobutylaluminium hydride (DIBALH) (0.1 mL from solution 1.0 M in THF, 0.14 mmol) was added dropwise under nitrogen to a solution of 9-(porpenoate)etioporphycene **2.48** (0.01 g, 0.016 mmol) in dry CH_2Cl_2 at -78 ºC. The reaction mixture was stirred at this temperature for more 2 h and quenched by adding small amounts of methanol (0.5 mL). A 50% v/v aqueous solution of ammonium chloride was added to the flask and the reaction allowed to stirr for 15 min. The organic layer was separated from the aqueous layer, and washed with water (4 × 50 mL). The organic fractions were combined and evaporated under reduced pressure. The resulting solid was purified by column chromatography over silica gel (CH_2Cl_2/MeOH = 3.5:1.5, v/v), yielding compound **2.49** (0.008 g, 85.7 5%). ^{1}H NMR ($CDCl_3$): δ (ppm) = 9.12 (s, *meso*-**H**, 1H), 9.08 (s, *meso*-**H**, 2H), 8.29 (d, *J* = 16 Hz, ethenyl –C**H**=, 1H), 6.56 (dt, *J* = 16 Hz, *J* = 8 Hz, ethenyl –C**H**=, 1H), 4.66 (d, *J* = 8 Hz, -C**H**$_2$-OH, 2H), 3.75-3.68 (m, -C**H**$_2$CH$_3$, 6H), 3.62 (q, *J* = 8 Hz, -C**H**$_2$CH$_3$, 2H), 3.41 (s, -C**H**$_3$, 3H), 3.39 (s, -C**H**$_3$, 6H), 3.27 (s. –C**H**$_3$, 3H), 1.68-1.58 (m, -CH$_2$C**H**$_3$, 12H), 1.56 (bs, -O**H**, 1H). ^{13}C NMR ($CDCl_3$): δ (ppm) = 165.7, 150.9, 150.5, 149.7, 148.2, 147.3, 146.3, 145.3, 144.4, 144.0, 143.3, 140.3, 132.7, 134.0, 133.7, 132.9, 130.3, 129.4, 129.0, 115.2, 109.2, 106.7, 105.7, 29.7, 23.3, 19.5, 19.2, 18.0, 17.7, 17.3, 15.5, 15.0, 14.9, 14.7, 14.6.. UV-Vis (CH_2Cl_2), λ_{max}, nm (ε × 10^{-3} M^{-1} cm^{-1}) = 399 (288.6), 623 (117.5). HMRS (CI+) m/z calculated for ($C_{35}H_{40}N_4NiO$) 590.2556, found ($C_{35}H_{40}N_4NiO$) 590.2565.

Appendix A

X-ray Experimental and Crystallographic Data

A.1 GENERAL PROCEDURES

All crystals for X-ray crystallographic analyses described in this appendix were grown by the author. All X-ray diffraction stuctures were solved by Dr. Vincent M. Lynch of this department. A general method as provided by Dr. Lynch used in obtaining these structures, along with relevant data tables for each structure now follows.

X-ray Experimental for compound 1.42•(CH_2Cl_2): Crystals grew as pale, yellow prisms by slow evaporation from dichloromethane and methanol. The data crystal had approximate dimensions; 0.28 x 0.20 x 0.08 mm. The data were collected on a Nonius Kappa CCD diffractometer using a graphite monochromator with MoKα radiation (λ = 0.71073Å). A total of 380 frames of data were collected using ω-scans with a scan range of 0.9° and a counting time of 149 seconds per frame. The data were collected at 153 K using an Oxford Cryostream low temperature device. Details of crystal data, data collection and structure refinement are listed in Table A.1. Data reduction were performed using DENZO-SMN.[1] The structure was solved by direct methods using SIR97[2] and refined by full-matrix least-squares on F with anisotropic displacement parameters for the non-H atoms using SHELXL-97. Structure analysis was aided by use of the programs PLATON98[4] and WinGX. The hydrogen atoms were calculated in idealized positions with Uiso set to 1.2xUeq of the attached atom (1.5xUeq for methyl hydrogen atoms).

A molecule of dichloromethane was disordered along a cylindrical region of the unit cell near 1/4, y, 1/4. Attempts to model the disorder were unsatisfactory. The contributions to the scattering factors due to this solvent molecule were removed by use of the utility SQUEEZE in PLATON98. PLATON98 was used as incorporated in WinGX.

The function, $\Sigma w(|F_o|^2 - |F_c|^2)^2$, was minimized, where $w = 1/[(\sigma(F_o))^2 + (0.0724*P)^2 + (0.3847*P)]$ and $P = (|F_o|^2 + 2|F_c|^2)/3$. $R_w(F^2)$ refined to 0.192, with R(F) equal to 0.0964 and a goodness of fit, S, = 1.12. Definitions used for calculating R(F),$R_w(F^2)$ and the goodness of fit, S, are given below. Neutral atom scattering factors and values used to calculate the linear absorption coefficient are from the International Tables for X-ray Crystallography (1992). All figures were generated using SHELXTL/PC. Tables of positional and thermal parameters, bond lengths and angles, torsion angles and figures are found elsewhere.

Figure A.1: View of compound **1.42** showing the atom labeling scheme. Displacement ellipsoids are scaled to the 50% probability level. The molecule lies on a crystallographic two-fold rotation axis at ¾, ½, z. Atoms with labels appended by "a" are related by 3/2 – x, 1 –y, z.

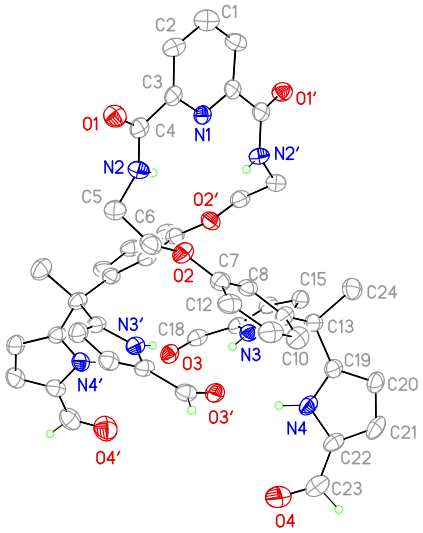

Table A.1: Crystal data and structure refinement for compound **1.42**.

Empirical formula	C48 H45 Cl2 N7 O8	
Formula weight	918.81	
Temperature	153(2) K	
Wavelength	0.71075 Å	
Crystal system	Orthorhombic	
Space group	Pnna	
Unit cell dimensions	a = 12.4901(15) Å	a= 90°.
	b = 15.769(2) Å	b= 90°.
	c = 22.940(3) Å	g = 90°.
Volume	4518.2(10) $Å^3$	
Z	4	
Density (calculated)	1.351 Mg/m^3	
Absorption coefficient	0.207 mm^{-1}	
F(000)	1920	
Crystal size	0.28 x 0.20 x 0.08 mm	
Theta range for data collection	2.96 to 25.00°.	
Index ranges	0<=h<=14, 0<=k<=18, 0<=l<=27	
Reflections collected	3980	
Independent reflections	3980	
Completeness to theta = 25.00°	99.7 %	
Absorption correction	Semi-empirical from equivalents	
Max. and min. transmission	1.06 and 0.951	
Refinement method	Full-matrix least-squares on F^2	
Data / restraints / parameters	3980 / 0 / 282	
Goodness-of-fit on F^2	1.123	
Final R indices [I>2sigma(I)]	R1 = 0.0964, wR2 = 0.1654	
R indices (all data)	R1 = 0.2230, wR2 = 0.1920	
Largest diff. peak and hole	0.234 and -0.236 $e.Å^{-3}$	

X-ray Experimental for *cis*-strapped Schiff-base calixpyrrole1.3•(4 CH_3OH): Crystals grew as long, yellow needles by slow evaporation from methanol. The data crystal was cut from a larger crystal and had approximate dimensions; 0.46 x 0.11 x 0.08 mm. The data were collected on a Rigaku SCX-Mini diffractometer with a Mercury 2 CCD using a graphite monochromator with MoKα radiation (λ = 0.71075Å). A total of 360 frames of data were collected using ω-scans with a scan range of 1° and a counting time of 75 seconds per frame. The data were collected at 163 K using a Rigaku XStream low temperature device. Details of crystal data, data collection and structure refinement are listed in Table A.2. Data reduction were performed using the Rigaku Americas Corporation's Crystal Clear version 1.40. The structure was solved by direct methods using SIR97 and refined by full-matrix least-squares on F^2 with anisotropic displacement parameters for the non-H atoms using SHELXL-97. Structure analysis was aided by use of the programs PLATON98[4] and WinGX. The hydrogen atoms were calculated in ideal positions with isotropic displacement parameters set to 1.2xUeq of the attached atom (1.5xUeq for methyl hydrogen atoms).

The crystal was twinned. The twin law was determined using TwinRotMat in PLATON98. The twin was by a 180° rotation about the 100 direct lattice direction. The twin law was (1,0,0; 0,-1,0; -0.851,0,-1). The twin fraction refined to 0.230(7).

The function, $\Sigma w(|F_o|^2 - |F_c|^2)^2$, was minimized, where $w = 1/[(\sigma(F_o))^2 + (0.1055*P)^2 + (24.5339*P)]$ and $P = (|F_o|^2 + 2|F_c|^2)/3$. $R_w(F^2)$ refined to 0.378, with R(F) equal to 0.123 and a goodness of fit, S, = 1.04. Definitions used for calculating R(F), $R_w(F^2)$ and the goodness of fit, S, are given below. The data were checked for secondary extinction but no correction was necessary. Neutral atom scattering factors and values used to calculate the linear absorption coefficient are from the International Tables for X-

ray Crystallography (1992). All figures were generated using SHELXTL/PC. Tables of positional and thermal parameters, bond lengths and angles, torsion angles and figures are found elsewhere.

Figure A.2: View of the *cis*-strapped Schiff-base calixpyrrole **1.3** showing the heteroatom labeling scheme. Displacement ellipsoids are scaled to the 30% probability level.

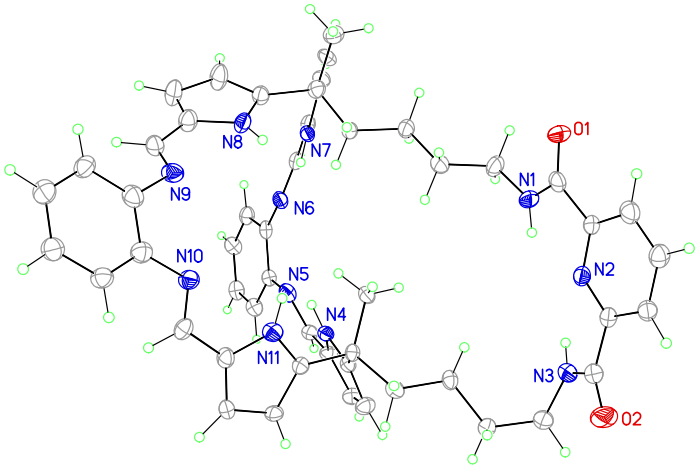

Table A.2: Crystal data and structure refinement for compound **1.3**.

Empirical formula	C55 H67 N11 O6	
Formula weight	978.19	
Temperature	153(2) K	
Wavelength	0.71073 Å	
Crystal system	monoclinic	
Space group	P 21/c	
Unit cell dimensions	a = 13.144(5) Å	a= 90°.
	b = 24.758(11) Å	b= 109.558(8)°.
	c = 16.705(6) Å	g = 90°.
Volume	5122(4) $Å^3$	
Z	4	
Density (calculated)	1.268 Mg/m^3	
Absorption coefficient	0.085 mm^{-1}	
F(000)	2088	
Crystal size	0.460 x 0.110 x 0.080 mm	
Theta range for data collection	3.043 to 24.998°.	
Index ranges	-15<=h<=14, -29<=k<=29, -11<=l<=19	
Reflections collected	9008	
Independent reflections	9008	
Completeness to theta = 25.242°	97.3 %	
Absorption correction	Mulit-scan	
Max. and min. transmission	1.00 and 0.590	
Refinement method	Full-matrix least-squares on F^2	
Data / restraints / parameters	9008 / 354 / 660	
Goodness-of-fit on F^2	1.038	
Final R indices [I>2sigma(I)]	R1 = 0.1230, wR2 = 0.3129	
R indices (all data)	R1 = 0.2576, wR2 = 0.3775	
Extinction coefficient	n/a	
Largest diff. peak and hole	0.603 and -0.485 $e.Å^{-3}$	

X-ray Experimental for Palladium(II) complex 1.50•$(THF)_2$: Crystals grew as thin yellow laths by slow evaporation from THF. The data crystal had approximate dimensions; 0.21 x 0.05 x 0.03 mm. The data were collected on a Rigaku AFC12 diffractometer with a Saturn 724+ CCD using a graphite monochromator with MoKa radiation (l = 0.71073Å). A total of 2136 frames of data were collected using w-scans with a scan range of 0.5° and a counting time of 24 seconds per frame. The data were collected at 100 K using a Rigaku XStream low temperature device. Details of crystal data, data collection and structure refinement are listed in Table A.3. Data reduction were performed using the Rigaku Americas Corporation's Crystal Clear version 1.40. The structure was solved by direct methods using SIR97 and refined by full-matrix least-squares on F^2 with anisotropic displacement parameters for the non-H atoms using SHELXL-97. Structure analysis was aided by use of the programs PLATON98 and WinGX. The hydrogen atoms were calculated in ideal positions with isotropic displacement parameters set to 1.2xUeq of the attached atom (1.5xUeq for methyl hydrogen atoms). The function, $\Sigma w(|F_O|^2 - |F_C|^2)^2$, was minimized, where $w = 1/[(s(F_O))^2 + (0.0985*P)^2]$ and $P = (|F_O|^2 + 2|F_C|^2)/3$. $R_W(F^2)$ refined to 0.246, with R(F) equal to 0.118 and a goodness of fit, S, = 1.16. Definitions used for calculating R(F), $R_W(F^2)$ and the goodness of fit, S, are given below. The data were checked for secondary extinction effects but no correction was necessary. Neutral atom scattering factors and values used to calculate the linear absorption coefficient are from the International Tables for X-ray Crystallography (1992). All figures were generated using SHELXTL/PC. Tables of positional and thermal parameters, bond lengths and angles, torsion angles and figures are found elsewhere.

Figure A.3: View of palladium(II) complex **1.50** showing the atom labeling scheme. Displacement ellipsoids are scaled to the 50% probability level.

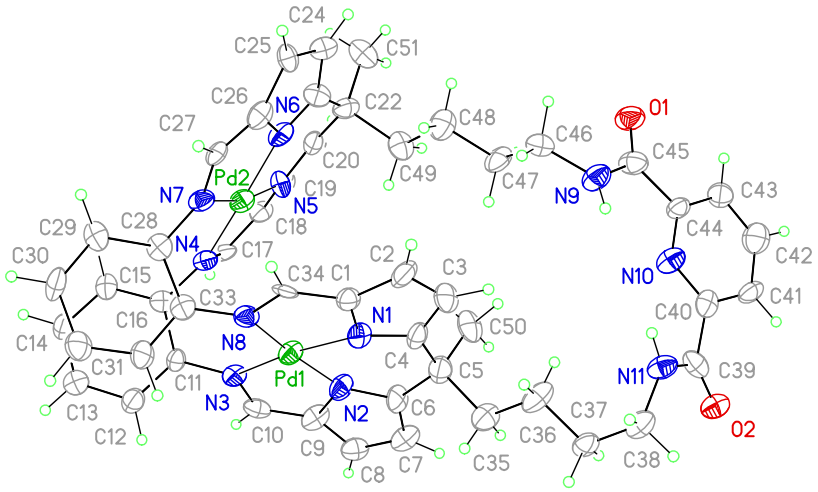

Table A.3. Crystal data and structure refinement for compound **1.50**.

Empirical formula	C59 H63 N11 O4 Pd2	
Formula weight	1203.00	
Temperature	100(2) K	
Wavelength	0.71075 Å	
Crystal system	Monoclinic	
Space group	P21/c	
Unit cell dimensions	a = 14.050(4) Å	a= 90°.
	b = 42.061(12) Å	b= 93.720(7)°.
	c = 8.976(3) Å	g = 90°.
Volume	5293(3) $Å^3$	
Z	4	
Density (calculated)	1.510 Mg/m^3	
Absorption coefficient	0.739 mm^{-1}	
F(000)	2472	
Crystal size	0.21 x 0.05 x 0.03 mm	
Theta range for data collection	2.99 to 25.00°.	
Index ranges	-14<=h<=16, -49<=k<=49, -10<=l<=10	
Reflections collected	59499	
Independent reflections	8912 [R(int) = 0.2255]	
Completeness to theta = 25.00°	95.5 %	
Absorption correction	Semi-empirical from equivalents	
Max. and min. transmission	1.00 and 0.343	
Refinement method	Full-matrix least-squares on F^2	
Data / restraints / parameters	8912 / 0 / 687	
Goodness-of-fit on F^2	1.160	
Final R indices [I>2sigma(I)]	R1 = 0.1180, wR2 = 0.2148	
R indices (all data)	R1 = 0.1939, wR2 = 0.2462	
Largest diff. peak and hole	1.832 and -0.955 $e.Å^{-3}$	

X-ray Experimental for 9-Formyletioporphycene 2.44: Crystals grew as clusters of thin, dark green needles by slow evaporation from dichloromethane. The data crystal was cut from a cluster and had approximate dimensions; 0.41 x 0.05 x 0.03 mm. The data were collected on a Rigaku AFC12 diffractometer with a Saturn 724+ CCD using a graphite monochromator with MoKa radiation (l = 0.71075Å). A total of 270 frames of data were collected using w-scans with a scan range of 1° and a counting time of 45 seconds per frame. The data were collected at 153 K using an Oxford Cryostream low temperature device. Details of crystal data, data collection and structure refinement are listed in Table A.3. Data reduction were performed using the Rigaku Americas Corporation's Crystal Clear version 1.40. The structure was solved by direct methods using SIR97[2] and refined by full-matrix least-squares on F^2 with anisotropic displacement parameters for the non-H atoms using SHELXL-97. Structure analysis was aided by use of the programs PLATON98[4] and WinGX. The hydrogen atoms were calculated in ideal positions with isotropic displacement parameters set to 1.2xUeq of the attached atom (1.5xUeq for methyl hydrogen atoms).

The Ni ion resides on a position with site symmetry 2/m. This imparts a symmetry on the ligand that it does not possess. The aldehyde group is disordered about four equivalent positions in the crystal. The atoms of the aldehyde group, C9, H9a and O1, were assigned site occupancy factors of ¼. The hydrogen atom attached to C5 was assigned a site occupancy factor of ¾ to comprise the formula for the complex of $(C_{33}H_{36}N_4O)Ni$.

The function, $\Sigma w(|F_O|^2 - |F_C|^2)^2$, was minimized, where $w = 1/[(s(F_O))^2 + (0.011*P)^2 + (13.8896*P)]$ and $P = (|F_O|^2 + 2|F_C|^2)/3$. $R_W(F^2)$ refined to 0.118, with R(F) equal to 0.0613 and a goodness of fit, S, = 1.13. Definitions used for calculating R(F), $R_W(F^2)$ and the goodness of fit, S, are given below. The data were checked for secondary extinction effects but no correction was necessary. Neutral atom scattering factors and values used to calculate the linear absorption coefficient are from the International Tables for X-ray Crystallography (1992). All figures were generated using SHELXTL/PC.[8]

Tables of positional and thermal parameters, bond lengths and angles, torsion angles and figures are found elsewhere.

Figure A.3: View of 9-formyletioporphycene **2.44** showing the atom labeling scheme. Displacement ellipsoids are scaled to the 50% probability level. The Ni ion sits on a position with crystallographic site symmetry of 2/m at ½, ½, ½. The crystallographic symmetry imposes a disorder on the aldehyde group around four equivalent positions on the ligand. Atoms C9 and O1 had site occupancies fixed at 1/4.

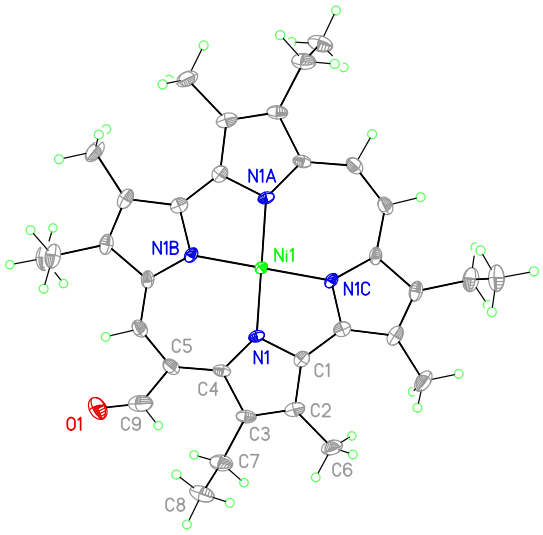

Table A.4: Crystal data and structure refinement for compound **2.44**.

Empirical formula	C33 H36 N4 Ni O	
Formula weight	563.37	
Temperature	100(2) K	
Wavelength	0.71075 Å	
Crystal system	Orthorhombic	
Space group	Cmca	
Unit cell dimensions	a = 25.575(6) Å	a= 90°.
	b = 4.9442(10) Å	b= 90°.
	c = 20.137(4) Å	g = 90°.
Volume	2546.3(9) $Å^3$	
Z	4	
Density (calculated)	1.470 Mg/m^3	
Absorption coefficient	0.798 mm^{-1}	
F(000)	1192	
Crystal size	0.41 x 0.05 x 0.03 mm	
Theta range for data collection	3.19 to 27.48°.	
Index ranges	-18<=h<=32, -6<=k<=6, -26<=l<=24	
Reflections collected	7175	
Independent reflections	1494 [R(int) = 0.0775]	
Completeness to theta = 27.48°	99.7 %	
Absorption correction	Semi-empirical from equivalents	
Max. and min. transmission	1.00 and 0.555	
Refinement method	Full-matrix least-squares on F^2	
Data / restraints / parameters	1494 / 12 / 106	
Goodness-of-fit on F^2	1.131	
Final R indices [I>2sigma(I)]	R1 = 0.0613, wR2 = 0.1083	
R indices (all data)	R1 = 0.0856, wR2 = 0.1175	
Largest diff. peak and hole	0.763 and -0.708 $e.Å^{-3}$	

Appendix B

Magnetic Measurements

Solution magnetic measurements were carried out using the Evans method.[1] Millimolar solutions of the metal complexes were prepared in $CDCl_3$ and placed in a 5 mm diameter NMR tube, while pure $CDCl_3$ was placed in a concentric capillary tube within the NMR tube containing the sample solution. NMR spectra were recorded using a Varian Mercury 400 MHz spectrometer. As shown in Eqs. 1 and 2, calculations of the magnetic moments (μ_{eff}) were based on the difference in chemical shift ($\Delta\delta$), in Hz) observed for the residual $CHCl_3$ signal in neat solvent and in the solution containing the paramagnetic species. This chemical shifts (δ) obtained in parts per million were converted to Hertz (Hz) for the calculations. The magnetic moments were derived using the formula reported by Grant,[2] as corrected for high-field superconducting NMR spectrometers according to the formula of Schubert.[3]

$$\chi_m = 477(\frac{\Delta f}{f2C}) \qquad \text{Eq. 1}$$

$$\mu_{eff} = 2.84\sqrt{\chi_m m * T} \qquad \text{Eq. 2}$$

Where,

Δf = difference in chemical shift between the sample and the reference (given in Hertz), f = the frequency of the NMR machine in Hertz, C = concentration (M), χ_m = molar succeptibility (cgi), T = temperature in Kelvin (K).

References

1. Evans, D. F. *J. Chem. Soc.* **1959**, 2003.
2. Grant, D. H. *J. Chem. Educ.* **1995**, *72*, 39.
3. Schunert, E. M. *J. Chem. Educ.* **1992**, *69*, 69.